Winter 2014

Mouse Oocyte Maturation and Embryo Development After Exposure to Vemurafenib (PLX4032), an Anti-Melanoma B-RAF V600E Inhibitor

Bo Liu
Old Dominion University

MOUSE OOCYTE MATURATION AND EMBRYO DEVELOPMENT AFTER EXPOSURE TO VEMURAFENIB (PLX4032), AN ANTI-MELANOMA B-RAF^{V600E} INHIBITOR

by

Bo Liu
Bachelor of Clinical Medicine, June 2009,
Guangzhou Medical University, Guangzhou, China

A Dissertation Submitted to the Faculties of
Old Dominion University
in Partial Fulfillment of the
Requirements for the Degree of

DOCTOR OF PHILOSOPHY

BIOMEDICAL SCIENCE

OLD DOMINION UNIVERSITY
December 2014

Approved by:

R. James Swanson (Director)

Christopher J. Osgood (Member)

Robert E. Ratzlaff (Member)

Silvina Bocca (Member)

ABSTRACT

MOUSE OOCYTE MATURATION AND EMBRYO DEVELOPMENT AFTER EXPOSURE TO VEMURAFENIB (PLX4032), AN ANTI-MELANOMA B-RAF^{V600E} INHIBITOR

Bo Liu
Old Dominion University, 2014
Director: Dr. R. James Swanson

Vemurafenib is a selective B-Raf^{V600E} inhibitor in melanoma targeted therapy which also inhibits the wild type B- and C-Raf. In oocyte maturation, the C-Raf/MAPK pathway acts as an important self-enhancing and promoting system, whereas in embryo development, the C-Raf/MAPK pathway participates in pre- and post- implantation embryo proliferation and differentiation.

The hypothesis: Vemurafenib has detrimental effects on oocyte maturation and/or embryo development. Mouse oocytes and one cell (1C) mouse embryos were tested by *ex vivo* culturing with Vemurafenib in serial dilution. Oocytes were evaluated by cell cycle morphology, spindle formation and chromosomal alignment by immunofluorescence (IF) staining as well as DNA integrity by Terminal Transferase dUTP Nick End Labeling. Embryo development was evaluated by morphological changes and the C-Raf bioactivity via a p-Mek 1/2 IF assay. *In vivo* exposure and subsequent morphological evaluation of *ex vivo* two-cell (2C) embryo development was conducted by pre-injections of Vemurafenib (10 mg/kg).

Ten μM or above produced oocyte toxicity, spindle formation disturbance, chromosome misalignment and DNA damage, whereas the therapeutic Vemurafenib concentration 1 μM did not display significant oocyte morphological toxicity to *ex vivo* oocyte maturation, spindle formation, chromosome alignment and DNA integrity.

Ten μM and 100 μM showed phosphorylation inhibition of embryo Mek 1/2, decreased C-Raf activity and obvious toxicity to 1C to 2C transition. However, the 1 μM Vemurafenib was not shown to have significant ex *vivo* preimplantation 1C embryo development toxicity on the 1C to 2C transition and no effect on C-Raf activity.

Ten mg/kg Vemurafenib pre-injections demonstrated only a mild delayed toxic influence throughout the embryo development. However, the majority of embryos

progressed to normal blastocysts and did not show significant *in vivo* degenerative preimplantation embryotoxicity.

Thus Vemurafenib, at its therapeutic concentration, was free of *ex vivo* oocyte and embryo morphological toxicity, but *in vivo* toxicity needs further clarification on mechanisms and survivability of collapsed unhatched embryos.

This thesis is dedicated to my Lord Jesus Christ, my mother Wang, Lin, my wife Huang, Ran and my advisor Dr. R. James Swanson for their continuous and unconditional support throughout the completion of my Ph.D. education.

ACKNOWLEDGMENTS

First of all, Praise and Thanks is direct to my dear LORD and Savior Jesus Christ for the innumerable, incredible and beautiful Blessings, Grace and Mercy undeservedly heaped upon me.

Completion of this doctoral dissertation was an impossible task without support from many people. I owe my sincere gratitude to all my beloved ones.

I am extremely grateful to Dr. R. James Swanson and his wife Gloria for their constant priceless guidance on my academic development, life and spiritual growth. He tolerated my failures and mistakes and melted difficulties by his immense knowledge, profession, enthusiasm and great patience. But what's more important is that I have learned how to live in Christ from them. Endless prayers encouragements and unconditional support were added to my blessings throughout my Ph.D. study from the very first eye I saw them. They mean more than teachers to me but are my dear father and mother.

None of these could be accomplished without the love and patience of my family. I must also acknowledge with deep thanks my mother, Wang, Lin, and the other half of me, Huang, Ran. They are my dearest parts and spend their lives to share my success and failure, sadness and joyfulness, smiles and tears, and moreover, my faith in Christ.

I also extend my thanks to the Dean, Dr. Ronnie Martin and all faculty and staff of Liberty University College of Osteopathic Medicine for their "salty" and warm hearts, sincerity of prayers, academic and financial support.

I also want to thank my committee members, Drs. Silvina Bocca, Christopher Osgood and Robert Ratzlaff, for their comprehensive instruction, insightful suggestions

and valuable time throughout this research.

This dissertation would not have come to a successful completion without the kind assistance received from my fellow classmates and spiritual friends Li, Fang and Yu, Liang. They are two of the best informative resources and consults to my project. And they have been very patient in taking care of me. They would search for any possible solution to my questions every time I turned to them and were never exhausted.

I want to thank Dr. Dayle Daines from Old Dominion University and Dr. Kimberly Mitchell from Liberty University. They have been so kind to extend their help beyond their responsibilities at various phases of this research whenever I approached them. Dr. Dayle Daines provided me with her research expertise and allowed me to use her equipment. Dr. Mitchell has been a profound biotechnology instructor to me. I thank them for their precious contributions.

My experience at Old Dominion University was greatly enhanced by friendships and fellowships made here. I extend my thanks to Dr. James Yuan and his wife Nancy. I especially enjoy their Chinese student bible study every Friday night, from where I gained the strength in my faith from the Lord. I appreciate Dr. Ralph Stevens and Janna Grubbs's support when I worked with them. I also give thanks to my American and international friends, Martin Morgan and his wife Edwina, Kurnia Foe and his wife Lian from Tabernacle Church of Norfolk, Si, Dong and his wife Yu, Huizhi, Yang, Shuo and others not mentioned. With their help, I could start my new adventure in Lynchburg.

NOMENCLATURE

1C	One Cell
2C	Two Cell
3C	Three Cell
4C	Four Cell
5C	Five Cell
6C	Six Cell
7C	Seven Cell
8C	Eight Cell
Akt (PKB)	Protein Kinase B
ANOVA	Analysis of Variance
BSA	Bovine Serum Albumin
CD	Cervical Dislocation
CDK	Cyclin-Dependent Kinase
CDKN2A	Cyclin-Dependent Kinase Inhibitor 2A
COC	Cumulus Oophorus Cells with Oocyte Complex
DAPI	4',6-Diamidino-2-Phenylindole
Deg	Degeneration
DMSO	Dimethyl Sulfoxide
DN	Dominant-Negative
eB	Early Blastocyst
EB	Expanded Blastocyst
EGTA	Ethylene Glycol Tetraacetic Acid
Em	Emission
Erk	Extracellular Signal-Regulated Kinases
Ex	Excitation
FDA	Food and Drug Administration
FGF	Fibroblast Growth Factor
FITC	Fluorescein Isothiocyanate

Frag	Fragment
FSH	Follicle Stimulating Hormone
G	Gauge
GnRH	Gonadotropin-Releasing Hormone
GV	Germinal Vesicle
GVBD	Germinal Vesicle Breakdown
H	Hatching
hB	Hatching Blastocyst
hCG	Human Chorionic Gonadotropin
h	Hours
I.P.	Imtraperitoneally
IACUC	Institutional Animal Care and Use Committee
IF	Immunofluorescence
IGF-1	Insulin-Like Growth Factor-1
IGF-1R	Insulin-Like Growth Factor-1-Receptor
I-R	Insulin Receptor
IU	International Unit
IUGR	Intrauterine Growth Retardation
IVF	In Vitro Fertilization
KA	Keratoacanthoma
kg	Kilogram
LH	Luteinizing Hormone
MAPK	Mitogen-Activated Protein Kinases
Mek (MAPKK)	Mitogen-Activated Protein Kinase Kinase
mg	Milligram
MI	Metaphase I
MII	Metaphase II
min	Minutes
MISS	MAPK-Interacting and Spindle-Stabilizing
mL	Milliliter

MM	Malignant Melanoma
mM	Millimolar
MPF	M Phase Promoting Factor
MTOC	Microtubule Organizing Center
mTORC	The mammalian target of rapamycin
MTSB	Microtubule-Stabling Buffer
nB	Normal Blastocyst
NC	Nontoxic Concentration
ηm	Nanometer
ODU	Old Dominion University
PB	Polar Body
PBS	Phosphate buffered Saline
PDGF	Platelet Derived Growth Factor
PI3K	Phosphoinositide 3-Kinase
PMSG	Pregnant Mare's Serum Gonadotropin
P-R	Progesterone Receptor
PTEN	Phosphatase and Tensin Homolog
QA/QC	Quality Assurance/Quality Control
RSK	Ribosomal S6 Kinase
RTK	Receptor Tyrosine Kinase
SCC	Squamous Cell Carcinoma
TC	Toxic Concentration
U	Unit
µL	Microliter
µM	Micromolar
µM	Micrometer
WT	Wild Type

TABLE OF CONTENTS

Page

LIST OF TABLES

LIST OF FIGURES

CHAPTER 1

INTRODUCTION

1.1 The Epidemiology of Malignant Melanoma (MM) with Pregnancy

Vemurafenib is an anti-cancer drug used in targeted chemotherapy for MM. Vemurafenib is not recommended for use in women that are pregnant or suspected to be pregnant because Hoffman La Roche, the patent holder, has not tested and most likely does not intend to test this drug for safely in embryo or fetal stages of mouse or human development. (FDA Reference ID: 3001518) Therefore a woman that is diagnosed with MM where Vemurafenib is the treatment-of-choice for the disease might have to choose between delivering a healthy neonate or death for both her and the child if she is pregnant at the time of diagnosis and treatment initiation. A clear understanding of the toxicity of Vemurafenib to the female gamete, pronuclear stage cell, and zygote-to-blastocyst stages is the initial starting point for understanding the potential dangers of Vemurafenib. If the toxicity is low enough to suggest use of Vemurafenib during pregnancy then further research could be performed on long-term effects to male and female gametes and on teratogenicity to the fetus/neonate.

In the United States (US), malignancies account for about 19.9% of the mortality in women between 15 and 34 years of age (Pavlidis, 2002). The MM is one of the leading causes of all malignancies and non-accidental deaths of women in the US (Langagergaard, 2011). Approximately 61,300 cases of melanoma were diagnosed *in situ* in 2013 (Siegel et al., 2013). "The incidence of MM in pregnancy has been estimated to range from 0.14 to 2.8 per 1,000 live births and melanoma accounts for about 8% of all malignant tumors arising during pregnancy" (Ernstoff MS et al., 2003). An increasing numbers of pregnancies in older women will result in more melanomas being seen. Women who often postpone their childbearing plans for various reasons make up one third of women diagnosed with MM in the US childbearing age (Lens et al., 2008). This data gives clear

direction for discovering the toxicity of Vemurafenib when used during pregnancy.

1.2 The Etiological Role of B-Raf in MM

While there is no current evidence for B-Raf in the mammalian eggs, the existence of B-Raf in the *Xenopus levis* has been documented (Sergiy I. Borysov et al., 2008). The fact that Vemurafenib is designed to target the mutated B-Raf does not exclude the role of wild-type B- and/or C-Raf in the process of mouse oocyte and embryo development. Therefore, understanding B-Raf's role is crucial in understanding C-Raf's role. The binding inhibition for mutated B-Raf^{V600E} is 31 nM; for wild-type B-Raf is 100 nM; and for C-Raf is 48 nM (Bollag G, et al., 2010). Based on the binding data, we can say that toxicity to normal wild-type oocytes and embryos is relevant in understanding the potential toxicity of Vemurafenib on oocyte and embryo development. The Raf serine/threonine protein kinases, including A- (68 kd), B- (95 kd) and C-Raf (74 kd), serve as the major downstream effectors of the Ras in the Mitogen-Activated Protein Kinase (MAPK) pathway. The MAPK signaling is activated by growth factors and/or cytokines through the receptor tyrosine kinases (RTK) which in turn activates Ras (Davies et al., 2002; White, 2011; Sosman et al., 2009). Mek is the only known substrate of B-Raf and C-Raf (Dhomen et al., 2007). The B-Raf mutation accounts for 50% of all melanoma cases, the majority of which are produced from unprotected intermittent UV exposure (Davies et al., 2002). Targeting melanoma B-Raf^{V600E} mutation with combination therapy has become the focus of ongoing clinical trials.

1.3 The Pharmacology of Vemurafenib

Vemurafenib, a crystalline form of PLX4032, is a highly selective mutated B-Raf^{V600E} kinase inhibitor (Sharma A, 2012). Vemurafenib is approved by the FDA because of its overall increase in survival rate and free progression period than its classical chemotherapeutic agent, dacarbazine in MM (Chapman et al., 2011). However, *in vitro*, siRNA-induced mutated B-Raf^{V600E} silencing leads to a decrease of downstream Erk activation and, to some degree, of apoptosis whereas the WT B-Raf silencing has a

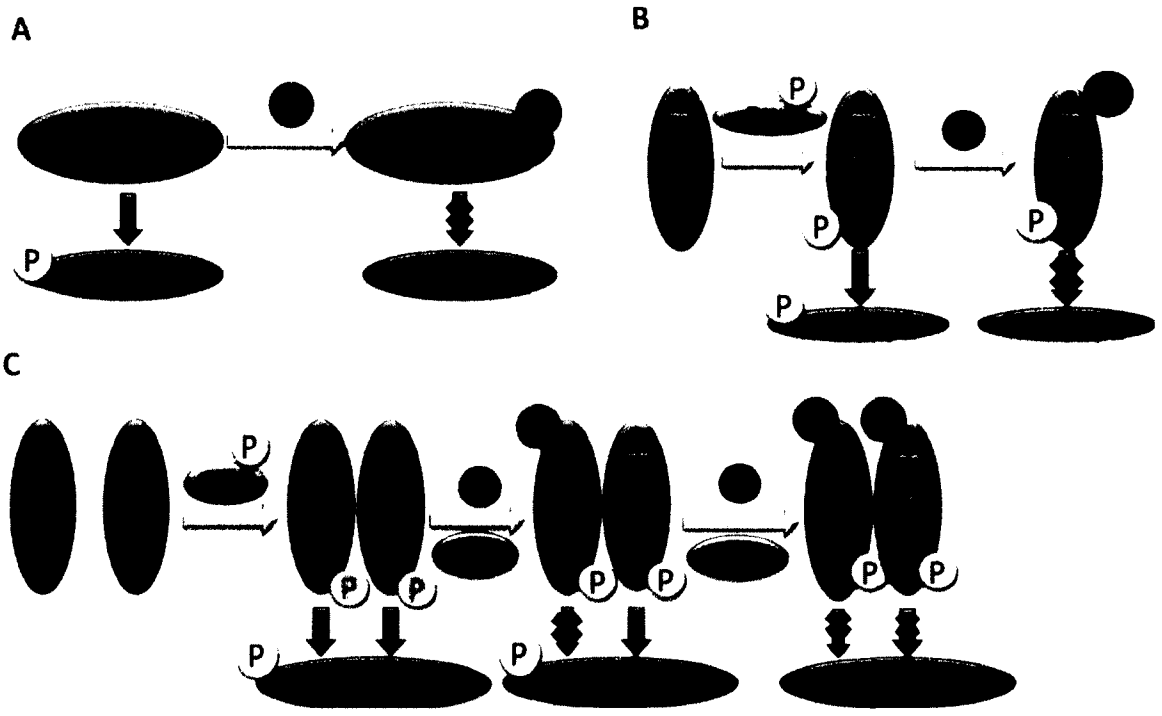

Figure 1. Vemurafenib's Pharmacological Mechanisms

(A) *In vivo* p (phosphorylated)-B-Raf^{V600E} mutated monomer in Melanoma. Vemurafenib completely blocks B-Raf activity of Mek phosphorylation. (Sharma A et al., 2012).

(B) *In vitro* Wild Type (WT) p-A-, p-B-, p-C-Raf monomer in other cells. Vemurafenib shows *in vitro* inhibitory effects on WT phosphorylated A-, B- and C-Raf and is potentially harmful to cell types such as like oocytes and embryos. (Poulikakos et al., 2011, Bollag G, et al., 2010)

(C) *In vivo* WT p-B-RAF homogenous & heterogeneous dimer in Melanoma. A low dose of Vemurafenib *in vivo* transactivates Mek by heterodimerizing with C-Raf, while a high dose of Vemurafenib blocks such an effect (Poulikakos et al., 2011; Heidorn, 2010; Hatzivassiliou, 2010).

trivial influence on melanoma growth (Hingorani et al., 2003). Moreover, several recent *in vivo* studies point to results similar to the *in vitro* B-Raf silencing test. In patients with both mutated and WT B-Raf melanoma cell, Vemurafenib not only inhibits B-Raf in the mutated B-Raf cell, but also causes MAPK pathway activation via transactivated C-Raf in WT B-Raf cells (Poulikakos et al., 2011; Heidorn, 2010; Hatzivassiliou, 2010).

Vemurafenib also inhibits Mek1/2 and Erk1/2 phosphorylation (Yang et al., 2010). Figure 3 compares the MAPK pathway transactivated via C-Raf *in vivo* (Figure 3C) with *in vitro* inhibition of WT B-Raf and C-Raf (Figure 3A). This activation results from transactivation of non-inhibited C-Raf dimerized with inhibited WT B-Raf. The mutated B-Raf^{V600E} cell monomer (Figure 3B) is inhibited (Poulikakos et al., 2011; Hatzivassiliou, 2010). In recent Vemurafenib phase I clinical trials, 90% of patients carrying the B-Raf^{V600E} mutation showed confirmed tumor shrinkage, with remarkable Erk signaling inhibition (Chapman, 2009; Flaherty, 2009).

1.4 Normal Oogenesis, Folliculogenesis, Morphology and Molecular Basis

1.4.1 Early Oogenesis: Primordial Oocyte to Primary Oocyte (Primordial Follicle)

A spermatozoon and an oocyte each provide half the genetic materials for embryo development and all the cytoplasmic materials for early (1C to 2C) embryo development.

Female oogenesis begins in the fetal ovary while in the uterine development and continues throughout reproductive stages. It is generally accepted that all oocytes in the ovary develop before the birth of the female fetus. In the fifth week of pregnancy, the primordial germ cells in early female fetal development multiply and slowly migrate from the yolk sac epithelium to the genital ridge, form the primitive medullary and sex cords, and later form the shape of the ovary. After this migration and proliferation, an estimated one to two thousand primordial germ cells, now called oogonia, are located in each ovary. This number increases by mitosis to approximately six to seven million oogonia by the fifth month of gestation (20th week) when proliferation ceases.

While growth factors, PGs, transforming growth factor beta (TGF- β) (Pangas SA et al., 2012), bone morphogenetic proteins (BMPs) (Margulis S et al., 2009) and antimullerian hormone (AMH) (Durlinger AL et al., 2002) are considered to be important in fetal ovary development. Information concerning the hormonal or factorial controls and regulations remains unclear.

Some oogonia located in the inner layer or ovarian cortex increase the size of the cell and perform drastic nuclear changes for further meiotic development. These cells are now called primary oocytes. These changes are endocrine independent. The DNA of the

primary oocyte replicates to form the sister chromatids, which are paired homologously with the same parental-oriented chromatids as the tetrads. The cells then enter meiosis. The cells arrest in meiotic prophase I at diplotene and is surrounded by a single flattened cuboidal layer of somatic epithelial cells (pre-granulosa cells). The primary oocyte-encapsulated somatic epithelium complex is now called the primary follicle. Oogenesis is closely connected with the folliculogenesis (Makabe S et al., 2006).

Once arrested, further development of the primordial follicle ceases until the initiation of sexual maturity in puberty. The primordial follicles remain in the resting state. Not every oogonium will successfully develop to form a primordial follicle. Depending on individual variation, only 50% to 90% of the fetal ovarian oogonia will finally enter the meiotic stage. The remainder of the oogonia, which failed to form primary oocytes and/or primordial follicles, undergo the physiological degenerative process called atresia. Only approximately two million primordial follicles will survive until the birth of the female fetus. However, the loss of gametes is a continual apoptotic process of the primordial follicles. From the 20^{th} week of gestation through pre-puberty, atresia of primordial follicles beginning with the death of the primary oocyte decreases the total number of primordial follicles to three to four hundred thousand by the onset of puberty (Tingen CM et al., 2009). By the onset of menopause at 45-55 years, all oocytes have been depleted and 99.9% of primordial follicles have never matured. The degradation of oocyte selection does not appear to be based on quality (Hartshorne GM et al., 2009).

1.4.2 Early Folliculogenesis and Endocrine Hormone Regulation

Onset of puberty is marked by the pulsing release of the gonadotropin releasing hormone (GnRH). Leptin is the putative initiator of GnRH release. Leptin receptors are located at the preoptic nucleus of the hypothalamus, where GnRH synthesis occurs. Leptin depletion leads to failure of GnRH release and the onset of puberty. Also, kisspeptin, the product of the gene Kiss1, a G-protein coupled receptor ligand for GPR54, is originally identified as a human metastasis suppressor gene that has the ability to

suppress melanoma and breast cancer. Kisspeptin-GPR54 signaling is understood to play an important role in initiating GnRH secretion at puberty.

GnRH, released from the hypothalamus and transported to the anterior pituitary gland via the infundibulum (hypothalamo- hypophyseal portal blood vessel system), stimulates the synthesis of the Follicle-Stimulating Hormone (FSH) and Luteinizing Hormone (LH). Both FSH and LH bind to their G-protein coupled receptors and activate the adenyl cyclase. Adenyl cyclase converts the ATP to cAMP, which in turn stimulates the protein kinase A (PKA) for further biological functions. FSH in the female stimulates estrogen secretion, mainly estradiol, growth of the ovarian follicles, and oocyte maturation; whereas LH facilitates luteinization of the follicle, ovulation stimulation and the progesterone secretion by the corpus luteum.

The activation of primordial follicle growth by FSH and LH is considered an irreversible process for the follicles toward either atresia or the mature Graafian follicle. In the primary oocyte, under the influence of systemic gonadotropins FSH and LH, the cell increases its total cytoplasm and secretes the zona pellucida, a transparent protective shell composed of four glycoproteins.

At the same time, the increase of FSH and LH concentration during the early stage of the menstrual cycle stimulates the numbers and layers from the single surrounding flattened layer to multiple cuboidal layers of granulosa cells, which in turn secrete transuding plasma inside the follicle and significantly increase the size of the follicle. This fluid-filled space, the antrum, is composed of multiple various-sized chambers. , Under the influence of LH, the thecal cell layer differentiates into the theca interna and theca externa. After this differentiation, the follicle is called a secondary follicle. Both granulosa cells and thecal cells are steroidogenic cells and are separated by a glassy layer of basement membrane.

Androstenedione is synthesized from cholesterol in the theca interna under the influence of LH and is delivered to the inner granulosa cells where it is synthesized into estradiol under the influence of both FSH and LH. Estradiol, the most biologically active estrogen, is responsible for the significant changes of secondary sex characteristics as well as oviduct and uterine preparation for the embryo implantation. Such preparations include enlarged and ciliated epithelia in the oviduct, increased size of the uterus and

stimulated epithelial, glandular and stromal cell proliferations of the endometrium. These cells become the secretory tissue in response to progesterone in the luteal phase in preparation for embryo implantation (Hedge G et al., 1987).

1.4.3 Graafian Follicle Formation

As the level FSH and LH increases, the number of granulosa cells increases. These granulosa cells are responsible for the fluid accumulated in the antrum. Multiple follicular pockets of fluid coalesce into a single tertiary follicle and finally form the Graafian follicle. As the antrum enlarges, the granulosa cells immediately adjacent to the primary oocyte are called corona radiata. The close contact of these cells to the primary oocyte through specialized gap junctions is critical to oocyte maturation resumption in information signaling and nutrition transportation and exchange. A group granulosa cells draws the primary oocyte off-centered to one side of the follicle, forming a cumulus oophorus. The cumulus oophorus in turn attaches to the mural granulosa cells, which are pressed by the antral fluid against the follicular wall like a stalk. The Graafian follicle, also known as the tertiary or preovulatory follicle, reaches the size of 12 to 19 mm. This dramatic change in size results in one Graafian follicle bulging and thinning one surface lining of the tunica albuginea, which is the dense connective tissue lining of the ovary.

1.4.4 LH surge, Follicular Rupture and Ovulation

Approaching day 14 of the normal 28 days of the menstrual cycle, the anterior pituitary produces a surge of LH in respond to the positive feedback of the estradiol secreted by granulosa cells. LH directly induces oocyte meiosis I resumption (section 1.5.6), and also causes the mural granulosa and cumulus cells to produce a minimal amount of follicular steroid hormone (progesterone), which indirectly induces oocyte maturation and initiates the ovulation process. Progesterone then causes follicular hyperemia and PGs secretion. As follicular fluid production and swelling increase (Russell DL et al., 2007), granulosa cells begin secrete proteolytic enzymes (like collagenase) to weaken the follicular wall of the Graafian follicle. The follicle swelling

and wall weakening lead to a blister-like thinned area called stigma. The stigma eventually ruptures and expels the secondary oocyte under the influence of LH (Peters H et al., 1980).

1.4.5 Oocyte Nuclear Maturation Morphology

By definition, oocyte maturation begins with meiotic prophase I. The arrested primary oocyte resumes its first meiotic division to progress into and arrest at meiotic nuclear metaphase II, which produces a secondary oocyte and accompanying cytoplasmic changes for proper conditions for fertilization and early embryo development. Therefore, both nuclear and cytoplasmic maturation are essential criteria for oocyte quality evaluation.

The most important feature of the arrested prophase I primary oocyte is its prominent microscopically intact nucleus, known as a germinal vesicle (GV). Inside the GV, the nucleolus can be clearly visualized by light microscope (Brunet S et al., 2007). In the Graafian follicle, formed by the LH surge, the most prominent microscopic structure is the metaphase II plate.

A very thin narrow space called the perivitelline space is located between the oocyte plasma membrane (oolemma) and the zona pellucida. The width of the perivitelline space is one of the critical criteria in assessing the quality of the secondary oocyte and embryo before implantation after the collection operation.

Meiosis resumption is characterized by the disappearance of the nuclear membrane and condensation of the chromatins into chromosome pairs aligned on the center of the barrel-shaped meiotic spinal apparatus at meiosis metaphase I. This dissolution of the nuclear membrane is termed germinal vesicle breakdown (GVBD). After separation of the paired chromosome at meiosis telophase I, the oocyte squeezes out its first polar body into the narrow perivitelline space, which contains half of the genetic materials with very little amount of cytoplasmic content. Then the oocyte progresses into meiosis II without being arrested in prophase, without DNA replication. Again, the chromatins of the oocyte at meiosis metaphase II are condensed and paired, aligning along the center of the barrel shaped meiotic spinal apparatus. The oocyte finally arrests at metaphase II to

await the signal to resume meiosis II after sperm penetration (oocyte activation).

1.4.6 Oocyte Cytoplasmic Maturation from Meiosis I Resumption to Meiosis II Arrest and Its Molecular Biology

Oocyte cytoplasmic maturation involves integration of the interaction of cumulus granulosa cells and the oocyte. Both cell types operate under the influence of hormone changes, and the oocyte's intracellular signaling network of cellular events (Meiosis I resumption, GVBD meiotic metaphase II arrest, and eventual ovulation). The steps of maturation involve:

- Surrounding cumulus granulosa cell regulation of oocyte cytoplasmic maturation. Meiosis prophase I arrest of the primary oocyte and the maintenance of the arrest state require bi-directional signaling communication between the cumulus granulosa cells and the oocyte. From the very beginning of folliculogenesis, the primary oocyte is responsible for the surrounding granulosa cells for their proliferation, functionalization, and differentiation. Developing granulosa cells build up the direct communicating gap junction channels by stringing themselves together and extending the cell membrane endings through the zona pellucida to the primary oocyte. These cell-to-cell communications convey the nutrient and signaling messages between granulosa cells and oocyte for maturational competence and the maintenance of the arresting state (Gershon E et al., 2008).
- Cx37 (also known as GJA4) is the major connexin (Cx) of the gap junction components between the cumulus granulosa cell and oocyte, whereas the Cx43 (also known as GJA1) is the gap junction component among the granulosa cells. The disruption and breakdown of the gap junction communication by the LH or human chorionic gonadotropin (hCG) are the characteristic signs of the primary oocyte meiosis I resumption (Kalma Y et al., 2004).
- LH binding to its G-protein coupled receptor in cumulus granulosa cells activates the Adenyl cyclase/cAMP/PKA and mitogen-activated protein kinase (MAPK) pathways,

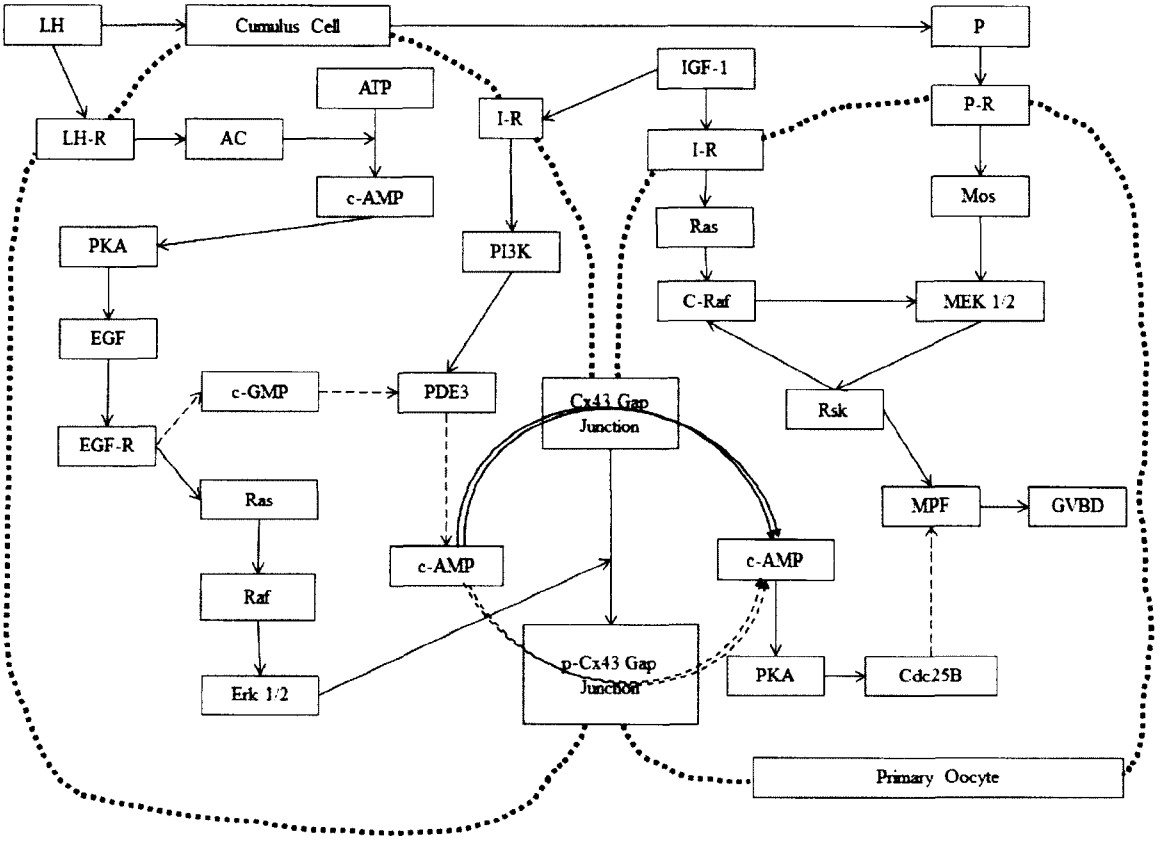

Figure 2. Signalings in Cumulus Cells Regulates Oocyte Maturation in LH Surge

The high c-AMP content delivered from cumulus cell to primary oocyte via Cx43 composed gap junction is the primary force of maintaining GV-intact oocyte from GVBD (Downs & Eppig 1984, Downs et al. 1986). The c-AMP in oocyte phosphorylates Cdc25B, an MPF inhibitor, via PKA keeps the GV-intact state (Gautier J et al., 1991). LH acts through G-protein-coupled receptor which in turn activates cAMP/PKA pathways to enhance the biosynthesis of EGF factor in cumulus cell (Conti M et al., 2002). EGF factor in turn activates the Ras/Raf/Erk 1/2 MAPK pathway mediates the oocyte meiosis resumption by phosphorylating downstrean effectors, nuclear transcriptions and gap junctions closure by Cx43 connexin phosphorylation(Kalma Y et al., 2004, Qing-Yuan Sun et al., 2009). IGF-1 activates PDE3 to degrade c-AMP in cumulus cell via I-R/PI3K pathway. IGF-1-Ras-Raf-MAPK pathway also acts as the self-enhancing and self-accelerating system in progesterone induced Mos-MAPK-GVBD (Bodart et al., 2005). LH-R (LH receptor), PDE3 (Phosphodiesterase 3), I-R (Insulin receptor), IGF-1 (Insulin-like Growth Factor-1), P (Progesterone), P-R (Progesterone receptor), GVBD (Germinal vesicle breakdown), MPF (Maturation Promoting Factor)

inhibits the expression of the Cx43 by phosphorylation, and disrupts the cell-cell gap junction communication (Conti M et al., 2002). Deletions of the MAPK effectors, Erk1 and Erk2, significantly block the gap junction breakdown. The LH-induced paracrine of progesterone from the surrounding cumulus cells towards the primary oocyte plays a pivotal role in adenyl cyclase inhibition, which decreases the total concentration of cAMP, and promotes the oocyte maturation promoting factor (MPF) complex formation.

- LH-induced epidermal growth factor (EGF) via cAMP/PKA, Ras and MAPK pathways together act as the intrafollicular gonadotropin-related signals from the cumulus granulosa cells to the primary oocyte. However, the detailed mechanisms remain elusive (Qing-Yuan Sun et al., 2009). Furthermore, insulin and insulin-like growth factor 1 (IGF-1) also bind to the IGF-1 receptor (IGF1R) to activate phosphor-inositol 3 kinase (PI3K). This binding brings the activity of phosphodiesterase 3 (PDE3) to breakdown the cAMP (Eppig JJ et al., 2004). Also, insulin and IGF-1-induced Ras/C-Raf/MAPK pathway enhance and promote the progesterone-induced Mos/MAPK pathway in MPF formation for GVBD in oocyte maturation resumption. By inhibiting Raf / MAPK pathway, the anti-melanoma drug Vemurafenib demonstrates potential cytotoxicity on the maturing oocyte.
- Before the LH surge, cAMP concentration within the pre-ovulated primary oocyte, is maintained at a high level. This high level of cAMP maintains the activation of PKA, which differs from functions of PKA in cumulus cells, inhibiting the early translation of maternal mRNAs in the primary oocyte from maturation and causing prophase I G2 arrest. PKA also directly targets and phosphorylates Cdc25B, which sustains the catalytic effect of component of MPF, the CDK1 (Cyclin-Dependent Kinase 1, also known as $p34^{cdc2}$) (Gautier J et al., 1991). This high concentration of cAMP may be partially produced by the adenyl cyclase from the primary oocyte but dominantly delivered externally from gap junctions from surrounding cumulus granulosa cell projections (Downs & Eppig 1984, Downs et al. 1986). 3', 5'-cyclic guanosine monophosphate (cGMP) from surrounding cumulus cells plays a similar role in increasing cAMP by inhibiting PDE3. The effect of EGF in decreasing cGMP by the cumulus cell's PDE leads to decrease of cAMP. The dissociation of gap junctions

after the LH surge cuts off the cAMP supply and reinitiates oocyte meiosis I from G2 arrest.

- Cumulus cells mechanically stripping or chemically digesting the intercellular gap junctions allow the oocyte to resume its progress toward maturation. This recovery after the PMSG injection is critical for the ex vivo oocyte maturation resumption in the culture medium.
- After reinitiating oocyte meiosis I, four stages of maturation from GVBD until the start of meiosis II include: (1) GVBD is initiated by phosphorylation of the nuclear lamins, which resemble the magnetic clips for the nuclear membrane integrity; (2) The nucleolus is completely dissolved; (3) The chromosomes are condensed by phosphorylation of the chromosome proteins, including histones; and (4) Barrel-shaped meiotic spindle apparatus led by centrosomes are formed and polymerized All condensed chromosomes are aligned vertically along the center of the axis of the spindle barrel. All four stages events require the prerequisites of successful GVBD, spindle apparatus formation, and correctly aligned chromosomes.
- Extensive reversible phosphorylation and dephosphorylation maximize the success of the progress from meiotic II through metaphase II arrest. Phosphorylation by kinases and dephosphorylation by phosphatases are the most important intracellular regulatory mechanisms in the primary oocyte. The cellular events of GVBD, spindle apparatus formation, and correctly aligned chromosomes are initiated by three principal kinases/phosphatases in the oocyte (1) Serine/threonine protein phosphatases (PP); (2) maturation promoting factor (MPF); and (3) MAPK pathway.
- The involvement of serine/threonine protein phosphatases (PP) in the GV oocyte includes protein phosphatase-1 (PP1) and 2A (PP2A) (Smith GD et al., 1998). Inactivation of MPF ($p34^{cdc2}$/cyclinB2) is positively regulated via tyrosine phosphorylation of $p34^{cdc2}$ by PP2A during prolonged prophase arrest of the oocyte (Rime, H et al., 1995). The endogenous form of PP2A also prevents progesterone-induced oocyte maturation (Iwashita, J et al., 1997). The PP1- and PP2A-inhibitor okadaic acid (OA) also demonstrates promotion of oocyte meiosis resumption (Smith, G.D et al., 1998). The depletion of PP2A is sufficient to initiate oocyte maturation (Maton, G., Lorca, 2005) and indicates blocking of the meiotic spindle apparatus

formation. Inhibition of PP1 also leads to the nuclear envelop dissolution and complete GVBD.

- Maturation promoting factor (MPF) (also known as mitosis-promoting factor or M-phase-promoting factor) is a heterodimer composed of Cyclin B and $p34^{cdc2}$ (CDK1). MPF strongly stimulates the meiotic activities by phosphorylating multiple target effectors required during oocyte meiosis resumption. MPF is undetectable in the GC-intact stage, gradually increases in GVBD, is peaks in metaphase I oocytes, and decreases in meiosis I anaphase and telophase (which dissembled and polyubiquitinated the Cyclin B by anaphase-promoting complex). However, MPF increases and stabilizes during secondary oocyte metaphase II arrest (Winston N et al., 1997).
- In 1971, MPF microinjected into the cytoplasm of progesterone-stimulated frog oocytes in G2 prophase I arrest stimulated resumption of the maturation process (Masui Y, Markert CL, 1971). Activated MPF phosphorylates and activates (1) condensins and histones (H1 and H3) for condensing the chromosomes; (2) various microtubule-associated proteins for the barrel-shaped spindle apparatus formation; and (3) lamins (lamin A, B and C) for the nuclear membrane depolymerization and dissolution (Maro B et al., 1994). Activation of the MPF plays a pivotal role in successful execution of the oocyte maturation events. For the activation of MPF, the activated the $p34^{cdc2}$ (CDK1) subunit must bind to Cyclin B for a complete functional unit. The threonine-161 (Thr-161) on the $p34^{cdc2}$ (CDK1) must be phosphorylated by a Cyclin Activating Kinase (CAK). Threonine-14 (Thr-14) and tyrosine-15 residues of the $p34^{cdc2}$ (CDK1) must be dephosphorylated to be activated by the Cdc25. However, Myt1 (Wee1) continues to phosphorylate theTyr-15, which could have been inactivated by the Mos-MAPK pathway (Oh JS et al., 2010). PP2A must be inactivated to dephosphorylate the Cdc25 for the activation to occur (Masatoshi Hara et al., 2013).
- The function of the Mitogen-Activated Protein Kinase (MAPK) pathway will be

discussed in section 1.6.

1.5 The Role of C-Raf in Normal Mouse Oocyte Development

Although Vemurafenib was developed against mutated B-Raf^{V600E}, its relevance is still valid in the normal ovum in relation to C-Raf as indicated by the binding data presented in section 1.2. During fetal development, mouse oocytes are arrested at the G_2 prophase stage of Meiosis I. At the onset of puberty, progesterone-induced meiosis maturation resumption is initiated by GVBD. GVBD is executed by the kinase activity of MPF activation, which is a binding complex of Cyclin B and Cdc2 (Nurse et al., 1998). The Myt1 (Wee1) is an inhibitor of MPF complex in the Meiosis I G_2 stage. Myt1is broken down by Ribosomal S6 Kinase (RSK) under direct activation of extracellular signal-regulated kinase 2 (Erk2) (Palmer et al., 1998). The activation of Erk2 by Mek 1/2 is followed by progesterone-induced Mos synthesis (Nebreda et al., 1993; Sagata et al., 1988). The small inhibitor RNA (siRNA) for Mos mRNA significantly inhibits Mos accumulation and progesterone-induced GVBD (Sagata et al., 1988; Barrett et al., 1990). However, the inhibition will not completely block the downstream MPF activation after the initiation of progesterone stimulation (Fisher et al., 1999). The fact that the MPF activation is not completely blocked indicates a secondary pathway working independently after Progesterone/Mos activation for complete activation of the MPF and the MAPK pathway. Meiotic resumption and GVBD has been shown to elicit insulin and IGF-1 via an RTK/Ras/C-Raf/Mek 1/2 pathway (Sudipta Paul et al., 2009). Blockage of Mos-induced activation of Mek 1/2 in the insulin pre-treated oocyte demonstrated a delayed GVBD rather than an abrupt inhibition (Frederic et al., 2003) and the impairment of the downstream Erk2 and RSK phosphorylation. However, at same time, the phosphorylation of C-Raf is also partially inhibited (Frederic et al., 2003).

At times the dominant-negative (DN) form of C-Raf results in the impairment of the Erk2 activation, Mos induced GVBD, and progesterone-induced meiotic maturation (Muslin et al., 1993). Furthermore, the DN form of Erk2 causes the down-regulation of

C-Raf, whereas over-expression of C-Raf at times accelerates GVBD progression (Shibuya et al., 1996).

A similar result is observed in maternal insulin-resistant mice where the mouse oocytes underwent oxidative stress. The resulting mitochondrial dysfunction led to impairment of oocyte maturation and implantation failure (Xiang-Hong et al., 2012). Mos is the only kinase phosphorylating Mek1, whereas complete Raf phosphorylation is achieved by phospho-Erk2 (Bodart et al., 2005). Thus, the Ras/C-Raf/MAPK pathway acts as an important self-enhancing and self-promoting system.

Barrel shaped spindle apparatus formation and stabilization, correct chromosome alignment, and segregation during in both Meiosis I and Meiosis II divisions are the key indicators of healthy oocyte maturation (Eichenlaub-Ritter et al., 1986). Oocyte toxic compounds are more likely to cause chromosome non- disjunction, meiotic delay and aster star-like spindle formation (Eichenlaub-Ritter et al., 1988). The MAPK pathway plays a pivotal role in meiotic spindle apparatus formation and chromatin organization. The MAPK pathway has been proven to be involved in Microtubule Organizing Center (MTOC) formation in mouse oocyte maturation (Verlhac et al., 1994). The same pattern of distribution has been observed for its downstream effector, RSK (Fan et al., 2003). Several studies have found that in the mouse oocyte, genetic knockouts along the MAPK pathway (like Mos, Erk2) showed a failure to achieve normal spindle assembly (Araki et al., 1996; Bodart et al., 2002; Choi et al., 1996; Zhao et al., 1991). Phosphorylation of p-Rsk substrates, MAPK- interaction, spindle-stabilizing protein (MISS), and DOC1R in mouse oocytes are responsible for microtubule organization and morphogenesis (Lefebvre et al., 2002; Terret et al., 2003). The spatial co-localization of MAPK with the metaphase spindle during meiosis I-to-II transition indicates a close relationship between them in mouse oocyte maturation (Hatch et al., 2001; Lee et al., 2000). Recent research shows that 75% MAPK activity causes a disturbed spindle with dispersed chromosomes, whereas 45% MAPK activity leads to a disintegrated spindle with scattered chromosomes (Wei Cui et al., 2012). This variable activity indicates the importance of the C-Raf enhancing circuit in spindle formation (Wei et al., 2012). A developmental morphology assay was the best means to evaluate toxicity and quality control of Vemurafenib on C-Raf of the cumulus cell free oocyte collection after the PMSG stimulation (Ackerman et

al., 1984). Spindle formation and chromosome alignment examined by IF staining as well as DNA integrity visualized by TUNEL assay were the best assays to demonstrate the consequences of oocyte C-Raf inhibition in oocyte maturation after Vemurafenib exposure (Negoescu A et al., 1998).

1.6 Normal Development of the Embryo

1.6.1 Embryo Development Stages and Morphological Changes

- After fertilization: After approximately 16 to 18h after the oocyte fertilization (sperm-oocyte fusion) and oocyte activation, the pronuclei are visible. The presence of two pronuclei observed under light microscope is perceived as normal fertilization. The number, alignment, distributions, and orientation of pronuclei relative to polar bodies can be used as assessment standards for higher blastocyst formation and implantation rate. For normal zygote development, the chromosomes from each pronucleus are well-aligned in pairs on the newly formed spindle apparatus and are prepared for the first mitotic division. Timing for one cell embryo collection should follow the standard that two pronuclei must be clearly observable. Fang Wu et al. detailed a timeline from pronuclear stages to syngamy formation after hCG injection, finding that the optimal time for the fertilized one-cell collection fell between 26 and 30h post-hCG injection since at that time two pronuclei had reached their largest size(Fang Wu et al., 2008). The first mitotic division cycle seems to consume a longer time compared to its later divisions, averaging 16h more than the second division (Bolton, V. N. et al., 1984; Flach, G et al., 1982; Latham, K. E. et al., 1991). The transition from 1C to 2C appears to be the transition between maternal and embryonic gene expression. Maternal materials from oocyte cytoplasm provide the essential support for meiosis, fertilization and first mitosis and are degraded at the onset of 2C stage (Braude, P et al., 1979; Pratt, H et al., 1983). The two-cell block in some outbred strains has been observed because of glucose

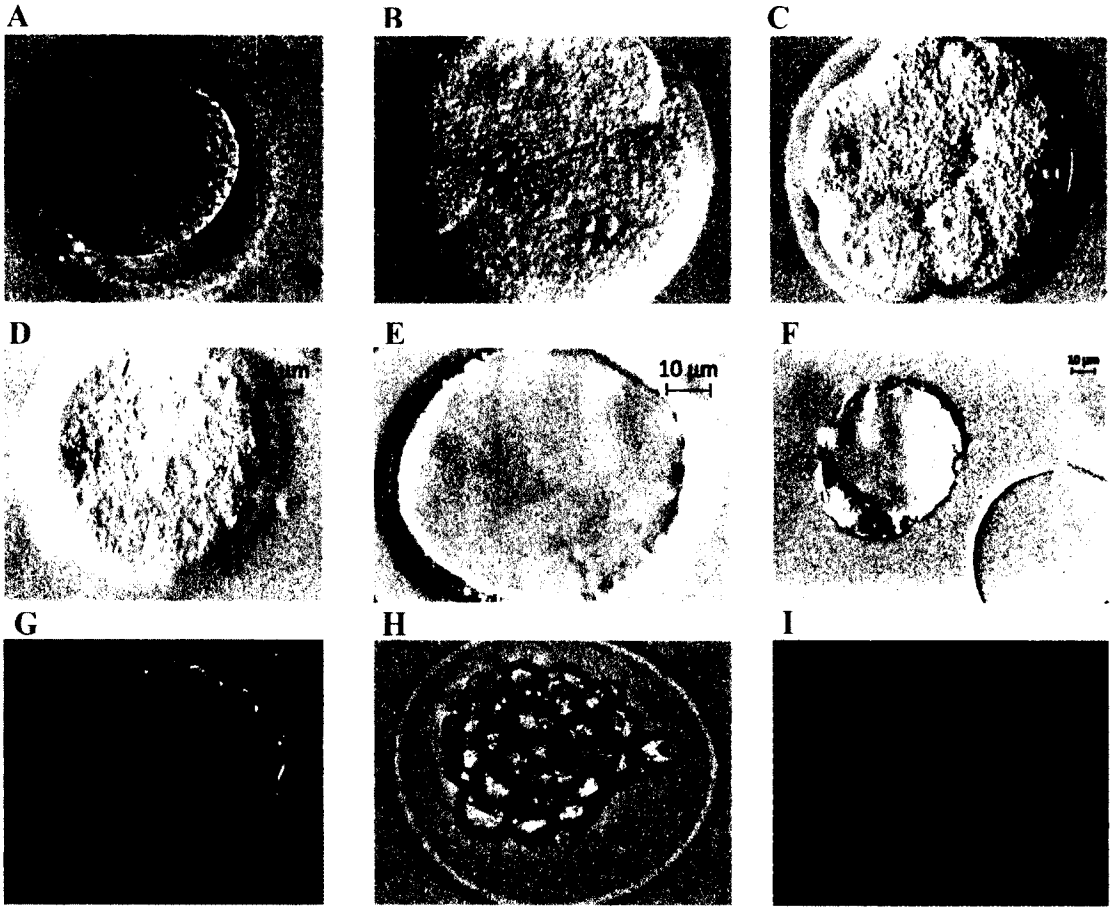

Figure 3. Developmental Stages of Normal and Abnormal Embryos

(A) Zygote embryo: Presence of two pro-nuclei with narrow perivitelline space and two small PBs

(B) 2 Cell Embryo (2 equal-sized blastomeres with narrow perivitelline space and two small PBs).

(C) 8 cell Embryo (8 equal sized blastomeres).

(D) Morula Embryo (cells begin to fuse: semi-circular cell outline with inner semi-circle fused together).

(E) Expanded blastocyst (cyst occupies 2/3 of the zona pellucida enclosed area).

(F) Hatched blastocyst (Blastocyst begins to hatch out of zona pellucida).

(G) Collapsed (deflated embryo after expansion).

(H) Fragmented (Frag: numerous and uneven-sized blastomeres or cytoplasmic blebs).

(I) Degenerated (condensed and granulated blastomeres).

inhibition. Gene expression of the embryo dominates the subsequent mitotic divisions (Flach, G et al., 1982). The embryonic genome expresses transcriptions at approximately 3h after G1 period (Poueymirou, WT et al., 1989; Latham, KE. et al., 1991). The Ras/C-Raf/MAPK pathway plays an important role in this 1C to 2C transition (see section 1.8).

- Cleavage stages: In cleavage stages, embryo cells normally divide into 4 cells on Day 2 and 8 cells on Day 3, with equal-sized cells and no fragmentation. Before the morula stage, single cells, also called blastomeres, is omnipotent and can develop into an individual organism when separated from the zona pellucida-encircled compact morula. Fewer numbers of cells in the corresponding days of the morula is considered as a developmental delay. Blastomere asymmetry, cytoplasmic inclusions, and blastomere multi-nucleation are all considered abnormal embryo development. The perivitelline space is squeezed into a very narrow space. The plasma membrane of blastomeres in the 8-cell stage begins to be connected by the gap junction, which exchanges nutrients and signaling information.
- Morula, blastocyst, and hatching stage: The eight-cell embryo begins to fuse together from the loosely-associated group cells on Day 3.5. The tight association of cells compacted together forms the morula, named from the fruit "mulberry." The cells continuously divide into approximately 30 cells in the zona pellucida. The failure of compaction indicates a loss of viability. A fragmentation outside the cell compact is considered non-viable.
- On the Day 4, the morula begins to differentiate to form a hollow space called blastocyst, which reaches 50~150 cells during the stage. The hollow cavity, or blastocoel, develops from a small chamber to an approximate 120 μM space. The embryo in this expanded space is called an expanded blastocyst. The outer layer of the blastocyst is called the trophectoderm (TE); the inner layer is the inner cell mass (ICM). ICM cells are often considered as pluripotent stem cells. ICM can develop into any cell type (ectoderm, mesoderm or endoderm) and will later differentiate to cells forming various tissues, organs, or extra-embryonic tissues such as amnion and yolk sac. The TE on Day 6, which further differentiates into cytotrophoblast and syncytiotrophoblast, the precursor components of the entire epithelial layer of the

placenta (Knofler M, et al., 2001). Some of the expanded blastocysts may be contracted or collapsed because of the failure of implantation in the medium culture. The collapsed blastocyst is a transient state which can be re-expanded once implanted (Keller G. et al., 2005). Deflating the blastocyst in vitrification becomes a common procedure in embryo cryopreservation.

- On Day 6, the expanded embryo hatches out of zona pellucida (blastocyst hatching or embryo hatching). The embryo-derived plasminogen activator seems to be a proteolytic enzyme participating in the hatching process. The hatched embryo is irregular in its border and ready to implant in the uterus.

1.6.2 Molecular Biology of Embryo Development

From the sperm-oocyte fertilization to an embryo implanted in the uterus, many signaling pathways are involved in embryo development and differentiation. Each signaling pathway is responsible for one or several biological processes (e.g., cell growth, division, migration, apoptosis, and polarity). The signaling pathways in embryo development are an extremely complex network (Figure 9). Little is known about which pathways play a more dominant role.

- MAPK pathways: Four MAPK pathways are involved in embryo development: (1) Ras/C-Raf (see section 1.8), (2) Jun N-terminal kinase (JNK), (3) p38 and (4) Erk5. The JNK and p38 MAPK pathways participate in the 8C to blastocyst stage, while p38 is a filamentous actin regulator (Paliga AJ et al., 2008). JNK and p38 pathways are also required in blastocoel formation during its expansion, since the inhibition of both pathways results in failure of cavity formation (Maekawa M et al., 2005).
- Wnt signaling pathway: The Wnt/β-catenin pathway is inactive until the blastocyst stage of embryo development. β-catenin is located in the nuclei of the ICM. The dorsal side distribution of the β-catenin indicates that Wnt/β-catenin is involved in dorsal-ventral axis formation (Lloyd S et al., 2003).
- PI3k/Akt pathway: The PI3K/Akt signaling pathway is responsible mainly for regulating the cell survival signal activated by growth-factor receptors. In

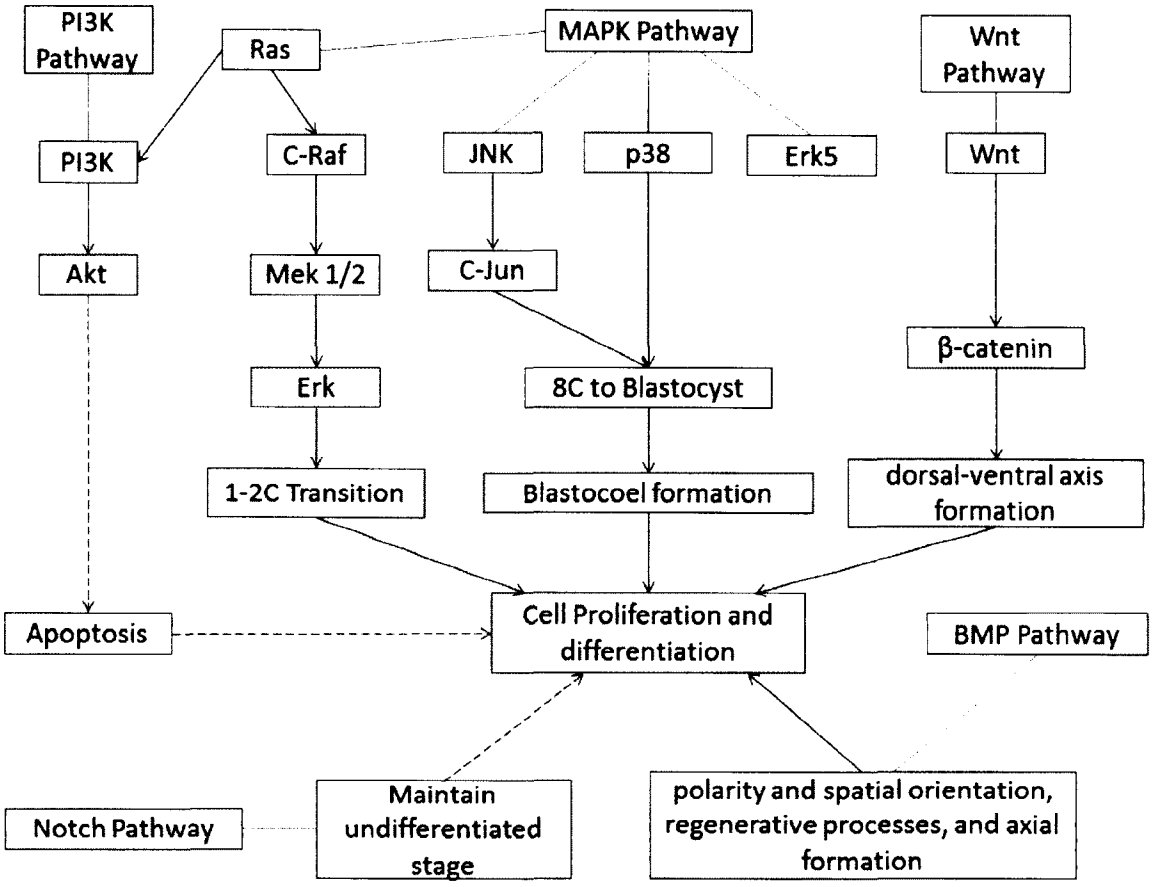

Figure 4. The Complexity of Preimplantation Embryo Signaling Pathway Interactions

The signaling pathways (MAPK, PI3k/Akt, Wnt, Notch, and BMP) involved in preimplantation embryo are performing as a complex network. PI3k/Akt is also activated by Ras, which demonstrates that the growth-factor related growth signal could drive the anti-apoptotic signal, preventing programmed cell death. The Notch dominated differentiation signal can synchronize with the MAPK-dominated growth signal by sharing JNK/c-Jun effectors, whereas the direction of the differentiation is the cooperative product of the BMP, Wnt and Notch pathways. The entire embryo preimplantation development demonstrates a coordination of the pathway network. Both must be present during the embryo development. The red-colored-solid lines indicate the pathways under a certain pathway family. The solid-arrowed lines indicate an direct effect towards the down-stream effector(s). The dash-arrowed lines indicate the indirect effect towards the down-stream effector(s).

preimplantation embryos, the PI3K/Akt pathway suppresses programmed cell death, which could be quickly induced by the PI3k inhibitor (Gross VS et al., 2005). Akt inhibition can also lead to delay of hatching in the preimplantation embryo (Riley JK et al., 2005).

- The Notch signaling pathway: This pathway forces the cell to remain in the undifferentiated stage and prevents its developing into the subsequent stage or other alternative developmental stages (Hansson EM, et al., 2004; Artavanis-Tsakonas S et al.. 1999).
- The BMP signaling pathway: BMP belongs to the TGF-β superfamily and involves in polarity and spatial orientation development of the preimplantation embryo. This pathway is heavily involved in differentiation, regenerative processes, and axial formation (Zernicka-Goetz M et al., 2002).

1.7 The Role of C-Raf in Normal Embryo Development

The Ras/C-Raf/Mek MAPK pathway, which functions as the downstream effectors of the FGF receptor and other Receptor Tyrosine Kinase (RTK) receptors, is one of four MAPK pathways involved primarily in the early embryo and the post-implantation development (Yufen et al., 2005). Ras inhibitions by either siRNA, DN Ras, or Ras mAb halted the mouse embryo in early 2C stage. The fact that such blockage is completely recovered by constitutive transduction of the C- Raf molecule indicates that C-Raf is the downstream effector of Ras in embryo development (Yamauchi et al., 1994). Later experiments showed that phosphorylated C-Raf activation was found in the M-phase-specific cell cycle in early cleavage stage of 2C embryos (Haraguchi et al., 1998). The 2C stage, which acts as the critical reprogramming transition from maternal to embryonic gene transcription and expression pattern (Flach et al., 1982), is a particularly sensitive stage during embryo development (Goddard et al., 1983). Further, the Mek 1/2 and the Erk, downstream effectors of the C- Raf, were shown to be expressed in the preimplantation embryo (Liu et al., 2004). The Erk inhibitor U0126-treated 2C embryos were reversibly arrested at G_2/M transition to the 4-cell (4C) stage and the entire p-Erk-dependent gene expression pattern was altered (Maekawa et al., 2007).

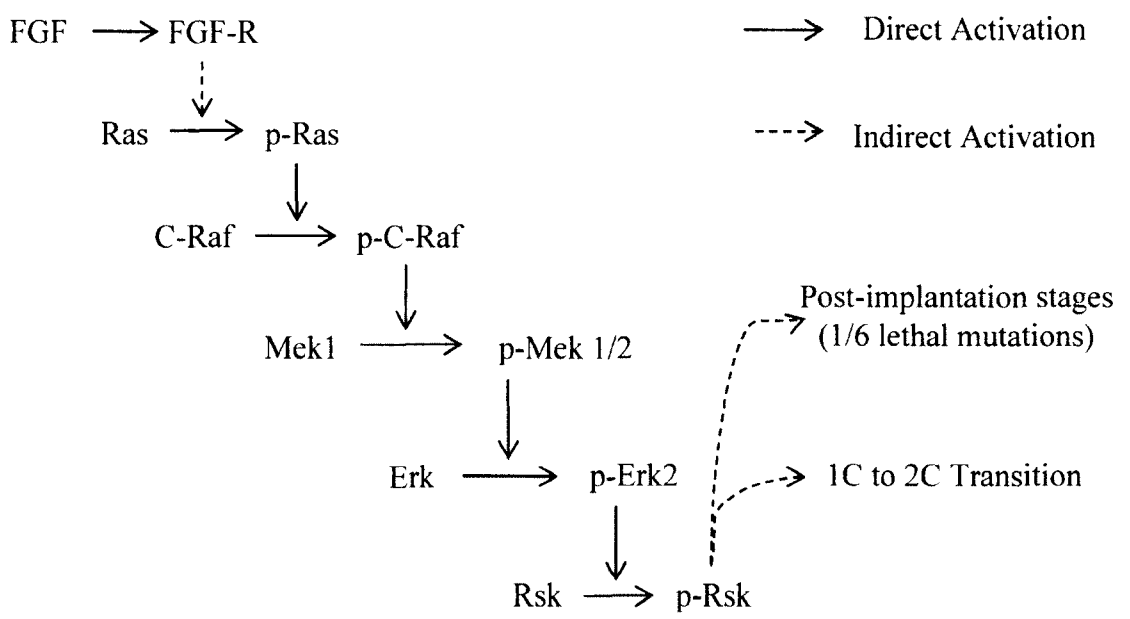

Figure 5. The Role of C-Raf in Normal Embryo Development

C-Raf plays an important role as a mediator in Ras MAPK pathway. The Ras MAPK pathway is involved in both pre- and post- implantation of embryo development. C-Raf is shown to be a key kinase in 1 cell to 2 cell transition and one of six lethal mutations in the post-implantation stages FGF (Fibroblast Growth Factor); FGF-R (FGF Receptor); pRas (Phosphorylated Ras); p-C-Raf (Phosphorylated Raf); p-Mek 1/2 (Phosphorylated Mek 1/2); p-Erk (phosphorylated Erk); p-Rsk (Phosphorylated Rsk).

The same study pointed out that the arrested 4C embryo showed a looser cell-cell adhesion than did the control group. The resumption of embryo development with normal 4-to-8 cell protein expression, driven by other pathways, was offset by adverse effects of loose cell adhesion and finally arrested at the 8-cell (8C) stage (Maekawa et al., 2007). Active pC-Raf in embryonic day 2.5 showed a membrane localization, which indicates C-Raf activates the MAPK pathway from the cell membrane instead of normally from nucleus (Wang et al., 2004).

On the other hand, preimplantation expression of C-Raf also showed several critical influences on post-implantation development. Individuals with vascular defects, including those with placental vascular bed defects, died in middle-gestation because of C-Raf deficiency in the embryonic stage (Wojnowski et al., 1997). Defects in placenta

and liver were observed in embryos possessing C-Raf preimplantation deficiency (Mikula et al., 2001). Later research showed that B-Raf and C-Raf are two of the six lethal null pre-implantation mutations resulting in the pre-implantation or placental lethality (Yufen Xie et al., 2005). Therefore, in this study, an *ex vivo* mouse embryo development study was initiated at the 1C stage to demonstrate potential pre-implantation toxicity. The p-Mek 1/2 *in situ* IF assay for C-Raf kinase bioactivity was performed at 14h after the 1C embryo collection, the optimal time to observe the toxic effect of Vemurafenib on the C-Raf expression in early embryo development.

1.8 The Vemurafenib in Pregnancy, Oocyte Maturation and Embryogenesis

The normal development of the embryo and fetus is perceived as the critical factor in evaluating the toxicity of any anticancer drug therapy. In the only case report available to evaluate the fetal toxicity of Vemurafenib during pregnancy (Maleka et al., 2013). Maleka et al. found that a 37-year-old woman diagnosed with generalized stage IV melanoma initiated Vemurafenib therapy 960mg twice a day during her 25^{th} week pregnancy after wide surgical excision and removal of the sentinel node. She successfully delivered an infant via Caesarian section procedure at the 30^{th} week of gestation and died 3.5 months later with a relapse of cerebral and dural metastasis. During pregnancy, her melanoma mutated -B-Raf^{V660E} was determined and treatment of 9% intrauterine growth retardation (IUGR) had been initiated because of tumor growth. In rapid response to Vemurafenib, the new metastasis disappeared and lactate dehydrogenase reached to the normal line at one month of treatment. The patient complained of the complications of skin itches and exanthema, which disappeared one week after treatment. At the time of delivery, IUGR reached 34% lower than the normal curve, indicating that the rapid response of Vemurafenib did not correct but aggravate the IUGR. The infant received 10.9 μg/mL Vemurafenib drug transmitted through the umbilical cord, compared to 24.3 μg/mL in the patient. This result indicated a possible fetal toxicity of Vemurafenib. However, their report lacks further evaluation of the neurological development of the child. A 30^{th} week premature baby case could not provide adequate testing for the safe use of Vemurafenib in term for pregnancy and

lactating mothers with MM. No risk of congenital malformations can be ruled out if embryogenesis occurs after exposure to cytotoxic drugs. Also, childhood development data of the fetus were not available to rule out certain specific cancer types (e.g., squamous cell carcinoma and KA) resulting from Vemurafenib exposure. Data for fetal and/or childhood organ and systemic differentiations, development, and function were also unavailable. Finally, currently no available animal oocyte and embryotoxicity data exist for Vemurafenib, which is a new first line treatment drug for unresectable MM. Therefore, much research is necessary to evaluate the drug safety of Vemurafenib. In this study, toxicity tests were performed on the mouse embryo development and oocyte maturation upon the exposure to Vemurafenib.

1.9 Innovation

The present study was the first research testing Vemurafenib exposure on mouse oocyte maturation and embryo developmental teratogenicity and toxicities. This research contributes background knowledge of the drug Vemurafenib based on detailed data in developmental morphology, TC_{50} and cytogenic analysis. Since many additional studies will be necessary to ensure that Vemurafenib is free of toxicity and teratogenicity, the current research serves as a reference for future studies on the detailed molecular mechanism of oocyte and embryo toxicity. An understanding of the effects of Vemurafenib on the mouse oocyte and embryo will shed light on (1) further modifications of Vemurafenib by pharmaceutical companies to insure that oocytes and embryos are protected from toxicity and teratogenicity; (2) better therapeutic agent(s) combinations to reduce Vemurafenib toxicity and teratogenicity; (3) normal clinical applications on pregnant, lactating and potentially-pregnant patients with MM; and (4)

unresolvable toxicological or teratogenic issues of Vemurafenib.

1.10 Specific Aims

Aim 1: To determine the toxic developmental effects of the anti-melanoma B-Raf^{V600E} inhibitor Vemurafenib on the ex vivo mouse oocyte (female gamete) maturation, GVBD, spindle formation, chromosomal alignment and DNA integrity.

While the anti-melanoma drug Vemurafenib principally inhibits mutated B-Raf^{V600E} in the MAPK signaling pathway, it also inhibits WT A-, B- and C-Raf monomers *ex vivo* (Bollag G, et al., 2010). However, Vemurafenib transactivates downstream Mek via drug-inhibited Raf dimer *in vivo* (Poulikakos et al., 2011). On the other hand, insulin-like growth factor-1 (IGF-1) induced Ras/C-Raf activation acts as a self-enhancing and self-promoting system in oocyte maturation including GVBD, spindle apparatus formation and chromosomal alignment (Kalma Y et al., 2004, Qing-Yuan Sun et al., 2009). Either activation or inhibition may cause significant adverse effects on later oocyte meiosis MII arrest formation. However, Vemurafenib toxicity on oocyte maturation is unknown. Therefore, mouse oocytes were stimulated and produced by an injection of pregnant mare serum gonadotropin (PMSG). Both female mouse ovaries were punctured, and oocytes were collected with cumulus cells stripped. Vemurafenib was directly exposed to cumulus-cell denuded oocytes at serial dilution from 0.01 μM to 100 μM. Developmental morphology was analyzed by inverted microscopy from the GV-intact oocyte to GVBD to the Meiosis MII stage oocyte by evaluating the point of 50% Toxic Concentration (TC_{50}). Spindle formation and chromosomal alignment were analyzed by IF staining. DNA integrity of the oocyte was visualized by the TUNEL assay.

Aim 2: To determine the effect of anti-melanoma B-Raf^{V600E} inhibitor Vemurafenib on preimplantation embryo development when exposed *ex vivo* from the 1C to hatching stages at the cellular level.

C-Raf plays an essential role in early 2C stage and post- implantation development in mouse embryos (Wang et al., 2004). Either activation or inhibition causes significant adverse effects in later embryonic and fetal development. Because the 1C stage embryo is considered to be vulnerable and sensitive to the surrounding environment, 1C mouse

embryos were produced by a superovulating injection of PMSG followed 48h later by an injection of human chorionic gonadotropin (hCG). 1C embryos with two prominent pro-nuclei were irrigated from oviducts excised after cervical dislocation (CD) euthanized plug-positive female mice between 26 to 30h post-hCG injection. Vemurafenib at concentrations from 0.01 μM to 100 μM were introduced into the culture medium for up to 110h incubation period for this *ex vivo* experiment. Thus, Vemurafenib was directly exposed *ex vivo* to 1C embryos for the entire culture period. Cell development morphology was evaluated and TC_{50} was calculated. Embryo C-Raf bioactivity at the two-cell stage after drug exposure was semi-quantified by a p-Mek 1/2 *in situ* IF assay.

Aim 3: To determine the effect at the cellular level of the anti-melanoma B-Raf^{V600E} inhibitor Vemurafenib on preimplantation embryo development from 2C to hatching stages when the gamete was exposed *in vivo* in the dam's i.p. cavity injection before mating and embryo collection but not exposed to the drug after embryo collection.

This group of superovulated mice was pre-injected in 7 doses i.p., with Vemurafenib (10 mg/kg) *in vivo* twice daily. The first injection was administered at 24-hour post-PMSG injection; the final dose was administered at 36-hour post-hCG injection). Females were placed with a fertile male immediately post-hCG injection until a positive vaginal mucous plug was observed. Two-cell embryos were collected 42h post-hCG injection with the same procedure as in Aim 2. Two-cell embryos were then cultured in either a drug-free medium for either control, or the 10 mg/kg experimental Vemurafenib concentrations, and observed up to 96h after collection. Cell division and morphology were evaluated under inverted microscopy and a TC_{50} was calculated.

CHAPTER 2

MATERIALS AND METHODS

2.1 Experimental Design

Determination of the toxicity of the anti-melanoma B-Raf^{V600E} inhibitor Vemurafenib to mouse oocytes and embryos provides an essential understanding for clinical physicians to benefit newly pregnant, lactating and potentially pregnant women with malignant melanoma (MM) who are urgently expecting and seeking effective medications. This novel research protocol also provides instructions for the physicians' prescriptions during their clinical practice as well as new directions for clinical researchers on the developmental evaluation, toxicity mechanism and combinational therapies for the drug. In order to test the hypothesis that Vemurafenib has detrimental effects on the oocyte maturation and/or embryo development, three major experiments were conducted as follows:

2.1.1 *In vitro* Oocyte Maturation Quality Control Assay

To determine the potential toxic developmental effects of anti-melanoma B-Raf^{V600E} inhibitor Vemurafenib on *ex vivo* mouse oocyte maturation from (1) GV-intact oocyte to (2) GVBD to (3) MII arrest, (4) spindle apparatus formation, (5) chromosomal alignment and (6) DNA integrity.

Experiment 1: Analysis of Vemurafenib toxicity on oocyte cell cycle progression during oocyte maturation resumption.

- Morphological evaluation of the dose-dependent serial dilutions of Vemurafenib toxicity on mouse oocyte maturation progression.
- Determination and evaluation of the TC_{50} and the effect of Vemurafenib on mouse oocyte maturation progression.

Experiment 2: Spindle formation and chromosome alignment IF Staining:

- Morphological and cytogenic analysis of spindle apparatus formation and chromosomal alignment were performed after exposure of Vemurafenib serial dilution.

Experiment 3: TUNEL assay for DNA integrity:

- DNA integrity of oocytes after Vemurafenib exposure was examined by DNA TUNEL assay for detecting oocyte DNA fragmentation.

2.1.2 *Ex vivo* 1C Mouse Embryo Development Quality Control Assay

To determine the effect of Vemurafenib on the embryo development from 1C to preimplantation hatching stage at cellular and subcellular levels of *ex vivo* embryos by the mouse embryo toxicity assay.

Experiment 1: Analysis of Vemurafenib toxicity with pre-implantation embryos on cell cycle progression during embryo development.

- Morphological evaluation of dose-dependent serial dilutions of Vemurafenib toxicity on mouse embryo development progression to the hatching (H) stage.
- Determination and evaluation of the TC_{50} and the effect of Vemurafenib on mouse 1C embryo development to H stage.

Experiment 2: Semi-quantification of the Embryo C-Raf bioactivity by p-Mek 1/2 *in situ* IF assay.

- Determine the overall C-Raf bioactivity of the 2C embryos after exposure to Vemurafenib.

2.1.3 *In vivo* Mouse Embryo Development Quality Control Assay

To determine the *in vivo* effect of anti-melanoma B-Raf^{V600E} inhibitor Vemurafenib on embryo development from 2C to H stage at the cellular level when the gamete was

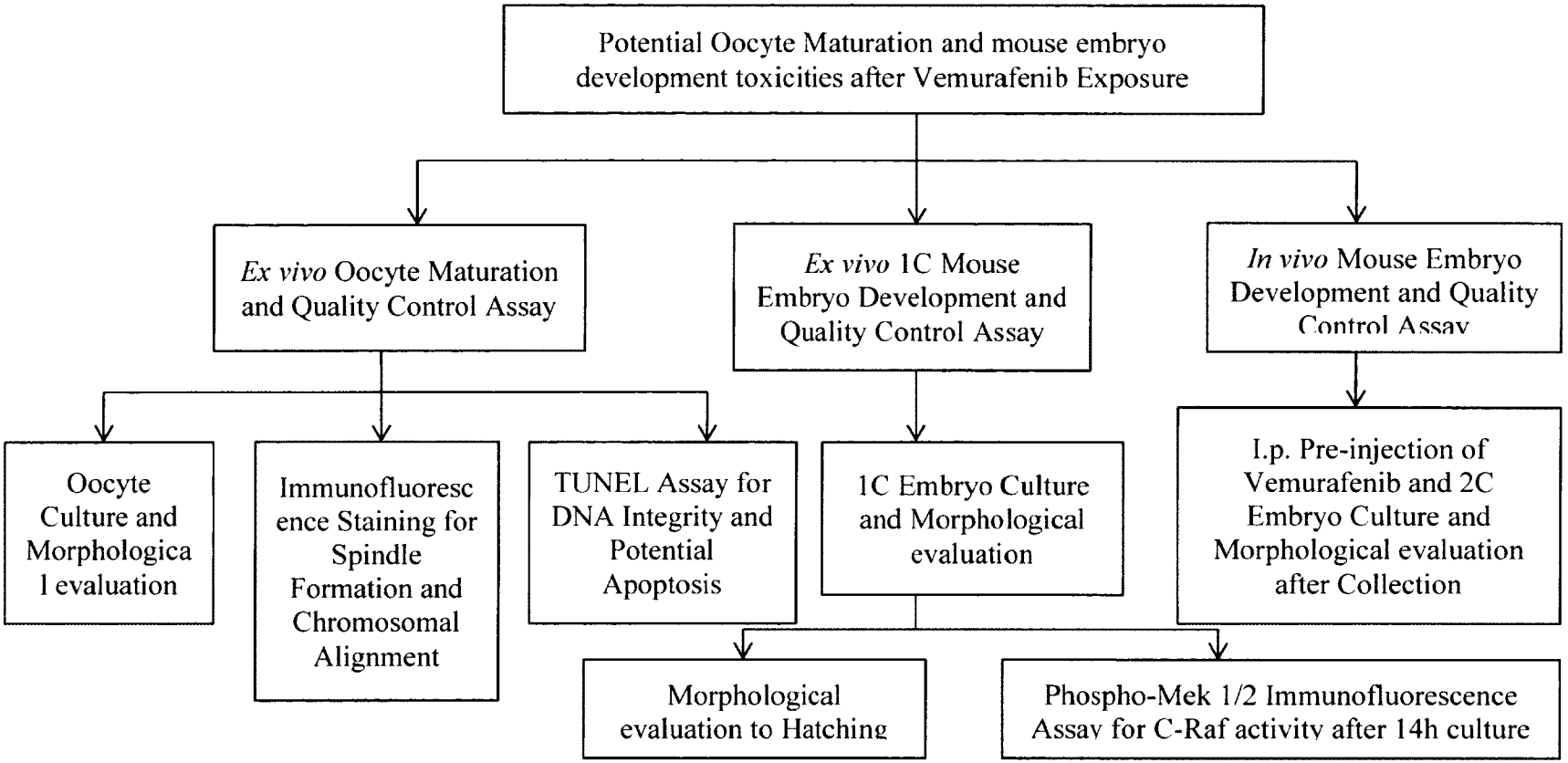

Figure 6. Experimental Design Flow Chart

In order to test the potential toxicities of Vemurafenib exposure on mouse gametes and embryos, *ex vivo* oocyte maturation and quality control assay was performed for morphology, immunofluorescence and TUNEL. The *ex vivo* 1C mouse embryo developmental and quality control assay was performed for morphology and p-Mek 1/2 IF to assess toxicity after Vemurafenib exposure. The *in vivo* mouse embryo assay took place with the pre-injection of Vemurafenib to mimic the actual clinical use of Vemurafenib. Morphological evaluation of the 2C embryo was examined.

exposed *in vivo* in the dam's i.p. cavity before mating and embryo collection but not exposed to the drug after embryo collection.

- Determination of *in vivo* therapeutic dose (10 mg/kg) effects of Vemurafenib on the overall mouse embryo development from oocyte maturation to embryo H stage.

1.2 Animals

The female B_6CBAF_1/J mice (C57B6 male/CBA female, both inbred) (Jackson Laboratory, Bar Harbor, ME, USA) were used in all experiments. The male CD1 outbred mice (Charles River Laboratories, Wilmington, MA, USA) were paired for mating in both *in vitro* and *in vivo* mouse embryo developmental assays. Animal health is critical for optimal reproductive results. Mice must not be stressed by constant exposure to noise, wet bedding, improper light cycle, or extreme temperature fluctuations. Upon arrival in the animal facilities of the Innovation Research Park Building 2 (IRP-2) at Old Dominion University, no more than five female mice were placed per cage with a minimum of 97 cm^2 floor area per animal and 13 cm height. The male mice were housed individually in similar caging. Purina 5001 laboratory rodent diet and water were freely accessible and provided *ad libitum*. Room temperature was maintained between 22-24°C (~74F), with 14 hour light/10 hour dark natural cycle for experiments which matches our exogenous hormonal superovulation timeline.

2.2.1 Justification of Animal Use

- Mouse oocyte and embryo developmental cultures are exquisitely sensitive to toxic compounds, chemicals and drugs. (Ackerman et al., 1984).
- The female B_6CBAF_1/J and male CD1 mouse strains (see section 2.2.2) are a well-established and commonly paired animal model for mouse oocyte maturation and embryo developmental quality control tests with a large volume of publications.
- Mouse oocyte maturation and embryonic development up to pre-implantation stage closely reflects the corresponding stages of the human embryo and can predict the successful *in vivo* fertilization (IVF) of the human embryo.

- The superovulation method in this paired mouse model produces a large collection of oocytes and embryos per female mouse significantly reducing the number of animals consumed by sequential PMSG and hCG hormonal stimulating injections.
- This work, begun in 1980, is a continuation of research on oocyte maturation and embryo developmental toxicity using the mouse model.

Experiments and animal use protocols were approved by the Institutional Animal Care and Use Committee (IACUC) (Assurance 13-011) at Old Dominion University. Euthanization by cervical dislocation (CD), approved by the American Veterinary Medical Association (AVMA), was used to eliminate the confounding factors of CO_2, Na-pentobarbital, isoflurane or other compounds during embryo and oocyte collection. No carefully-crafted simulator could mimic the cooperative complexity of oocyte maturation and embryo developments and differentiation that occurs in the biological whole-animal model. No cell culture, computer program, invertebrate or other lower species could substitute for the mouse oocyte and embryo toxicity test.

2.2.2 Justification of the Animal Selection

Consistent mouse strain use is important to the success of assays conducted in the laboratory. Embryos from different strains behave differently during culture. Culture conditions that are ideal for one mouse strain or combination of pure strains may not be acceptable for different purposes. An animal strain is considered an inbred strain when it has been maintained by brother with sister mating or offspring with parent mating for a minimum of 20 consecutive generations. The result is a genetically defined strain nearly homologous in every way, aside from the difference of sex chromosome contribution.

The B_6CBAF_1/J strain of mouse is the hybrid result of breeding two different inbred mouse strains (CBA/J males and C57B6/J (B6) females). The coat color of these animals is agouti. The strain designation for male stud mice used in all experiments was CD1, an outbred albino mouse (ICR) strain.

Consistency of animal strains is essential to the uniformity of assay results. Because females of a hybrid strain are crossed with CD1 males from an outbred strain, embryos of this inbred/outbred cross are unpredictable and completely unsuitable for further use. If a

plug-negative female is actually pregnant, the offspring should be removed and euthanized prior to reproductive competency. Because embryos from our chosen mating-pair hybrid strain (B_6CBAF_1/J crossed with CD1) do not exhibit the 2C block in development, these embryos can be used in both the 1C and 2C stages which gives us some control over embryo variability throughout all experiments in this study.

2.2.3 Animal Mating Conditions

Generally, weanling animals at four weeks of age have the best oocyte and embryo production. Stud males must be a minimum 9 weeks of age before being placed into service and may require several trial matings before producing high-quality embryos. Non-plugged superovulated female mice were put into separate cages and recycled for use after two weeks' rest. An individual female mouse superovulated more than three times without having a positive plug was removed from the colony and euthanized by CD. Males failing to mate over four consecutive opportunities were removed from the colony and euthanized by CD. Both strains over 10 months in age were removed from the colony. Successful mating will produce vaginal plug rates ranging from 70-100 percent and oocyte and embryo production will average 20 and 25 respectively per female. These figures will vary in relation to stability of the animal facility, quality of the hormone, age and health of the males and females, seasonal timing, and strain of mouse used, as well as other lesser factors. Reconstituted hormones can be reliably stored at -20°C for approximately 12 months without significant reduction in biological potency.

2.3 Reagent Preparation

2.3.1 Vemurafenib Solutions

Ex vivo mouse oocyte maturation and embryo developmental assays with Vemurafenib 100X stock solution and *in vivo* 10 mg/kg mouse embryo assay injection solutions were prepared.

According to the FDA drug evaluation and research report, both crystalline solid and

form II Microprecipitated Bulk Powder (MBP) of Vemurafenib has poor aqueous media solubility at 37°C of less than 0.26 mg/1000mL and thus a low bioavailability. While preparing the solutions, white insoluble particles formed in modified Krebs bicarbonate-buffered medium (mKBB) or M16 medium due to this insoluble characteristic was precipitated at the bottom of each well during culture in the 96-well Falcon sterile culture plate (Cat No. 353072, Fisher Scientific). Heating to 56°C and stirring the mKBB or M16-Vemurafenib particle mixture did not increase solubility of the drug. Filtering a 200 mL lot through a 0.22 μm filter unit (Nalge NUNC) to remove any microorganism contamination during solution preparation caused complete blockage of a white particle film on the filter. The final concentration of the drug was lowered and varied from well to well, which did not reflect the actual potential toxicity or teratogenicity of the drug and significantly decreased the authentication of test result. In polar dimethyl sulfoxide (DMSO), a sterile liquid solvent, the dissolvability of Vemurafenib reaches nearly 98 mg/mL. When DMSO is placed in the culture media up to 2% v/v concentration it shows no significant change in the survival rate with cultured embryos. One caveat is that DMSO is a potent stress proteins inducer (Hallare A et al., 2006). Ten mg Vemurafenib powder was dissolved in 204 μL of sterile DMSO (Sigma) and sequentially dissolved in 204 mL of mKBB or M16 medium with a final concentration of 100 μM/L (100X) with 0.1% DMSO as stock solution. M16 and mKBB media both have penicillin and streptomycin supplement, but the solution preparation procedure took place in a laminar flow hood to guarantee solution sterility. The 100X stock solution of Vemurafenib was serially diluted 1:10 for the lower concentrations in both *ex vivo* oocyte maturation and 1C embryo development assays. One mL of the higher concentrated solution was mixed with 9 mL of mKBB or M16 medium to make the lower concentration solutions. For the *in vivo* mouse embryo assay, the 10 mg/kg Vemurafenib stock solution was made by sequentially dissolving 10 mg Vemurafenib into 8 μL DMSO and then into 8 mL mKBB or M16 solutions. The maximum volume for mouse i.p. injection was 200 μL per injection and the solution was cloudy without being fully dissolved. During dilution

procedures, vortexing was used to assure the final concentration at the lower doses.

2.3.2 Modified Kreb's Bicarbonate Buffer (mKBB) Medium, Microtubule Stabilizing Buffer (MTSB) and Immunofluorescence Blocking Buffer Preparations

- The mKBB medium preparation (Ackerman, S et al., 1983): The mKBB was

Table 1. Components of the mKBB Medium (400 mL)

Components	Cat. No.	Volume (g)	Final Concentration (mM)
NaCl	S5886, Sigma	2.1996	94.0900 mM
KCl	P5405, Sigma	0.1424	4.7800 mM
$CaCl_2.2H_2O$	C7902, Sigma	0.1008	1.9200 mM
KH_2PO_4	P5655, Sigma	0.0644	1.1800 mM
$MgSO_4$	M2643, Sigma	0.0572	1.1900 mM
$NaHCO_3$	S5761, Sigma	0.8436	25.1100 mM
DL-Lactate	L4263, Sigma	1.6 mL	3.3 µL/mL
Sodium Pyruvate	P2256, Sigma	0.0220	0.5000 mM
D-(+)-Glucose	G7021, Sigma	0.4000	5.5500 mM
BSA (fraction V)	A4503, Sigma	1.6000	4.0000 mg/mL
Pen/Strep (5k IU)	P0781, Sigma	4.0 mL	50.0 IU/mL

prepared fresh each month by using the formula in Table 1. Each new batch of medium was tested using the 2C mouse embryo assay to reach at least 85% passing rate. A Mettler analytical balance (Model No B214825957, Mettler) and stir bar were used with constant stirring while adding ingredients to approximately 150 mL of Milli-Q deionized water in the listed order on the preparation formula. After adding all dry and wet ingredients, including BSA, to the mixture was stirred until

the protein was fully dissolved. The medium was transferred into a 200 mL Class A volumetric flask for final volume by adding water up to the 200 mL line.

This medium was subjected to filtration through a 500 mL, 0.22 μm Nalgene filter. The first three filtration passes used approximately five milliliters as a filter rinse before filtering the remainder for use. The initial 10-15 mL rinse fluid was used for osmolality and pH measurements. The medium pH was between 7.7 and 8.0 as measured by Mettler SevenCompact pH meter Ion S220 (Serial No. B2026211682, Mettler). The osmolality was between 270 and 300 mOsm/kg H_2O (Advanced® model 3250 single-sample, freezing point depression osmometer). If the osmolality was above 300 mOsm/kg H_2O it was brought down according to the following formula:

$$V_2 = \frac{(mOsm_i - mOsm_d)}{mOsm_i} x V_1$$

Where the $mOsm_i$ = the initial osmolality; $mOsm_d$ = the desired osmolality; V_1 = volume of the medium sample, and V_2 = the volume of the medium to be removed then replaced with the same amount of H_2O respectively.

Table 2. Microtubule Stabilizing Buffer (MTSB) Preparation (100 mL)

Components	Cat. No.	Volume	Final Concentration
PBS	P5493, Sigma	97 mL	1X
PIPES	P6757, Sigma	3.02400 g	100.0000 mM
$MgCl_2$	M8266, Sigma	0.02605 g	5.0000 mM
Triton X-100	X100, Sigma	1.0 mL	1.0%
Formaldehyde	F8775, Sigma	2.0 mL	2.0%
EGTA	E3889, Sigma	0.09506 g	2.5000 mM

- For embryo culture, the protein supplement mirrors the human plasma physiology which is approximately 4 mg/mL. This protein supplement reduced the adhesive characteristic of oocytes and embryos, blocked the electrical charges on the outer surface of the cells and provided a secondary source of amino acids. While performing experiments, all media was overlaid with toxicity-negative light mineral oil. The oil provided a physical barrier to prevent the medium from evaporation with osmolality increase. Oil also increased the time of CO_2 equilibration so mKBB and M16 media were pre-incubated at least 24h before each experiment. M2 medium was HEPES-buffered and did not need the 24-hour pre-incubation. Media were not kept in incubator more than 3 days due to ammonia accumulation from protein breakdown.
- The MTSB solution preparation: The MTSB solution for the oocyte fixation and permeation in the *ex vivo* oocyte maturation assay was prepared in accordance to Table 2 (Eichenlaub-Ritter, U, 1986, 1989; Soewarto, D et al., 1995). Fixation and permeation is the key step in stabilizing the depolymerization process of the spindle apparatus. EGTA acts as the chelating agent for blocking calcium related bioactivities like apoptosis. Triton X-100 permeates the unfixed (or lightly fixed) oolemma and decreases the surface tension of the MTSB solution during IF staining. Formaldehyde cross-links and denatures the cytoplasmic and nuclear proteins, including histones, and chromosomal DNA. The pH was adjusted by PBS to the final volume.
- IF blocking buffer preparation: Blocking buffer was prepared according to Table 3 for blocking the reactive antigens and reducing the background stain in the IF staining process. Universal blocking of the mouse-derived miscellaneous antigens was accomplished with mouse serum, BSA and non-fat dry milk. And the sodium azide is bacteriostatic, stopping bacterial growth. The pH was adjusted by PBS to

Table 3. IF Stain Blocking Solution (100 mL) (Liu, L et al., 2002)

Components	Cat. No.	Volume	Final Concentration
NaN_3	S2002, Sigma	0.0200 g	0.0200%
Triton X-100	X100, Sigma	0.01 mL	0.01%
Glycine	50046, Sigma	0.75070 g	100.0000 mM
Mouse Serum	M5905, Sigma	2.0 mL	2.0%
Non-Fat Dry Milk	M7409, Sigma	0.2000 g	0.2000%
BSA	A4503, Sigma	2.0000 g	2.0000%
PBS	P5493, Sigma	97.99 mL	1X

Table 4. Component Differences Between M16 And M2 Media in g/L

Components	M16 concentration	M2 concentration
NaCl	5.53193	5.53193
KCl	0.35635	0.35635
$CaCl_2 \cdot 2H_2O$	0.25137	0.25137
KH_2PO_4	0.162	0.162
$MgSO_4$	0.1649	0.1649
$NaHCO_3$	2.101	0.35
DL-Lactate	2.95	2.95
Sodium Pyruvate	0.0363	0.0363
D-(+)-Glucose	1	1
BSA with FV	4	4
HEPES	N/A	5.42726

the final volume.

2.3.3 Difference of M16 and M2 Media

Both M16 (Cat No. M7292, Sigma-Aldrich) and M2 (Cat No. M7167, Sigma-Aldrich) media are the most commonly used media for *in vitro* culture for oocyte maturation and pre-implantation embryo development. The difference of the composition is shown in Table 4.

Both of them contain the components of modified Krebs-Ringer bicarbonate buffered medium, which is very similar to Whitten's medium. Both M2 and M16 include lactate and pyruvate which is benefit for the early stage of the embryo development since embryo in this stage does not utilize glucose efficiently, whereas the M2 medium is the modified version of the M16 medium by substituting some sodium bicarbonate with HEPES buffer which is an intracellular phosphate buffer. Therefore, M16 medium is suitable for the CO_2 incubator culture to mimic the true fallopian tube environment. M2 is suitable for extended operations and procedures outside the incubator like oocyte recovery and 1C embryo collection. Both of them add phenol red as the indicator for pH change and are stored in the refrigerator.

2.4 Toxicity of Vemurafenib on *Ex Vivo* Oocyte Maturation and Quality

While gametes and embryos in childbearing mothers with the B-Raf mutated MM would have a very low probability of having a simultaneously mutated C-Raf, the mouse gametes and embryos without the mutation successfully circumvent the development retardation bias caused by the malignancy cachexia while testing drug toxicity. Therefore, a mouse without this mutation in gametes and embryos should be an accurate model for determining the drug's toxicity. Female B_6CBAF_1/J mice were chosen for their continuity of 1C to 2C transition without blockage which excluded the blockage bias caused by other mouse strains. Oocyte follicular growth was over stimulated by the PMSG and primary oocytes were recovered by puncturing the large antral follicles. Cumulus cells were gently striped away. Denuded oocytes with an intact GV were

collected and tested in different concentrations of Vemurafenib. The control group was treated exactly like experimental groups but without Vemurafenib. Since the Vemurafenib could only be dissolved in the DMSO with 0.1% final concentration, a control group with 0.1 % DMSO medium solution was simultaneously tested. After 16h culture, the number of GV intact, GVBD, MII arrested and fragmented/degenerated oocytes were recorded. TC_{50} was calculated. Oocyte cellular and subcellular levels of cell morphology were analyzed by IF staining on spindle formation and chromosomal alignment. Also, the DNA integrity was visualized by TUNEL assay. Experiments were run in triplicate.

2.4.1 Mouse Oocytes Recovery Procedure

Eight female B_6CBAF_1/J mice (Jackson Laboratory) 4-week-old to 6-month-old were i.p. injected with 0.1 mL (5 IU) PMSG (Cat. No. G4877, Sigma -Aldrich) to stimulate the ovarian follicular growth. After 48h post-injection, mice were euthanized by cervical dislocation (CD). The ovaries with fat pads were carefully removed with sterile scissors and watchmaker forceps (Cat. No ST-JFC-7, ASSI). The ovaries were transferred to a 35 mm petri-dish (Cat. No 134738, NUNC) with 3 mL of M2 medium (Cat. No. M7167, Sigma-Aldrich) supplemented with penicillin/streptomycin 120 U/mL (Cat. No P4333, Sigma-Aldrich) pre-warmed in a Nuaire AutoFlow NU-4750 Water Jacket CO2 Incubator (Cat No NU4750, Nuaire). The M2 medium was overlaid with 2 mL of toxicity negative mineral oil to prevent the osmolality change from water evaporation. Under a Zeiss Discover V8 Stereo Dissecting Microscope (Serial No. 3911005189, Zeiss), the large antral follicles were punctured through by using a 1mL syringe (Cat. No. 02G088A, Norm-Ject) with 30-gauge/½-inch needle (Cat. No. 305106, B-D). Oocytes were either (1) gently aspirated in and out of a Stripper® (Cat No. MXL3-STR, Origio) to strip off the surrounding cumulus cells. The denuded oocyte with the intact GV (Diameter = 70~80um) were collected and transferred to the M2 medium. Nude oocytes found before stripped by micropipettes were discarded for the possible maturation prior collection because of the loss of the inhibitory cumulus

cells maintaining the G2 prophase arresting state.

2.4.2 Denuded Oocytes Cultured with Various Vemurafenib Concentrations

Vemurafenib was dissolved in the sterile DMSO (Cat No D8418, Sigma-Aldrich) and sequentially added to the M16 medium to a final concentration of 100 μM/L in 0.1% DMSO, as the stock solution. The Vemurafenib serial dilutions in each well was created by a serial dilution ratio of 1:10 producing 10 μM/L, 1 μM/L, 0.1 μM/L, and 0.01 μm/L concentrations. To maintain blind evaluation of data by Investigator I, Investigator II dispensed and coded the different concentration solutions into two 4-well Falcon dishes (Cat No. 08-772-1B, Fisher Scientific) without identifying the codes. Denuded oocytes from each mouse were assigned into wells containing a final volume of 0.8 mL mKBB medium with each serial dilution of the Vemurafenib. One control oocyte group was cultured with 0.8mL of mKBB medium without Vemurafenib. The other control oocyte group was cultured with 0.8mL mKBB in 0.1% DMSO. All oocytes were cultured for 16h at 37°C; 5% CO_2; and 100% humidity. Both experimental and control oocyte groups were assigned to wells in 20 min intervals to ensure that oocytes were synchronously developed in each well, which accounted for the handling time interval.

2.4.3 Oocyte Development Morphological Evaluation

After 16h *in vitro* culture, the number of oocytes from the lowest to highest developmental stages in all groups were counted and evaluated. Four developmental stages were defined as the following: (1) GV: Oocytes with an intact GV and prominent nucleolus are arrested at the Meiosis I G2 prophase stage of the cell cycle; (2) GVBD, MI: The meiotic resumption which oocytes experience with GV disintegration in Metaphase of meiosis I; (3) MII-arrest: Oocytes progress to MII arrest of meiosis II after expelling the first polar body (PB1). (4) Fragment (Frag): Various and uneven-sized

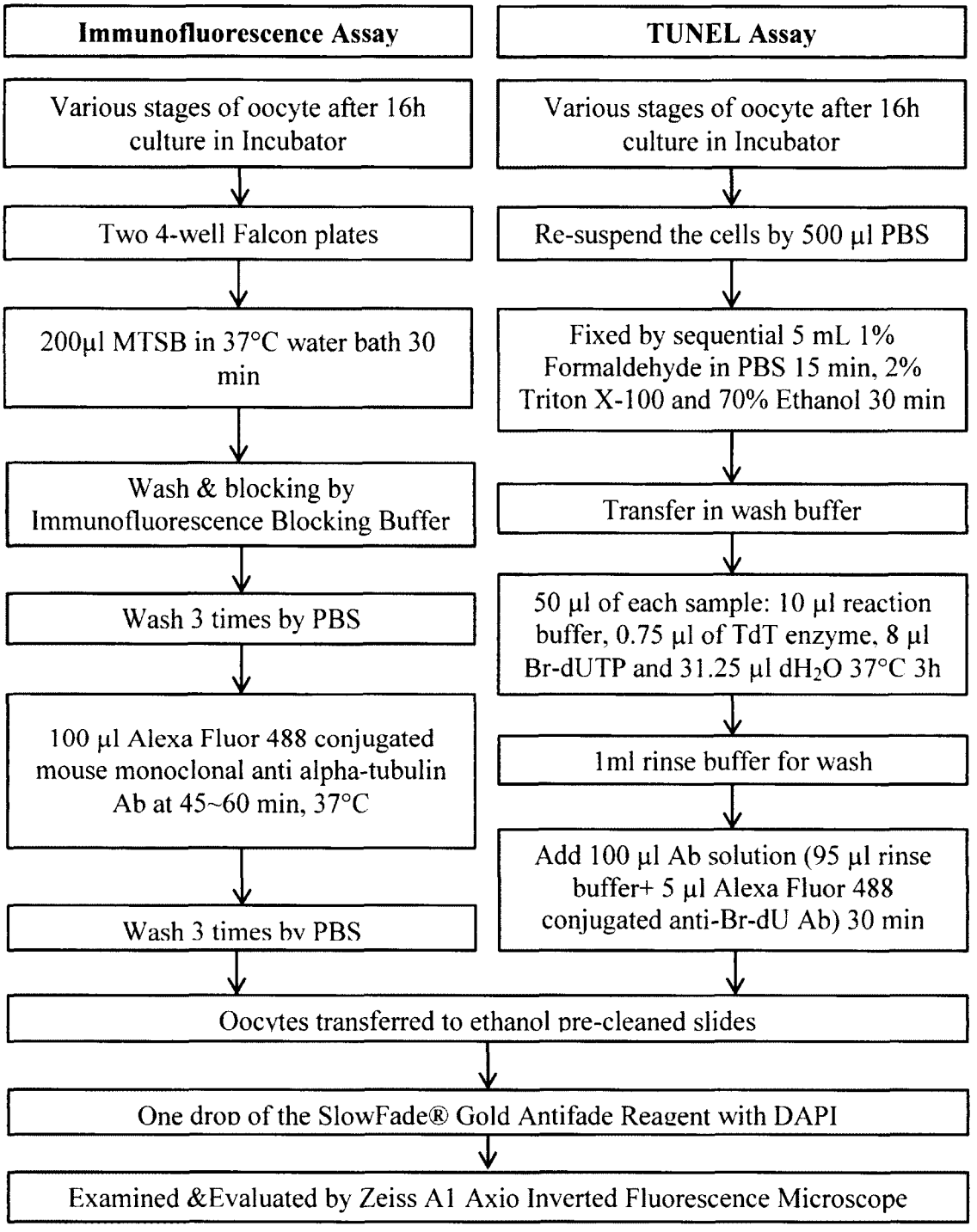

Figure 7. The Flow chart of IF and TUNEL assay

The staining procedure conducted was classical direct immunofluorescence staining. TUNEL assay procedures were followed through Life Technologies APO-BrdU™ TUNEL Assay Kit manual instruction.

Table 5. Oocyte Developmental Stages Definition

Stages	Definition
GV	Oocytes with an intact germinal vesicle and prominent nucleolus are arrested at the Meiosis I G2 prophase stage of the cell cycle.
GVBD or MI	The meiotic resumption which oocytes experience with GV disintegration in Metaphase of meiosis I.
MII-arrest	Oocytes progress to MII arrest of meiosis II after expelling the first PB.
Frag.	Fragmented: Various and uneven-sized cytoplasmic blebs.
Deg.	degenerated: condensed and granulated blastomeres

cytoplasmic blebs. Investigator II decoded the concentrations after IF staining, and recording of data by Investigator I. The TC_{50} is defined as a Vemurafenib concentration at 16h which (1) inhibits 50% of the oocytes from showing a metaphase plate or expelling the first PB; (2) causes DNA damage, (3) shows disoriented spindle formation; and/or (4) shows chromosome misalignment. Nontoxic concentration (NC) is defined as a lack of statistical difference on oocyte maturation to meiosis II arrest upon exposure to Vemurafenib compared with the control group. Normally, at least 85% of the oocytes will extrude the first PB within 16h culture in an *in vitro* control group (Eichenlaub-Ritter, U, 1995). Four developmental stage images were captured through a Zeiss Vert A1 Axio inverted research microscope fitted with a Zeiss AxioCam ICm1 camera unit (Cat. No. 426113, Zeiss). Oocytes images of each stage were photographed with an Axio Version Special Edition 64 bit Release 4.9.1 software (Zeiss).

2.4.4 IF Staining and Microscopy for the Cytological Analysis

Vemurafenib-exposed oocytes and two control group oocytes progressing to GVBD with PB (meiosis II arrest) or without PB (meiosis I arrest) were stained in separate wells of two 4-well Falcon plates through direct tubulin and chromosome IF labeling to

examine the spindle formation and chromosome alignment. The entire staining procedure was conducted at room temperature unless otherwise specified. Oocytes were fixed and permeated in each well 30 min in a 37°C water bath by a 0.8 mL Microtubule-stabling buffer (MTSB) (Eichenlaub-Ritter, U, 1986, 1989; Soewarto, D et al., 1995). The oocytes were then washed and blocked in a 4°C moist chamber overnight by a blocking solution (Liu, L et al., 2002). Oocytes were washed in a 0.8 mL PBS and incubated in darkness with 200 μL of Alexa Fluor 488 (Ex/Em=495/519 nm) conjugated mouse monoclonal anti alpha-tubulin antibody (1:20~1:40 PBS, Cat No. 322588, Life Scientific) 45-60 min in a 37°C water bath. Oocytes were washed in a 0.8 mL PBS and transferred to ethanol pre-cleaned slides. One drop of the SlowFade® Gold Antifade Reagent with DAPI (Cat No. 36939, Life Scientific) was added to each slide in darkness for 15-20 min or overnight at 4°C for chromosome staining. Slides were examined under a Zeiss Vert A1 Axio inverted fluorescence microscope using a combination of two filter sets: (1) DAPI filter (Cat No. 49000, Chroma Technology) (Ex/Em=345/455) for the chromosome alignment visualization and (2) FITC/ Alexa Fluor 488/Fluo3/Oregon Green filter (Cat No.49011, Chroma Technology) (Ex/Em=495/519nm) for spindle apparatus formation visualization. Images were taken by Axio Version Special Edition 64 bit Release 4.9.1 software. The number of oocytes with either normal or abnormal spindle formation or aligned or disordered chromosomes was recorded in each treated and control group.

2.4.5 Terminal Transferase dUTP Nick End Labeling (TUNEL) Assay

Morphologically normal chromosomal alignment and spindle apparatus formation is not sufficient and conclusive for stating that DNA is intact without damage during Vemurafenib exposure. The TUNEL assay is a common method for detecting DNA fragmentation which results only from apoptotic signaling cascades. Therefore, potential apoptosis after Vemurafenib exposure was measured by the TUNEL assay. Vemurafenib-exposed oocytes and two control group PC oocytes progressing to GVBD with PB (MII arrest) or without PB (MI arrest) were subjected to a DNA TUNEL assay analysis. Procedures were carefully followed through the *APO-BrdU™ TUNEL Assay*

Kit manual instruction (Cat No. A23210, Life Technologies) (Figure 13). Oocytes were transferred among a Sigmacoat-coated 4-well Falcon dish to avoid sticky oocytes after the wash step. For the final step, one drop of SlowFade® Gold Antifade Reagent with DAPI (Invitrogen) was added to the slides without light for 15-20 min or 4°C overnight instead of the propodium iodide in the kit for chromosome staining. Slides were examined under a Zeiss Vert A1 Axio inverted fluorescence microscope using a combination of two filter sets: (1) DAPI filter (Ex/Em=345/455) for the chromosome alignment visualization and (2) FITC/Alexa Fluor 488/Fluo3/Oregon Green filter (Ex/Em=495/519nm) for the DNA damage visualization. Images were taken by an Axio Version Special Edition 64 bit Release 4.9.1 software. Since oocyte is composed of only one cell and its polar body is perceived as internal positive control. So the TUNEL assay stained oocytes were observed individually. The number of oocytes with either intact or damaged DNA or aligned or disordered chromosomes were recorded in each treated and control groups.

2.4.6 Statistical Analysis

Because oocyte stages, spindle formation, chromosome alignment, and DNA integrity results are considered as discrete data, both oocyte morphology and cytogenic examination results were evaluated by one-way ANOVA test via SPSS v.21 to determine whether a significant difference exists among groups. A p value<0.05 was considered statistically significant. (*$p \leq 0.05$, **$p \leq 0.01$, ***$p \leq 0.001$).

2.5 Toxicity of Vemurafenib on *Ex Vivo* 1C Mouse Embryo Development and Quality

Mouse embryo growth and development from 1C to blastocyst hatching upon exposure of toxic compounds has been considered the most reliable methodology for quality assurance/quality control (QA/QC) since 1984 (Ackerman S et al., 1984; Tucker KE et al., 2004). Embryos exposed to various concentrations of Vemurafenib were

obtained by irrigating oviducts from CD-euthanized female mice after PMSG/hCG injection with mating. Embryo development from 1C to hatching blastocyst were evaluated morphologically at 38, 62, 86, and 110h after culture. Tests were repeated in triplicate.

2.5.1 Superovulation and Mating

Four-week to seven-month-old female B_6CBAF_1/J mice were superovulated by 0.1 mL (5 IU) i.p. injection of PMSG followed by an i.p injection of 0.1 mL (5 IU) hCG 48h later using a 1 mL-syringe with a 30 gauge/½ inch needle (Hogan B et al., 2002). Each female mouse and one young fertile CD1 male mouse were placed together in a single cage for mating. Mating normally occurs within 6h. After 16h post-hCG injection mated female mice were examined through the vagina for a coitus mucous plug.

2.5.2 Embryo Collection

Plug-positive female mice were euthanized by CD between 26 and 30h after hCG injection. The skin of the mouse was pulled on the upper end and lower end to produce a sterile surgical field, free of hair and contaminants. A V-shaped incision was made on the abdominal musculature to pull upward and expose the xiphoid process. The small intestine was pushed to one side to expose the uterus. Tubal scissors were used to pierce the membranes under the uterus to cut the ovarian ligament. A slight amount of traction was maintained on the uterine horn so that the oviduct was torn off. And the uterine horn was stretched to the xiphoid process and the oviduct was excised from the uterine horn on the uterine side. After both oviducts had been harvested from each mouse, all oviducts containing embryos were freed and transferred into 3 mL pre-warmed equilibrated mKBB culture medium supplemented with 0.4% BSA (pH 7.6~7.8) (Ackerman, S et al., 1983) in a sterile 35-mm Nunclon culture dish. The medium was sterilized by filtering through the 0.22 μm filter unit (Nalge Co) and successfully pre-tested to determine toxicity. To be considered non-toxic, more than 75% of the embryos were required to pass over at least the morula stage. 1C embryos were flowed out from the oviducts by

using a 30 gauge needle connected to an mKBB medium filled 1mL syringe through fimbria (Swanson, R et al., 1992) under a Zeiss Discover V8 Stereo Dissecting Microscope.

2.5.3 Embryo Culture with Vemurafenib at Different Concentration

Vemurafenib was first dissolved in sterile DMSO, and then dissolved in an mKBB medium with a final concentration of 100 μM with 0.1% DMSO as the stock solution. A Vemurafenib serial dilution was created by serial dilution at a ratio of 1:10 to 10 μM/L, 1 μM/L, 0.1 μM/L and 0.01 μM/L. Each of the two negative control groups were incubated with a solution of either: (1) 200 μL mKBB with 0.1% DMSO or 200 μL mKBB medium without Vemurafenib. The positive control was treated with a mixture of 0.0000025% Zephiran Chloride with mKBB. For the blind evaluation of data by Investigator I, Investigator II coded and dispensed the various concentration solutions into rows in a 96-well Falcon sterile plate (Cat No 08-772-17, Fisher Scientific) without identifying labels. Depending on the number of embryos in each mouse, additional plates were used. All embryos from one mouse were transferred into a single row with one embryo per well. One row represented one replicate on any one experimental day. Two pro-nuclei with a narrow perivitelline space and two small PBs were visible in each morphologically-acceptable 1C embryo. All embryos were cultured in a 37℃ incubator with 100% humidity and a 5% CO_2 Air supplement.

2.5.4 Embryo Development Evaluation

All embryo developmental stages were defined as in Table 5. The numbers of embryos in each stage from lowest to highest development were recorded and morphologically evaluated at 38, 62, 86, and 110h of culture using a Zeiss Vert A1 Axio inverted research microscope fitted with a Zeiss AxioCam ICm1 camera unit. Embryo images at each stage were captured by an Axio Version Special Edition 64 bit Release 4.9.1 software. Investigator I recorded the results; Investigator II decoded the concentrations afterward. TC_{50} was defined as the Vemurafenib concentration that

inhibited 50% of embryos progressing to 2C, 4C, morula, blastocyst, and hatching stages at 38, 62, 86, and 110h of culture respectively compared with the control group; while negative control was designated as no statistical difference on embryo development with exposure to Vemurafenib. Positive control was designated as the presence of a statistical difference on embryo development with exposure to Vemurafenib.

2.5.5 The *Ex Vivo* 1C Embryo p-Mek 1/2 *In Situ* IF Staining for Embryo C-Raf Activity

Twenty embryos of all concentrations after 14h culture, regardless of

Table 6. Embryo Developmental Stages Definition

Stages	Definition
1C	presence of two pro-nuclei with a narrow perivitelline space and two small PBs
2C	2 equal sized blastomeres with a narrow perivitelline space and two small PBs
3-4C	3-4 cell: 3-4 equal sized blastomeres with a narrow perivitelline space
5-6C	5-6 equal sized blastomeres with a narrow perivitelline space
7-8C	7-8 equal-sized blastomeres with a narrow perivitelline space
cM	cells begin to fuse: semi-circular cell outline with inner semi-circle fused
M	morula cells fully fused
eB	early blastocyst: cyst formation begins
nB	normal blastocyst cyst: occupies half of the zona pellucida enclosed area
EB	expanded blastocyst: cyst occupies 2/3 of the zona pellucida enclosed area
hB	hatched blastocyst: Blastocyst begins to hatch out of zona pellucida
H	fully Hatched: Blastocyst fully hatches out of zona pellucida
Deg	degenerated: condensed and granulated blastomeres
Frag	fragmented: numerous and uneven-sized blastomeres or cytoplasmic blebs
Col	collapsed: deflated embryo after expansion

developmental stages (1C, 2C or Frag./Deg.), were subject to embryo p-Mek 1/2 *in situ* IF Staining for embryo C-Raf activity. The entire staining procedure was conducted at room temperature unless otherwise specified. Embryos were fixed in 2% paraformaldehyde for 20 minutes and permeated in each well 5 minutes with 2% Triton X-100. The embryos were then washed and blocked at least 4h with a blocking solution (Liu, L et al., 2002). Embryos were washed in PBS in wells incubated with 1mL 1:100 rabbit anti-phospho-Mek 1/2 (Ser 217/221) Antibody (Car. No. 9121S, Cell Signaling Technology) overnight. Embryos then were washed with PBS in wells and incubated with 1:40 PBS biotinylated Goat Anti-Rabbit secondary antibody (Cat. No. 65-6140, Life Technologies) in 37°C for at least 2h. Embryos were then washed in PBS in wells again and transferred to ethanol pre-cleaned slides and incubated with Alexa Fluor 488 (Ex/Em=495/519 nm) conjugated streptavidin (Car. No. S-11223, Life Technologies) in darkness for 30 minutes. Then slides were added one drop of SlowFade® Gold Antifade Reagent with DAPI (Cat No. 36939, Life Scientific) was added to each slide in darkness for 5 minutes for chromosome staining. Slides were examined under a Zeiss Vert A1 Axio inverted fluorescence microscope using a combination of two filter sets: (1) DAPI filter (Cat No. 49000, Chroma Technology) (Ex/Em=345/455) for chromosome alignment visualization and (2) FITC/ Alexa Fluor 488/Fluo3/Oregon Green filter (Cat No.49011, Chroma Technology) (Ex/Em=495/519nm) for Mek 1/2 phosphorylation. Images were taken by an Axio Version Special Edition 64 bit Release 4.9.1 software.

2.5.6 Statistical Analysis

Developmental stage scoring ranged from -1 to 5 points: -1 for degenerated (Deg.) or fragmented (Frag.); 0 for 2C; 1 for 3-4C; 2 for 5-8C; 3 for morula; 3.5 for collapsed blastocyst; 4 for blastocyst and 5 for hatching. Each row was calculated by the mean rank of scores. Scores represent a continuous type of data for multiple means with single variables. However, because the parametric assumptions for normal distribution and equal number of samples could not be satisfied, the One-way analysis of variance (ANOVA) by Kruskal-Wallis rank test was performed via SPSS v.21 to determine the developmental difference between the groups. For the same reason, the Mann-Whitney

test with Bonferroni adjustment test was used as the follow-up test between treated and control groups. The pvalue≤0.05 was considered as statistically significant (*p ≤0.05, **p ≤0.01, ***p ≤0.001). Because embryo stages are considered as the discrete data, a one-way ANOVA test was applied to embryo development in different embryonic stages.

2.6 Toxicity of Vemurafenib on *In Vivo* Mouse Embryo Development and Quality

Ex vivo assays used to analyze advanced molecular biochemical and cytogenic mechanisms do not mimic the actual *in vivo* environment and precise responses to drug exposure. For example, on Day 7 after zygote formation, the cell number of the blastocyst in *in vitro* development is 125 ±19, whereas the *in vivo* development cell number is 186 cells. This phenomenon indicates that embryos collected and cultured in an *in vitro* medium were delayed by one day.

In the *in vivo* test, superovulated mice were pre-injected with 7 doses i.p. of Vemurafenib (10 mg/kg) twice daily. The first injection was given12h after the PMSG injection; the last dose was administered 36h after the hCG injection). The long half-life (57h) of the drug and 12 hour delay injection strategy maximized the length of time of drug exposure to the embryo. The regimen of 10 mg/kg of the drug dissolved in DMSO and injected i.p. with 100 μL PBS has been successfully tested by Richard C. Koya et al. as the normal therapeutic dose of Vemurafenib. Although accurate measurement of the drug serum concentration could not be assured because of technical limitations, the direct opening of mouse oviducts into the abdominal cavity at their fimbriated end provided an accurate exposure of the drug at the injected concentrations. Both 0.1 % DMSO and negative control mice were also injected in the same manner. After hCG injection 48h post-PMSG injection, each female mouse was placed with a fertile male until a positive vaginal mucous plug was observed post-mating. 2C embryos were collected *ex vivo* as the standard of 2 equal sized blastomeres with narrow perivitelline space and two small PBs. Embryo collection from all mice followed the same operational procedure and qualified standards as described in section 2.5.2 (control groups and Vemurafenib injected groups). Embryos were transferred into 96-well Falcon sterile plates and coded by Experimenter II. Experimental (10 mg/kg) and negative controls (plain control and

0.1%DMSO control) were incubated with 200μL mKBB medium without Vemurafenib in a 5%CO_2 incubator culture with 100% humidity. Cell division and morphology were evaluated under a Zeiss A1 Axio inverted microscope. Results were recorded by Investigator I and decoded by Investigator II for further TC_{50} calculation and statistical analysis. The remaining experimental procedures, morphological evaluations and statistics were identical to Aim 2.

CHAPTER 3

RESULTS

3.1 *Ex Vivo* Oocyte Maturation Quality Control Assay

3.1.1 Cytological Morphology Evaluation of Cell Cycle in Control *Ex Vivo* Oocytes

GV-intact oocytes were isolated from sexually mature female mice by puncturing follicles. Collected oocytes were cultured with the anti-melanoma drug Vemurafenib in various concentrations to test its potential toxicity and teratogenicity. By stripping off the cumulus granulosa cells, the majority of GV-intact oocytes would experience GVBD in 2h, observed under a Zeiss A1 inverted microscope. The majority of control cells progressed to MII stage characterized by extrusion of the first polar body. Only a few oocytes were incompetent to progress to MII metaphase stage and were arrested in either GV-intact, MI prophase stage or Frag./Deg. (Table 7).

3.1.2 The Progression of Cell Cycle of Oocytes in the Presence of Vemurafenib

Normal oocyte development after LH stimulation will undergo GVBD, progressing from G_2 GV-intact resting stage to MI stage and then to the MII-arrested stage. Normal morphological developmental stages were defined as follows: (1) GV: Oocytes with an intact GV and prominent nucleolus arrested at meiosis I G2 prophase stage of the cell cycle; (2) GVBD or MI: meiosis resumes and oocytes experience GV disintegration in metaphase of meiosis I; (3) MII arrest: Oocytes progress to MII arrest by extruding the first polar body (PB1) and having a metaphase plate structure. (Figure 8) To detect the Vemurafenib morphological toxicity on oocytes, a one-way ANOVA test of oocyte maturation was evaluated. One-way ANOVA results showed a significant difference among groups of Vemurafenib serial dilution after 16h of culture compared to 0.1% DMSO and negative control groups. In follow-up statistical tests, concentrations at or below

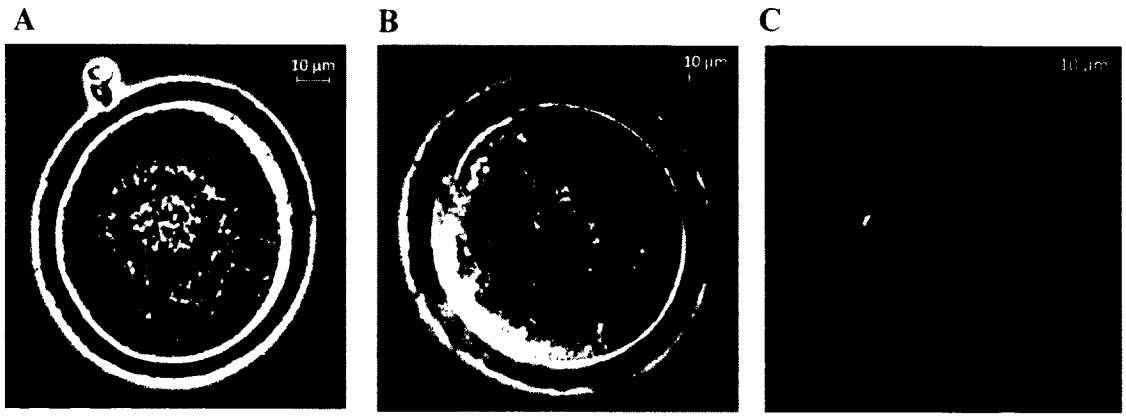

Figure 8. The Normal Morphological Developmental Stages of the Oocyte

(A) GV: Oocytes with an intact GV are arrested at Meiosis I G2 prophase stage of the cell cycle (400x).

(B) GVBD: The meiosis resumption oocytes experience GV disintegration in Metaphase I (400x).

(C) MII arrest: Oocytes progress to MII arrest of the meiosis II after extracting the first polar body (400x).

the therapeutic concentration did not appear to be significantly different compared to control groups in maturation stages (Table 7). The majority of oocytes from 1 µM to the 0.1% DMSO control successfully progressed to the MII-arrest stage and all oocytes in the negative control group progressed to the MII-arrest stage. Only a few oocytes in these groups were confined to GV-intact, MI and Fragmented/Degenerated stages. However, the concentration of 10 µM and 100 µM showed a significant difference from the control groups [11 ± 1 (73% ± 7%), $p = 0.014$] and [4 ± 2 (29% ± 10%), $p \leq 0.001$] versus [14 ± 1 (95% ± 4%)] at MII-arrest stage oocytes respectively (Table 7). The difference showed that the majority of oocytes were incompetent to mature into MII-arrest stage. Most oocytes in the 100 µM group were arrested at the MI stage [5 ± 2 (36% ± 10%) versus 0 ± 1 (2% ± 4%) at MI stage]. Fragmentation and degeneration could also be seen in this group. The 100 µM group's pattern was similar to the positive control group which

Table 7. Triplicate Evaluation of *ex vivo* Oocytes at 16h Development in Vemurafenib Solutions

Groups	Replicate Number	Mean of the Number of Oocytes ±SD (Mean of Percentage ±SD)			
		GV	GVBD, MI	MII	Frag/Deg
Positive Control[a]	3	2 ± 1 (13 ± 7)**	6 ± 1 (43 ± 6)***	3 ± 1 (18 ± 4) ***	4 ± 1 (25 ± 5)***
Negative Control[b]	3	0 ± 1 (2 ± 4)	0 ± 1 (2 ± 4)	14 ± 1 (95 ± 4)	0 ± 0 (0 ± 0)
0.1 % DMSO[c]	3	1 ± 1 (5 ± 4)	0 ± 0 (0 ± 0)	13 ± 2 (90 ± 9)	1 ± 1 (5 ± 4)
100 μM[d]	3	3 ± 1 (18 ± 4)**	5 ± 2 (36 ± 10)***	4 ± 2 (29 ± 10) ***	3 ± 1 (18 ± 4)***
10 μM[d]	3	1 ± 1 (9 ± 3)	2 ± 1 (13 ± 7)	11 ± 1 (73 ± 7)*	1 ± 1 (5 ± 4)
1 μM[d]	3	1 ± 1 (7 ± 7)	1 ± 1 (9 ± 3)	13 ± 1 (84 ± 8)	0 ± 0 (0 ± 0)
0.1 μM[d]	3	1 ± 1 (5 ± 4)	1 ± 1 (5 ± 4)	13 ± 1 (91 ± 4)	0 ± 0 (0 ± 0)
0.01 μM[d]	3	0 ± 0 (0 ± 0)	1 ± 1 (9 ± 3)	13 ± 1 (91 ± 4)	0 ± 1 (2 ± 4)

*** Highly significantly different from negative control, $p \leq 0.001$.

** Significant difference from negative control, $p \leq 0.01$

* Significant difference from negative control, $p \leq 0.05$

a. Positive Control: composed of 0.0000025% Zephiran Chloride with modified Kreb's Bicarbonate Buffer (mKBB), which has proven gemmate/embryo toxicity.

b. Negative Control: mKBB without DMSO.

c. 0.1% DMSO: DMSO dissolved in mKBB at a final concentration of 0.1% as DMSO control.

d. Serial dilution: Serially diluted from 100X stock solution made by Vemurafenib dissolved in DMSO and subsequently in mKBB to reach the concentration of 100 μM Vemurafenib 0.1% DMSO mKBB. And each concentration was adjusted to maintain the final DMSO concentration to 0.1%

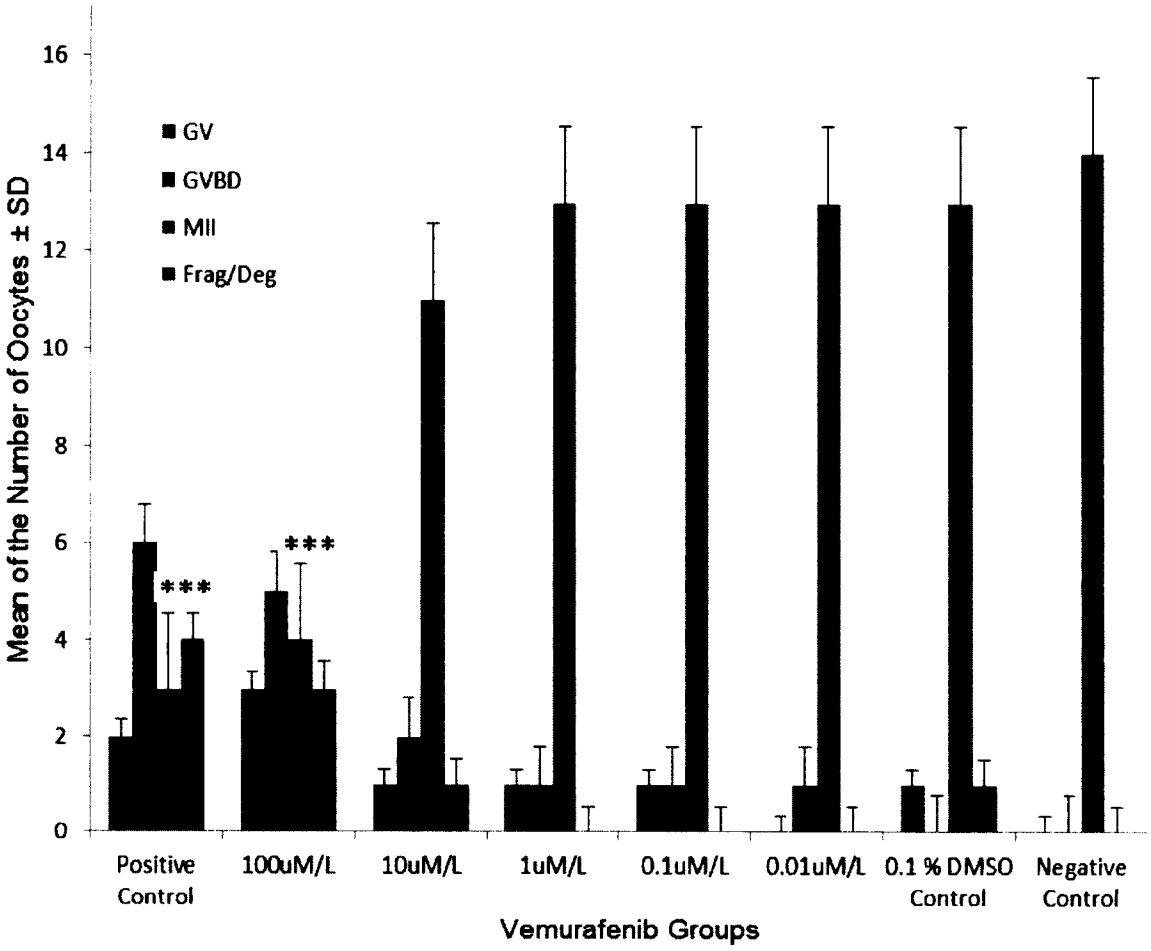

Figure 9. Concentration-Dependent Response of Oocyte Maturation

Concentration related response by percentage of oocyte maturation (GV, GVBD, MII and Frag/Deg shown) after 16h in presence of Vemurafenib is shown. The concentration of 10 μ M and 100 μ M showed a significant difference from the control groups [11 ± 1 (73% ± 7%), p =0.014] and [4 ± 2 (29% ± 10%), p ≤ 0.001] versus [14 ± 1 (95% ± 4%)] at MII-arrest stage oocytes respectively. Positive Control: composed of 0.0000025% Zephiran Chloride with modified Kreb's Bicarbonate Buffer (mKBB), which has proven gemmate/embryo toxicity. Negative Control: mKBB only without DMSO. 0.1% DMSO: DMSO dissolved in mKBB as final concentration of 0.1% as DMSO control.

produced a clear oocyte toxic effect ($p \leq 0.001$).

3.1.3 Spindle Apparatus and Chromosome Alignment Shape in Oocytes in the Presence of Vemurafenib after 16h of Culture

Abnormal morphological change leads to abnormal spindle formation and chromosome alignment. However, normal morphology in oocytes arriving at the MII-arrest stage does not guarantee that the spindle apparatus and chromosomes are formed and aligned correctly to support future fertilization and embryonic life.

The Alexa-flour 488 fluorescent dye conjugated anti-tubulin antibody directly stained the microtubules a bright green color and the DAPI stained chromosomes were blue. Immunofluorescent images of oocyte spindle formation and chromosomes were taken and evaluated after 16h culture with Vemurafenib. GV-intact ova had no microtubules to evaluate but their chromosomes could be scattered in an unordered pattern. The spindle fibers and chromosomes of the polar body were usually disturbed and unaligned, even in controls, due to depletion of ATP compared to the oocyte. With higher concentrations of Vemurafenib (10 μM or 100 μM), the following normal and damaged spindle apparatus and chromosome organization is shown in Figure 15: (1) barrel spindle and aligned chromosome in MII-arrest oocyte; (2) misaligned spindle and unaligned chromosome in MII-arrest oocyte; (3) barrel spindle and aligned chromosome in MI oocyte; (4) barrel spindle and unaligned chromosome in MI oocyte; and (5) misaligned spindle and unaligned chromosome in MI oocyte. With 1 μM, 0.1 μM and 0.01 μM of Vemurafenib, 0.1% DMSO control, and negative control groups, most of the oocytes could proceed to MII-arrest with barrel-shaped spindle apparatus and equator - aligned chromosomes (Figure 8). Interestingly, both intact and misaligned spindle fibers could be found in unaligned chromosome MI oocytes which indicated the MI spindle could be formed without correct chromosomal alignment. A disturbed spindle apparatus could produce complete chromosomal disorientation which indicated that successful chromosomal alignment relies on the guidance of barrel shaped spindle fibers. Chromosomal abnormalities could not predict the outcome of spindle shapes.

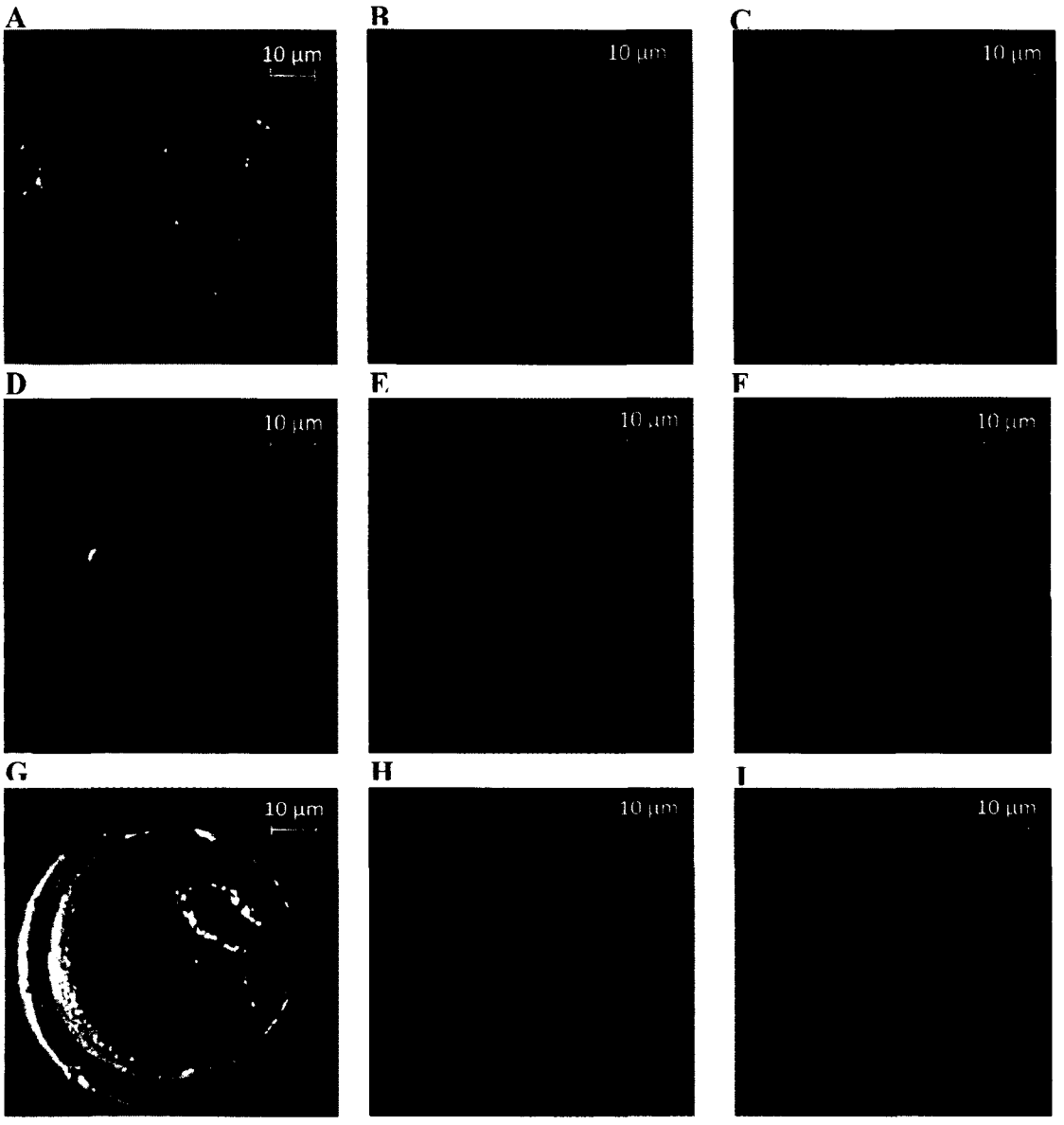

Figure 10. Oocyte Responses of Spindle Formation and Chromosome Alignment after 16h Vemurafenib Exposure

(A, B and C) from one cell, A, MII; B, Barrel shaped spindle; C, aligned chromosome. (D, E and F) from one cell, D, MII; E, Misaligned spindle; F, unaligned chromosome. (G, H and I) from one cell, G, MI; H, Barrel shaped spindle; I, unaligned chromosome. Concentration related response of spindle apparatus formation and chromosome alignment (GV, GVBD, and MII) after 16h in the presence of Vemurafenib. Figures showed the immunofluorescence staining of different responses of oocytes under the influence of Vemurafenib. MI = Metaphase I; MII = Metaphase II. Cell was taken by phase. Spindle fiber was stained as green and chromosomes were stained as blue.

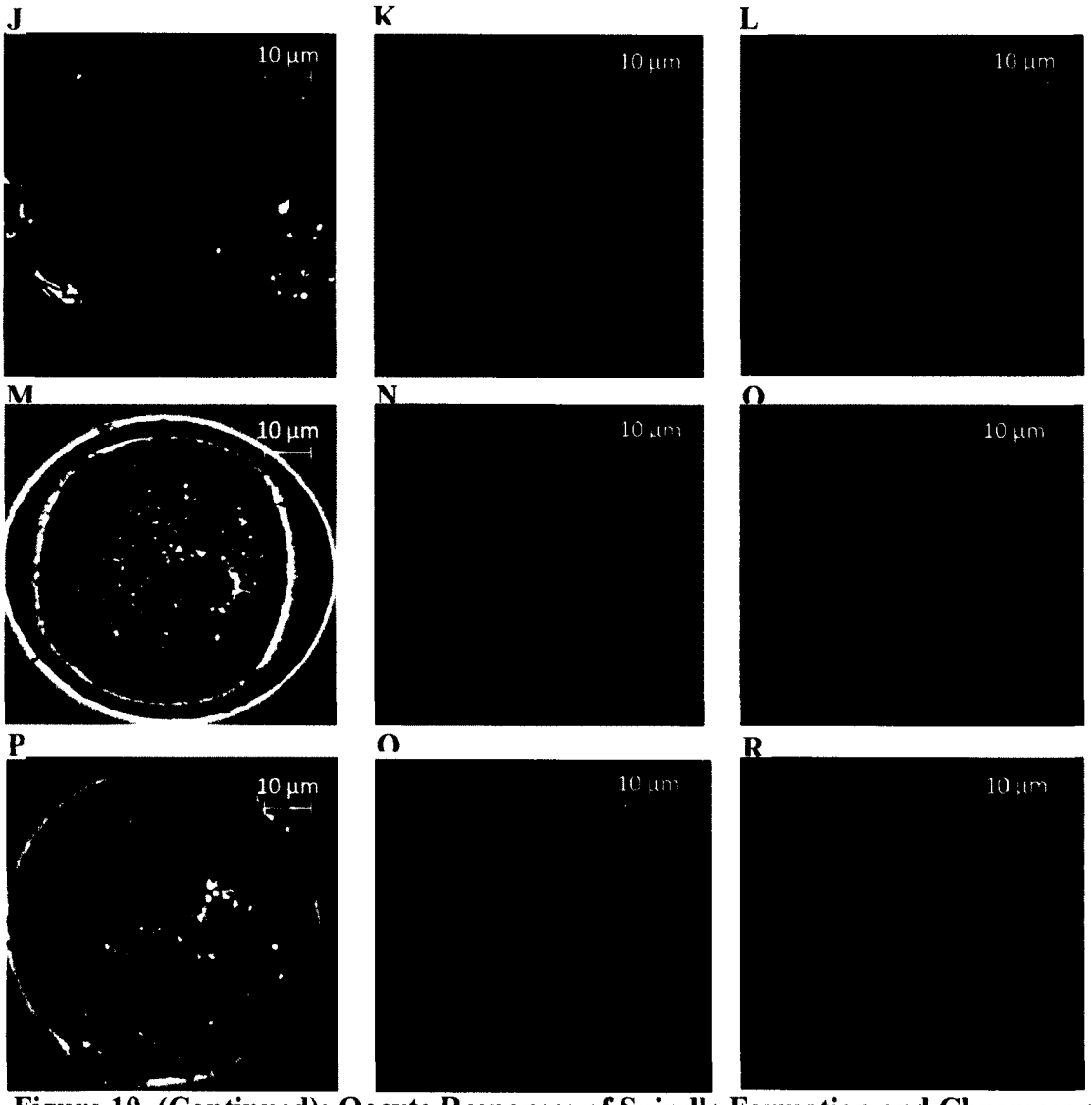

Figure 10. (Continued): Oocyte Responses of Spindle Formation and Chromosome Alignment after 16h Vemurafenib Exposure

(J, K, and L) from one cell, J, MI; K, Barrel shaped spindle; L, aligned chromosome. (M, N, and O) from one cell, M, MI; N, Misaligned spindle; O, unaligned chromosome. (P, Q, and R) from one cell show P, GV; Q, no spindle fibers; R, unaligned chromosome. Concentration related response of spindle apparatus formation and chromosome alignment (GV, GVBD, and MII) after 16h in the presence of Vemurafenib. Figures showed the immunofluorescence staining of different responses of oocytes under the influence of Vemurafenib. MI = Metaphase I; MII = Metaphase II; GV = Germinal Vesicle intact. Cell was taken by DIC phase. Spindle fiber was stained as green and chromosomes were stained as blue.

Table 8. Triplicate Analysis of Spindle Apparatus Morphology and Chromosomal Alignment in Oocytes 16h Post-Vemurafenib Treatments

Groups	Replicate Number	Mean Number of Oocytes ±SD (Mean Percentage ±SD)			
		Normal Spindle	Abnormal Spindle	Normal Chrom.	Abnormal Chrom.
Positive Control[a]	3	4 ± 3 (25 ± 19)***	11 ± 3 (75 ± 19)***	1 ± 1 (5 ± 8)***	14 ± 1 (95 ± 8)***
Negative Control[b]	3	14 ± 1 (95 ± 4)	1 ± 1 (5 ± 4)	14 ± 1 (95 ± 4)	1 ± 1 (5 ± 4)
0.1 % DMSO[c]	3	14 ± 1 (91 ± 8)	1 ± 1 (9 ± 8)	14 ± 1 (91 ± 8)	1 ± 1 (9 ± 8)
100 μM[d]	3	7 ± 3 (46 ± 16)***	8 ± 3 (54 ± 16)***	3 ± 1 (28 ± 13)***	12 ± 1 (72 ± 13)***
10 μM[d]	3	14 ± 1 (69 ± 9)	4 ± 1 (31 ± 9)***	7 ± 0 (47 ± 0)***	8 ± 0 (53 ± 0)***
1 μM[d]	3	14 ± 0 (93 ± 7)	1 ± 0 (7 ± 7)	13 ± 1 (87 ± 7)	2 ± 1 (13 ± 7)
0.1 μM[d]	3	14 ± 1 (93 ± 0)	1 ± 1 (7 ± 0)	13 ± 0 (87 ± 0)	2 ± 0 (13 ± 0)
0.01 μM[d]	3	12 ± 4 (95 ± 4)	0 ± 0 (5 ± 4)	13 ± 0 (89 ± 3)	2 ± 1 (11 ± 3)

*** Highly significantly difference from negative control, $p \leq 0.001$

a. Positive Control: composed of 0.0000025% Zephiran Chloride with modified Kreb's Bicarbonate Buffer (mKBB), which has proven gemmate/embryo toxicity.

b. Negative Control: mKBB without DMSO.

c. 0.1% DMSO: DMSO dissolved in mKBB at a final concentration of 0.1% as DMSO control.

d. Serial dilution: Serially diluted from 100X stock solution made by Vemurafenib dissolved in DMSO and subsequently in mKBB to reach the concentration of 100 μM Vemurafenib 0.1% DMSO mKBB. And each concentration was adjusted to maintain the final DMSO concentration to 0.1%

According to the statistics, after 16h of culture with Vemurafenib, the 100 μM concentration showed a highly significant difference from control groups. This mirrored the morphological pattern ($p \leq 0.001$). The 100 μM Vemurafenib caused 8 ± 3 (54% ± 16%) aberrant spindle formations and a majority (72% ± 13%) of chromosomal misalignments (Table 8). However, the concentration 1 μM or below, which is the therapeutic concentration and below, showed no significant difference from control groups in spindle apparatus formation. Almost all oocytes progressed to the MII-arrest stage with barrel shaped spindle fibers and correctly aligned chromosomes.

The 10 μM concentration of Vemurafenib which was morphologically normal compared to control groups became significantly different in chromosomal alignment when compared to control groups ($p \leq 0.001$). 8 ± 0 (53% ± 0%) oocyte chromosomes misaliged ($p = 0.0009$) after 16h 10 μM Vemurafenib exposure. Besides GV-intact, MI and Frag./Deg. oocytes, the morphologically normal MII-arrested oocytes with abnormalities of the spindle formation and chromosome alignment contributed to another 31% ± 6% weight to the actual incompetency of MII-arrest oocytes after 10 μM Vemurafenib culture. Similarly, 24% ± 11% actual incompetency was added to the morphologically normal MII-arrested oocytes in the100 μM Vemurafenib group. In all results combined, 100 μM Vemurafenib showed a highly significant difference than the control groups ($p \leq 0.0001$), in which 82% ± 4% of oocytes were incapable of further events such as fertilization, early embryo formation and implantation. Similar to 100X Vemurafenib, a significant statistical difference ($p \leqslant 0.001$) was found in 10 μM, in which 53% ± 9% of the oocytes were incapable of further developmental events. All other groups showed no difference from the 0.1% DMSO and negative control groups. TC_{50} is considered as 10 μM,

Table 9. Triplicate Analysis of Spindle Apparatus Morphology and Chromosomal Alignment in GVBD/MI and MII-Arrest Oocytes 16h Post-Vemurafenib Treatment

Groups	Replicate Number	Mean Number of Oocytes ±SD (Mean Percentage ±SD)			
		MI (Barrel, Aligned)	All Other MI	MII (Barrel, Aligned)	All Other MII
Positive Control[a]	3	0 ± 1 (3 ± 6)	6 ± 1 (12 ± 7)	0 ± 0 (0 ± 0)***	3 ± 1 (32 ± 11)***
Negative Control[b]	3	0 ± 0 (0 ± 0)	0 ± 1 (4 ± 2)	14 ± 1 (98 ± 4)	0 ± 0 (0 ± 0)
0.1 % DMSO[c]	3	0 ± 0 (0 ± 0)	0 ± 1 (5 ± 3)	13 ± 2 (97 ± 5)	0 ± 0 (0 ± 0)
100 μM[d]	3	1 ± 1 (7 ± 6)	1 ± 1 (10 ± 6)	3 ± 1 (28 ± 7)***	2 ± 1 (24 ± 11)***
10 μM[d]	3	0 ± 1 (2 ± 4)	1 ± 0 (4 ± 2)	7 ± 1 (54 ± 11)***	4 ± 1 (31 ± 6)***
1 μM[d]	3	1 ± 1 (5 ± 4)	0 ± 0 (0 ± 0)	13 ± 1 (90 ± 4)	0 ± 1 (2 ± 4)
0.1 μM[d]	3	0 ± 0 (0 ± 0)	1 ± 0 (4 ± 2)	13 ± 0 (95 ± 4)	0 ± 0 (0 ± 0)
0.01 μM[d]	3	0 ± 0 (0 ± 4)	0 ± 0 (0 ± 0)	13 ± 1 (91 ± 4)	0 ± 1 (2 ± 4)

*** Highly significantly difference from negative control, $p \leq 0.001$

a. Positive Control: composed of 0.0000025% Zephiran Chloride with modified Kreb's Bicarbonate Buffer (mKBB), which has proven gemmate/embryo toxicity.

b. Negative Control: mKBB without DMSO.

c. 0.1% DMSO: DMSO dissolved in mKBB at a final concentration of 0.1% as DMSO control.

d. Serial dilution: Serially diluted from 100X stock solution made by Vemurafenib dissolved in DMSO and subsequently in mKBB to reach the concentration of 100 μM Vemurafenib 0.1% DMSO mKBB. And each concentration was adjusted to maintain the final DMSO concentration to 0.1%

Table 10. Triplicate Overall Results of Morphology, Spindle Apparatus Shape and Chromosome Alignment in Oocytes 16h Post-Vemurafenib Treatment

Groups	Replicate Number	Mean Number of Oocytes ±SD (Mean Percentage ±SD)	
		MII-Arrest, Barrel Spindle, Aligned Chromosome	All Other Stages
Positive Control[a]	3	0 ± 0 (0 ± 0)***	15 ± 1 (100 ± 0)***
Negative Control[b]	3	14 ± 1 (98 ± 4)	0 ± 1 (2 ± 4)
0.1 % DMSO[c]	3	13 ± 2 (90 ± 9)	1 ± 1 (10 ± 9)
100 μM[d]	3	3 ± 1 (18 ± 4)***	12 ± 1 (82 ± 4)***
10 μM[d]	3	7 ± 1 (47 ± 9)***	8 ± 1 (53 ± 9)***
1 μM[d]	3	13 ± 1 (84 ± 8)	2 ± 1 (19 ± 2)
0.1 μM[d]	3	13 ± 0 (89 ± 3)	2 ± 1 (11 ± 3)
0.01 μM[d]	3	13 ± 1 (91 ± 8)	1 ± 1 (9 ± 8)

*** Highly significantly difference from negative control, $p \leq 0.001$

a. Positive Control: composed of 0.0000025% Zephiran Chloride with modified Kreb's Bicarbonate Buffer (mKBB), which has proven gemmate/embryo toxicity.

b. Negative Control: mKBB without DMSO.

c. 0.1% DMSO: DMSO dissolved in mKBB at a final concentration of 0.1% as DMSO control.

d. Serial dilution: Serially diluted from 100X stock solution made by Vemurafenib dissolved in DMSO and subsequently in mKBB to reach the concentration of 100 μM Vemurafenib 0.1% DMSO mKBB. And each concentration was adjusted to maintain the final DMSO concentration to 0.1%

whereas NC is 1 μM.

3.1.4 The DNA Integrity of Oocytes in the Presence of Vemurafenib

Similar to spindle formation and chromosome alignment, abnormal morphological change does not lead to intact DNA. However, normal morphological changes in oocytes to the MII-arrest stage are not sufficient to conclude that the DNA is free of massive damage caused by the drug. Barrel-shaped spindle apparatus and correct spindle equator-aligned chromosomes cannot guarantee intact DNA either. However, this experiment showed similar result patterns as the spindle formation and chromosome alignment. The Alexa-flour 488 fluorescent dye conjugated anti-Br-dU antibody indirectly stained the Br-dUTP labeled nick end caused by DNA damage provided an easily identifiable bright green color. The blue DAPI stained chromosomes provided the reference for corresponding DNA damage labeling. Immunofluorescent images of TUNEL assay results photographed after 16 hour culture of Vemurafenib were evaluated under a Zeiss A1 inverted fluorescent microscope. Generally, GV-intact after 16h culture of Vemurafenib without any progress in development always possessed DNA massive damage. Also, the DNA in the polar body was usually damaged because of the scarcity of an energy source compared with the oocyte. Except for GV-intact oocytes, other combinations of morphological appearance and DNA integrity could be shown in higher concentrations of Vemurafenib (10 μM or 100 μM) (see Figure 16): (1) TUNEL negative DNA intact MII arrest oocyte; (2) TUNEL positive DNA damaged MII-arrest oocyte; (3) TUNEL positive MI oocyte. Most of the oocytes in the 0.1% DMSO control group, negative control groups and 1 μM, 0.1 μM, 0.01 μM of Vemurafenib formed MII-arrest oocytes with a DNA intact negative TUNEL effect (Table 11). All GV and MI oocyte polar bodies, whether the oocytes were from control group or in 100 μM group, showed clear DNA damage after 16h culture of Vemurafenib. Based on the statistical results, the 100 μM Vemurafenib showed a highly significant difference from the control groups, which showed a pattern similar to the morphological evaluation ($p \leq 0.001$). The 100 μM Vemurafenib caused DNA fragmentations in $13 \pm 2\%$

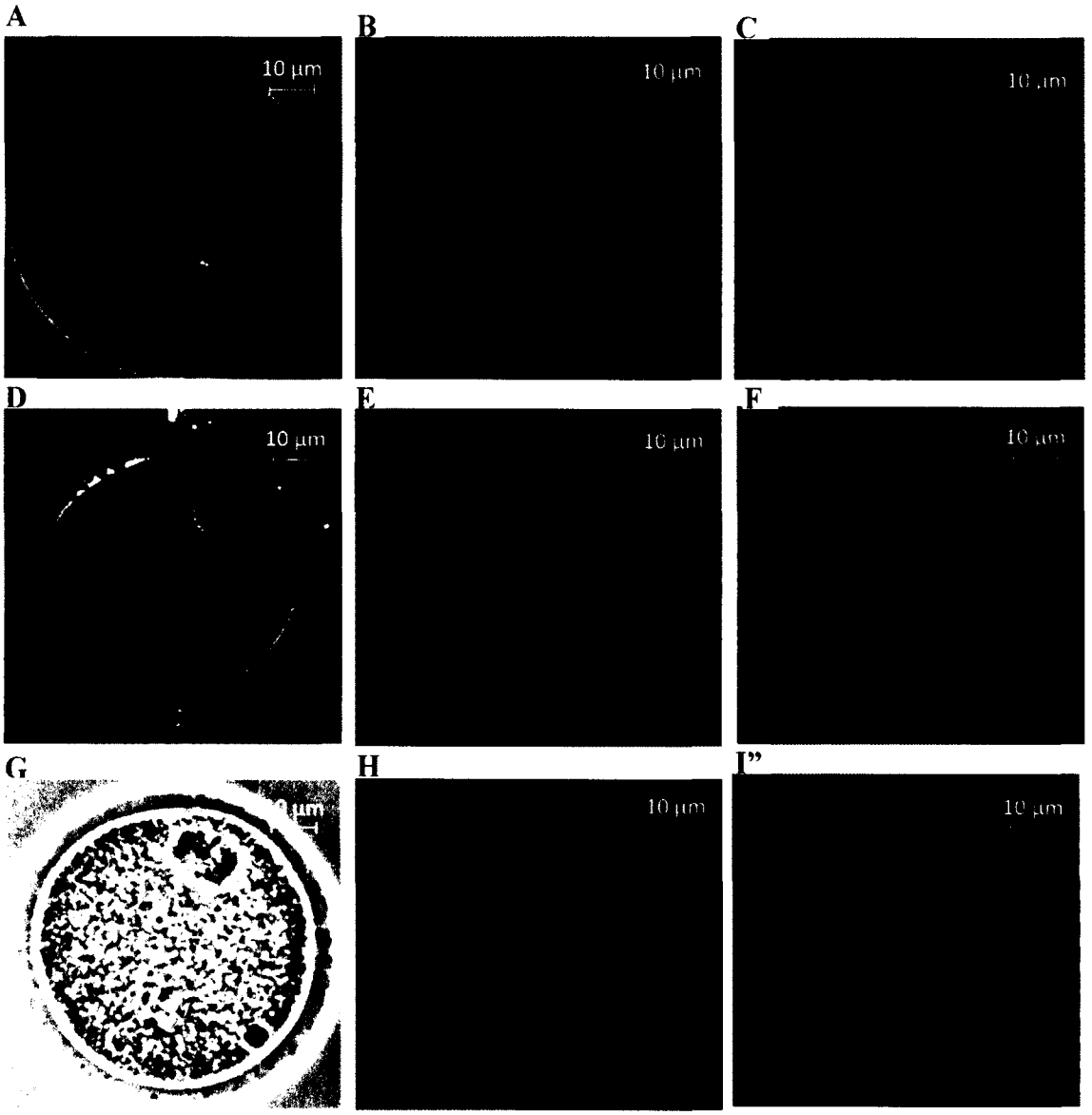

Figure 11. Oocyte Responses of DNA Integrity after 16h Vemurafenib Exposure

(A, B, and C) from one cell A, MII stage; B, aligned chromosome; C, TUNEL negative. (D, E, and F) from one cell D, MII stage; E: unaligned chromosome; F, TUNEL positive. (G, H, and I) from one cell G, MI stage; H: unaligned chromosome; I, TUNEL positive. Concentration related response of DNA integrity (GV, MI, and MII) after 16h in presence of Vemurafenib. Figures showed the TUNEL immunofluorescence staining of different responses of oocytes under influence of the Vemurafenib. MI: Metaphase I; MII: Metaphase II. Cell was taken by DAC phase. Positive TUNEL was stained as green and chromosomes were stained as blue. All Polar body showed a positive TUNEL (Green).

Table 11. Triplicate 16h *ex vivo* Oocyte Development Evaluation in the Presence of Vemurafenib Solutions

Groups	Replicate Number	Mean Number of Oocytes ±SD (Mean Percentage ±SD)			
		GV	GVBD, MI	MII	Frag/Deg
Positive Control[a]	3	3 ± 1 (18 ± 4)***	4 ± 1 (28 ± 4)***	4 ± 1 (24 ± 3) ***	4 ± 1 (28 ± 4)***
Negative Control[b]	3	0 ± 1 (2 ± 4)	0 ± 0 (0 ± 0)	14 ± 1 (95 ± 4)	0 ± 1 (2 ± 4)
0.1 % DMSO[c]	3	0 ± 1 (2 ± 4)	0 ± 1 (2 ± 4)	14 ± 1 (96 ± 8)	0 ± 0 (0 ± 0)
100 μM[d]	3	3 ± 1 (20 ± 7)***	6 ± 1 (40 ± 7)***	4 ± 2 (29 ± 10) ***	2 ± 1 (11 ± 3)
10 μM[d]	3	1 ± 1 (9 ± 3)	3 ± 1 (17 ± 8)*	11 ± 2 (71 ± 10)	0 ± 1 (2 ± 4)
1 μM[d]	3	1 ± 1 (5 ± 4)	1 ± 1 (5 ± 4)	14 ± 1 (91 ± 3)	0 ± 0 (0 ± 0)
0.1 μM[d]	3	0 ± 1 (2 ± 4)	1 ± 1 (5 ± 4)	13 ± 2 (93 ± 7)	0 ± 0 (0 ± 0)
0.01 μM[d]	3	1 ± 1 (5 ± 4)	0 ± 1 (2 ± 4)	14 ± 1 (93 ± 7)	0 ± 0 (0 ± 0)

*** Highly significantly difference from negative control, $p \leq 0.001$

a. Positive Control: composed of 0.0000025% Zephiran Chloride with modified Kreb's Bicarbonate Buffer (mKBB), which has proven gemmate/embryo toxicity.

b. Negative Control: mKBB without DMSO.

c. 0.1% DMSO: DMSO dissolved in mKBB at a final concentration of 0.1% as DMSO control.

d. Serial dilution: Serially diluted from 100X stock solution made by Vemurafenib dissolved in DMSO and subsequently in mKBB to reach the concentration of 100 μM Vemurafenib 0.1% DMSO mKBB. And each concentration was adjusted to maintain the final DMSO concentration to 0.1%

Table 12. Triplicate Analysis of DNA Integrity in Oocytes 16h Post-Vemurafenib Treatment

Groups	Replicate Number	Mean Number of Oocytes ±SD (Mean Percentage ±SD)	
		TUNEL Positive	TUNEL Negative
Positive Control[a]	3	15 ± 1 (98 ± 4)***	0 ± 1 (2 ± 4)***
Negative Control[b]	3	1 ± 1 (8 ± 4)	14 ± 1 (95 ± 4)
0.1 % DMSO[c]	3	1 ± 1 (9 ± 3)	14 ± 1 (91 ± 3)
100 μM[d]	3	13 ± 2 (86 ± 7)***	2 ± 1 (14 ± 7)***
10 μM[d]	3	8 ± 0 (53 ± 0)***	7 ± 0 (47 ± 0)***
1 μM[d]	3	3 ± 1 (18 ± 4)	12 ± 1 (82 ± 4)
0.1 μM[d]	3	1 ± 1 (7 ± 7)	13 ± 2 (93 ± 7)
0.01 μM[d]	3	1 ± 1 (9 ± 8)	14 ± 1 (91 ± 8)

*** Highly significantly difference from negative control, $p \leq 0.001$

a. Positive Control: composed of 0.0000025% Zephiran Chloride with modified Kreb's Bicarbonate Buffer (mKBB), which has proven gemmate/embryo toxicity.

b. Negative Control: mKBB without DMSO.

c. 0.1% DMSO: DMSO dissolved in mKBB at a final concentration of 0.1% as DMSO control.

d. Serial dilution: Serially diluted from 100X stock solution made by Vemurafenib dissolved in DMSO and subsequently in mKBB to reach the concentration of 100 μM Vemurafenib 0.1% DMSO mKBB. And each concentration was adjusted to maintain the final DMSO concentration to 0.1%

(86% ± 7%) of the oocytes (Table 12). However, the concentration 1 μM or below, which is below the therapeutic concentration, showed no significant difference from the control groups ($p = 0.103$). Almost all MII-arrested oocytes demonstrated a negative response to the DNA damage effect of Vemurafenib.

However, after culturing with 10 μM Vemurafenib 16h, oocytes which morphologically normal MII oocytes [11 ± 2 (71% ± 10%)] revealed a significant difference in DNA integrity compared with the control groups. Oocytes showed 8 ± 0 (53% ± 0%) to be TUNEL positive ($p \leq 0.001$). After correction, the morphologically normal MII-arrested oocytes with disintegration of DNA contributed another 24% weight to the actual incompetency of MII-arrested oocytes after 16h 10 μM Vemurafenib culture. In addition to GV-intact, MI and Frag./Deg. oocytes, 10 μM Vemurafenib revealed a significant statistical difference ($p = 0.002$) were found in 10 μM in which 8 ± 0 (53% ± 0%) of oocytes were incapable of further developmental events. Similarly, 100 μM Vemurafenib showed a highly significant difference from the control groups ($p \leq 0.0001$), with 86% ± 7% of the oocytes incapable of further development. An approximate 15% decrease in ability to survive was observed in morphologically normal MII-arrested oocytes in the100 μM Vemurafenib group (Table 12). The positive TUNEL assay showed massive DNA damage, which would prevent further development of the oocytes regardless of the morphological appearance. Finally, all other 1x or lower concentration groups showed no difference from the 0.1% DMSO and negative control groups. TC_{50} is considered as 10 μM, whereas NC is 1 μM.

3.2 *Ex Vivo* 1C Mouse Embryo Development Quality Control Assay

3.2.1 Evaluation of 1C Embryo Development

The 1C embryos with two prominent pronuclei and narrow perivitelline space were collected from sexually mature B_6CBAF_1/J female mice. The 3-week-old females were subjected to sequential 5 IU PMSG and 5 IU hCG injection 48h apart, followed immediately by mating with CD1 males. Embryos in fallopian tubes from plug-positive females 16h post-mating were isolated and cultured in pre-tested mKBB culture medium

with the serial dilutions of anti-melanoma B-Raf^{V600E} drug Vemurafenib. Embryos in each developmental stage were evaluated by scoring. Different developmental stages were scored range from -1 to 5 points after exposure to different Vemurafenib concentrations after 38, 62, 86, 110h culture: -1 point for degenerate or fragmented stage embryos; 0 point for 2C stage embryos; 1 point for 3-4C stage embryos; 2 points for 5-8C stage embryos; 3 points for morula stage embryos; 4 points for blastocyst stage embryos; 5 points for hatching stage embryos and 3.5 points for collapsed embryos.

Treated (Vemurafenib serial dilutions) groups and control (positive, negative, 0.1% DMSO) groups were ranked by calculating and statistically analyzing the mean rank of embryo development staging scores of groups in non-parametric one-way analysis of variance test (ANOVA Kruskal-Wallis test). To evaluate the embryonic toxicity and teratogenicity threshold of the Vemurafenib serial dilutions, the mean ranks of treated groups for each concentration were compared with each other as well as with control groups. The higher the developmental score, the better the embryo developed.

A post-hoc comparison test (Mann-Whitney test) was run for testing the statistical ranking differences between paired comparisons groups of each concentration and with control groups. To reduce the type I error of small degree of freedom of compared groups and increase the accuracy of the test, a Bonfeeroni adjustment (0.05/ [n (n-1)/2]) for small degree of freedom was used to increase the continuity of the test results, where n is equal to the number of the groups. The Observed Curve of the mean rank scores was plotted to explain the developmental behavior of 1C embryos in the serial dilutions of Vemurafenib exposure. The Observed Curve was closely represented by the Best-fit Curve, which is the theoretical curve. The closer the regression coefficient (R^2) to 1, the more accurate the Best-fit Curve represents the Observed Curve. The regression formula and the R2 value were presented in 36, 62, 86 and 110h graphs.

All preimplantation embryos in each concentration and control groups were regrouped into four developmental categories to magnify and pinpoint the toxicity effects of the Vemurafenib in 62, 86 and 110h post-culture. The categories were defined as: premorula (1-2C, 3-4C and 5-8C stages); morula-blastocyst (morula, blastocyst and collapsed blastocyst stages); hatching and fragmented-degenerated. The one-way ANOVA test was applied for evaluating statistical differences. The negative control

group was shown to contain the most embryos progressing from the 1C to the hatching stage. Only a few embryos were incompetent to develop and proceed to either fragmented or degenerated embryos. Therefore, all the negative control groups the highest scores and best morphological results among all groups.

A p value of $\leqslant 0.05$ throughout the results, was considered as statistically significant (*$p \leqslant 0.05$, **$p \leqslant 0.01$, ***$p \leqslant 0.001$).

3.2.2 The *Ex Vivo* 1C Embryo Development Evaluation in Presence of Vemurafenib

To detect Vemurafenib toxicity on the 1C embryos, a mean rank of the embryo development scoring was evaluated by comparing negative control and 0.1% DMSO control. The result of Kruskal-Willis test showed a significant difference among groups. In the Mann-Whitney paired comparison, concentrations below 10 μM, which was 10X the therapeutic concentration or lower, did not appear to be significantly different compared with control groups at 38, 62, 86 and 110h (Table 13). A concentration of 100 μM, which is 100X the therapeutic concentration, shows a significant difference from the control groups (Table 13), beginning at the initiation of the drug exposure [Mean rank score 100 μM (33.73 ± 10.92) versus negative control (63.57 ± 14.07), 38h after culture, pairwise $p \leq 0.0001$]. Significant toxic effect was observed at 100 μM, where embryos failed to develop to the blastocyst hatching stage. Embryos in 100X concentration of Vemurafenib showed massive fragmentation and degeneration at the early stage of culture. Toxicity remained to the end of the 110h observation frame. The toxicity of Vemurafenib in the concentration of 100 μM was even greater than the positive control [mean rank score 100 μM (33.73 ± 10.92) versus positive control (30.30 ± 11.64)] when compared to 38h after culture. The positive control mean rank score was reduced by the massive embryo degenerations and fragmentations. Embryonic

Table 13. Triplicate *ex vivo* 1C Embryo Development Evaluation in the Presence of Vemurafenib

Groups	Replicate Number	Kruskal-Willis Mean Rank ANOVA Test of Embryo scorings ±SD			
		38 h	62 h	86 h	110 h
Positive Control[a]	3	30.30 ± 11.64***	13.78 ± 5.94***	13.80 ± 5.52 ***	15.50 ± 3.97***
Negative Control[b]	3	63.57 ± 14.07	74.03 ± 12.45	74.36 ± 12.94	69.36 ± 12.45
0.1 % DMSO[c]	3	57.69 ± 10.84	66.17 ± 10.86	63.47 ± 8.87	63.70 ± 6.86
100 μM[d]	3	33.73 ± 10.92***	25.74 ± 5.14***	25.08 ± 1.51 ***	19.84 ± 3.41***
10 μM[d]	3	48.45 ± 14.83	56.00 ± 17.08	44.83 ± 26.13	49.64 ± 23.26
1 μM[d]	3	59.46 ± 20.92	58.68 ± 20.36	63.33 ± 12.96	70.70 ± 15.94
0.1 μM[d]	3	64.65 ± 17.45	60.68 ± 16.45	69.17 ± 16.45	65.61 ± 14.64
0.01 μM[d]	3	62.39 ± 11.12	62.34 ± 21.04	66.33 ± 12.81	66.06 ± 9.78

*** Highly significantly different from negative control, $p \leq 0.001$

a. Positive Control: composed of 0.0000025% Zephiran Chloride with modified Kreb's Bicarbonate Buffer (mKBB), which has proven gemmate/embryo toxicity.

b. Negative Control: mKBB without DMSO.

c. 0.1% DMSO: DMSO dissolved in mKBB at a final concentration of 0.1% as DMSO control.

d. Serial dilution: Serially diluted from 100X stock solution made by Vemurafenib dissolved in DMSO and subsequently in mKBB to reach the concentration of 100 μM Vemurafenib 0.1% DMSO mKBB. And each concentration was adjusted to maintain the final DMSO concentration to 0.1%

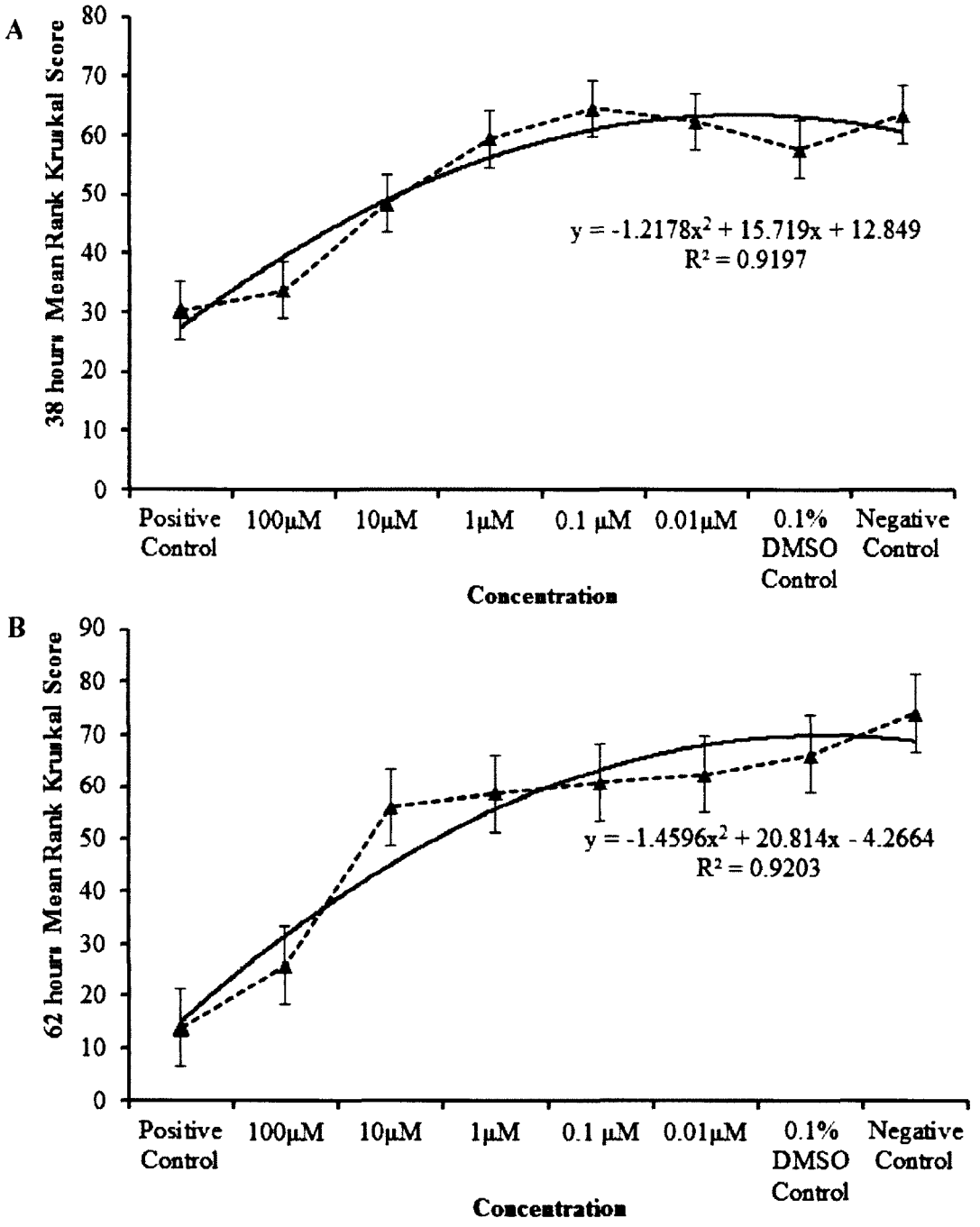

Figure 12. The Plotted Observed and Best-Fit Curve of Mean Rank Scores of Embryo Development in Presence of Vemurafenib at 38h and 62h of Culture

(A and B) Concentration-related response of embryo developmental Best-fit Curve at 38 and 62h of culture in presence of Vemurafenib. Dashed curves represent observed data. Solid triangles are the mean rank scores of embryo development in various concentrations. The solid curve (Best-fit Curve) explains the observed curve. R^2: Regression coefficient.

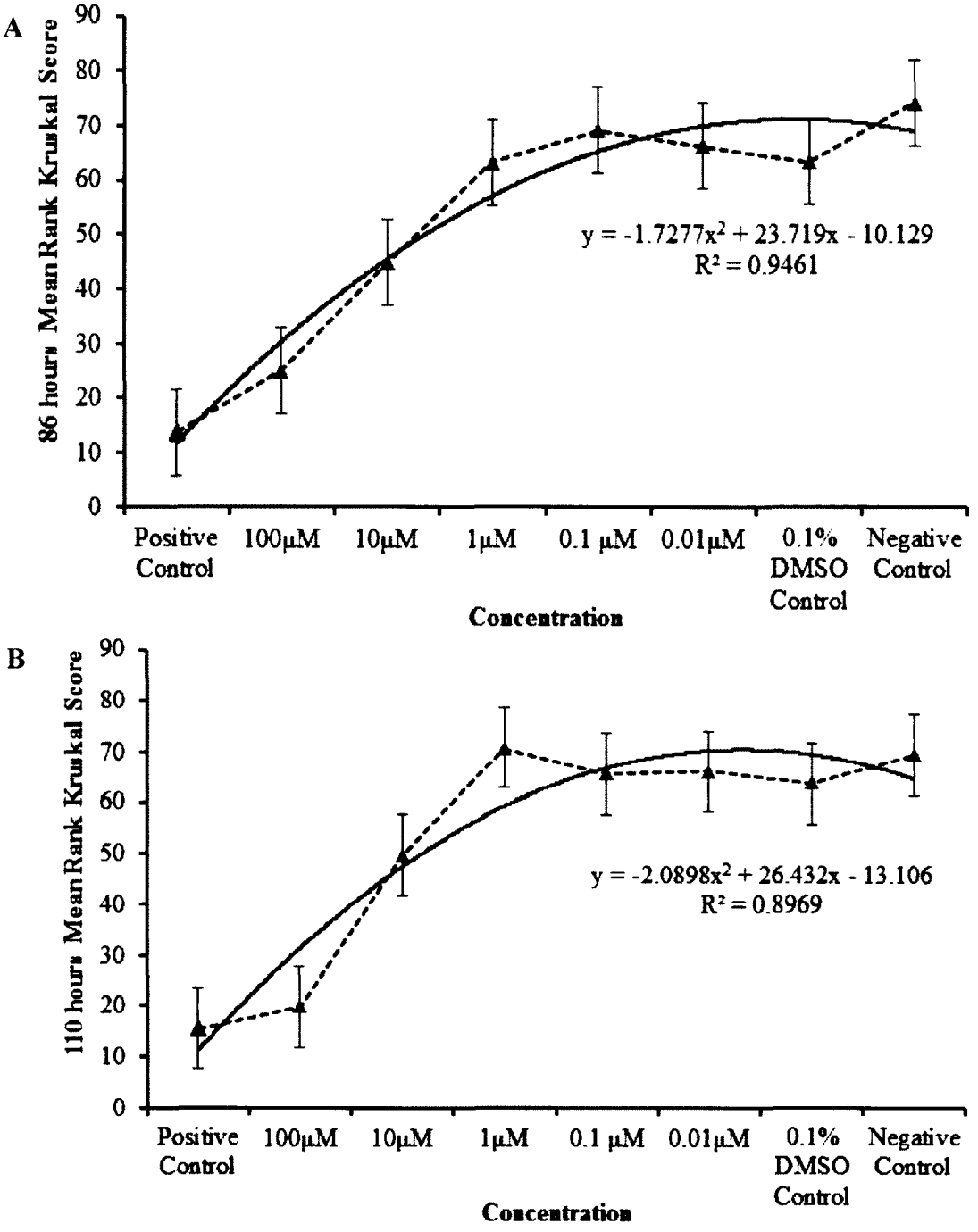

Figure 13. The Plotted Observed and Best-Fit Curve of Mean Rank Scores of Embryo Development in Presence of Vemurafenib at 86h and 110h of Culture

(A and B) Concentration related response of embryo developmental Best-fit Curve at 86 and 110h of culture in presence of Vemurafenib. The dash curves represent the observed data. The solid triangles are the mean rank scores of embryo development in various concentrations. The solid curve (Best-fit Curve) explains the observed curve. R^2: Regression coefficient.

Table 14. Triplicate 38h *ex vivo* 1C Embryo Development Evaluation in the Presence of Vemurafenib Solutions

Groups	Replicate Number	Mean Number of Embryos ±SD (Mean Percentage ±SD)			
		Premorula	Morula-Blastocyst	Hatched	Frag/Deg
Positive Control[a]	3	12 ± 2 (98 ± 4)	0 ± 0 (0 ± 0)	0 ± 0 (0 ± 0)	0 ± 1 (2 ± 4)
Negative Control[b]	3	14 ± 2 (100 ± 0)	0 ± 0 (0 ± 0)	0 ± 0 (0 ± 0)	0 ± 0 (0 ± 0)
0.1 % DMSO[c]	3	12 ± 2 (100 ± 0)	0 ± 0 (0 ± 0)	0 ± 0 (0 ± 0)	0 ± 0 (0 ± 0)
100 μM[d]	3	14 ± 5 (98 ± 4)	0 ± 0 (0 ± 0)	0 ± 0 (0 ± 0)	0 ± 1 (2 ± 4)
10 μM[d]	3	13 ± 4 (100 ± 0)	0 ± 0 (0 ± 0)	0 ± 0 (0 ± 0)	0 ± 0 (0 ± 0)
1 μM[d]	3	12 ± 3 (100 ± 0)	0 ± 0 (0 ± 0)	0 ± 0 (0 ± 0)	0 ± 0 (0 ± 0)
0.1 μM[d]	3	11 ± 3 (97 ± 6)	0 ± 1 (3 ± 6)	0 ± 0 (0 ± 0)	0 ± 0 (0 ± 0)
0.01 μM[d]	3	12 ± 2 (100 ± 0)	0 ± 0 (0 ± 0)	0 ± 0 (0 ± 0)	0 ± 0 (0 ± 0)

a. Positive Control: composed of 0.0000025% Zephiran Chloride with modified Kreb's Bicarbonate Buffer (mKBB), which has proven gemmate/embryo toxicity.

b. Negative Control: mKBB without DMSO.

c. 0.1% DMSO: DMSO dissolved in mKBB at a final concentration of 0.1% as DMSO control.

d. Serial dilution: Serially diluted from 100X stock solution made by Vemurafenib dissolved in DMSO and subsequently in mKBB to reach the concentration of 100 μM Vemurafenib 0.1% DMSO mKBB. And each concentration was adjusted to maintain the final DMSO concentration to 0.1%

developmental pattern was compared at 38, 62, 86 and 110h culture in the presence of Vemurafenib. Each mean rank score from each hour point of culture at different concentrations was represented by the solid triangle.

The Observed Curve connected mean rank scores by a dashed line, whereas the Best-fit Curve was represented by a solid line. The Best-fit Curve explained the Observed Curve in 92% (R^2) at 38h, 92% at 62h, 95% at 86h and 90% at 110h. All curves showed an obvious sharp incline and a plateau from 100 μM to the negative control (Figures 12 and 13). The Best-fit curve further proved that the concentration in 100 μM of Vemurafenib prevented over half the embryos from developing to the blastocyst hatching stage. Therefore, the TC_{50} for the 1C embryo development assay set at 100 μM. The categorized data analyzed by one-way ANOVA showed a pattern similar to the mean rank Kruskal ANOVA analysis. But the one-way ANOVA categorized analysis focused primarily on the general trend of embryo development. At 38h culture, no major difference was found among groups (Table 14). However, at 62h culture, not only 100 μM Vemurafenib showed a highly significant difference in embryo development, but also 10 μM in concentration of Vemurafenib solution demonstrated a delay in embryo development (Table 15). However, most embryos in the categorized premorula stage in 10 μM were at 7C or 8C stage (data not shown) and soon regained the rate of embryo development compared to control group (Table 15). Concentrations below 10 μM did not demonstrate a significant difference from control groups at 38, 62, 86 and 110h (Table 14, 15, 16 and 17). Therefore, embryotoxicity has been clearly observed at 100X of the therapeutic concentration. At the same time, potential delayed toxicity was observed in 10X Vemurafenib. However, the drug showed no significant morphological toxicity *in vitro* preimplantation 1C embryos.

3.2.3 The *Ex Vivo* 1C Embryo p-Mek 1/2 *In Situ* Immunofluorescence Staining for Embryo C-Raf Activity in Presence of Vemurafenib after 14h Culture.

The Mek 1/2 is the direct and only substrate of C-Raf in the MAPK pathway. Phosphorylation of Mek 1/2 directly mirrors the kinase function and activity of C-Raf,

Table 15. Triplicate 62h *ex vivo* 1C Embryo Development Evaluation in the Presence of Vemurafenib Solutions

Groups	Replicate Number	Mean Number of Embryos ±SD (Mean Percentage ±SD)			
		Premorula	Morula-Blastocyst	Hatched	Frag/Deg
Positive Control[a]	3	7 ± 0 (56 ± 9)***	0 ± 0 (0 ± 0) ***	0 ± 0 (0 ± 0)	6 ± 2 (44 ± 9)***
Negative Control[b]	3	0 ± 0 (0 ± 0)	14 ± 2 (100 ± 0)	0 ± 0 (0 ± 0)	0 ± 0 (0 ± 0)
0.1 % DMSO[c]	3	1 ± 1 (11 ± 2)	11 ± 1 (87 ± 6)	0 ± 0 (0 ± 0)	0 ± 1 (2 ± 4)
100 μM[d]	3	9 ± 4 (73 ± 41)***	1 ± 1 (4 ± 6) ***	0 ± 0 (0 ± 0)	4 ± 7 (23 ± 35)***
10 μM[d]	3	5 ± 1 (39 ± 10)*	8 ± 3 (61 ± 10)*	0 ± 0 (0 ± 0)	0 ± 0 (0 ± 0)
1 μM[d]	3	4 ± 6 (33 ± 51)*	8 ± 7 (67 ± 51)*	0 ± 0 (0 ± 0)	0 ± 0 (0 ± 0)
0.1 μM[d]	3	3 ± 3 (31 ± 34)*	8 ± 5 (69 ± 34)*	0 ± 0 (0 ± 0)	0 ± 0 (0 ± 0)
0.01 μM[d]	3	3 ± 4 (29 ± 39)*	9 ± 5 (68 ± 36)*	0 ± 0 (0 ± 0)	0 ± 1 (3 ± 5)

*** Highly significantly difference from negative control, $p \leq 0.0001$

* Significantly difference from negative control, $p \leq 0.05$

a. Positive Control: composed of 0.0000025% Zephiran Chloride with modified Kreb's Bicarbonate Buffer (mKBB), which has proven gemmate/embryo toxicity.

b. Negative Control: mKBB without DMSO.

c. 0.1% DMSO: DMSO dissolved in mKBB at a final concentration of 0.1% as DMSO control.

d. Serial dilution: Serially diluted from 100X stock solution made by Vemurafenib dissolved in DMSO and subsequently in mKBB to reach the concentration of 100 μM Vemurafenib 0.1% DMSO mKBB. And each concentration was adjusted to maintain the final DMSO concentration to 0.1%

Table 16. Triplicate 86h *ex vivo* 1C Embryo Development Evaluation in the Presence of Vemurafenib Solutions

Groups	Replicate Number	Mean Number of Embryos ±SD (Mean Percentage ±SD)			
		Premorula	Morula-Blastocyst	Hatched	Frag/Deg
Positive Control[a]	3	1 ± 2 (12 ± 21)	0 ± 0 (0 ± 0) ***	0 ± 0 (0 ± 0)	11 ± 4 (88 ± 21)***
Negative Control[b]	3	0 ± 0 (0 ± 0)	12 ± 4 (82 ± 21)	2 ± 3 (18 ± 21)	0 ± 0 (0 ± 0)
0.1 % DMSO[c]	3	0 ± 1 (3 ± 5)	10 ± 3 (80 ± 21)	1 ± 1 (9 ± 9)	1 ± 1 (7 ± 7)
100 μM[d]	3	1 ± 2 (10 ± 16)	5 ± 4 (37 ± 30) ***	0 ± 0 (0 ± 0)***	8 ± 9 (54 ± 44)***
10 μM[d]	3	1 ± 1 (12 ± 10)	9 ± 4 (65 ± 14) ***	0 ± 1 (2 ± 3)*	3 ± 1 (21 ± 8)***
1 μM[d]	3	0 ± 1 (3 ± 5)	12 ± 3 (94 ± 5)	0 ± 1 (3 ± 6)	0 ± 0 (0 ± 0)
0.1 μM[d]	3	0 ± 0 (0 ± 0)	10 ± 4 (84 ± 13)	1 ± 1 (12 ± 7)	0 ± 1 (3 ± 6)
0.01 μM[d]	3	1 ± 0 (0 ± 0)	12 ± 2 (95 ± 5)	0 ± 1 (3 ± 5)	0 ± 1 (2 ± 4)

*** Highly significantly difference from negative control, $p \leq 0.0001$

* Significantly difference from negative control, $p \leq 0.05$

a. Positive Control: composed of 0.0000025% Zephiran Chloride with modified Kreb's Bicarbonate Buffer (mKBB), which has proven gemmate/embryo toxicity.

b. Negative Control: mKBB without DMSO.

c. 0.1% DMSO: DMSO dissolved in mKBB at a final concentration of 0.1% as DMSO control.

d. Serial dilution: Serially diluted from 100X stock solution made by Vemurafenib dissolved in DMSO and subsequently in mKBB to reach the concentration of 100 μM Vemurafenib 0.1% DMSO mKBB. And each concentration was adjusted to maintain the final DMSO concentration to 0.1%

Table 17. Triplicate 110h *ex vivo* 1C Embryo Development Evaluation in the Presence of Vemurafenib Solutions

Groups	Replicate Number	Mean Number of Embryos ±SD (Mean Percentage ±SD)			
		Premorula	Morula-Blastocyst	Hatched	Frag/Deg
Positive Control[a]	3	0 ± 0 (0 ± 0)	0 ± 0 (0 ± 0)***	0 ± 0 (0 ± 0) ***	13 ± 2 (100 ± 0)***
Negative Control[b]	3	0 ± 0 (0 ± 0)	3 ± 4 (22 ± 23)	11 ± 2 (78 ± 23)	0 ± 0 (0 ± 0)
0.1 % DMSO[c]	3	0 ± 0 (0 ± 0)	4 ± 4 (27 ± 23)	8 ± 3 (69 ± 31)	1 ± 1 (7 ± 7)
100 μM[d]	3	0 ± 1 (2 ± 4)	2 ± 1 (13 ± 7)	0 ± 1 (2 ± 4) ***	12 ± 5 (82 ± 12)***
10 μM[d]	3	0 ± 0 (0 ± 0)	5 ± 1 (37 ± 12)*	5 ± 4 (37 ± 17)***	3 ± 1 (26 ± 7)**
1 μM[d]	3	0 ± 0 (0 ± 0)	3 ± 4 (18 ± 25)	10 ± 1 (81 ± 20)	0 ± 1 (3 ± 5)
0.1 μM[d]	3	0 ± 0 (0 ± 0)	4 ± 4 (28 ± 23)	8 ± 1 (69 ± 22)	0 ± 1 (3 ± 6)
0.01 μM[d]	3	0 ± 0 (0 ± 0)	4 ± 4 (27 ± 23)	8 ± 2 (71 ± 27)	0 ± 1 (2 ± 4)

*** Highly significantly difference from negative control, $p \leq 0.0001$

** Significantly different from negative control, $p \leq 0.01$

* Significantly different from negative control, $p \leq 0.05$

a. Positive Control: composed of 0.0000025% Zephiran Chloride with modified Kreb's Bicarbonate Buffer (mKBB), which has proven gemmate/embryo toxicity.

b. Negative Control: mKBB without DMSO.

c. 0.1% DMSO: DMSO dissolved in mKBB at a final concentration of 0.1% as DMSO control.

d. Serial dilution: Serially diluted from 100X stock solution made by Vemurafenib dissolved in DMSO and subsequently in mKBB to reach the concentration of 100 μM Vemurafenib 0.1% DMSO mKBB. And each concentration was adjusted to maintain the final DMSO concentration to 0.1%

the potential target of Vemurafenib. C-Raf activity is responsible for the transition of 1C to 2C and one of six lethal knockouts in post-implantation development. Therefore, the present study tested whether p-Mek 1/2 in morphological normal and abnormal embryos after 14h of culture mirrors the function of C-Raf kinase.

A biotin-streptavidin signal amplification system was used to test the small amount of endogenous p-Mek 1/2. The biotin conjugated secondary antibody was used to bind the anti-p-Mek 1/2 (Ser217/221) antibody, followed by the Alexa-flour 488 fluorescent dye conjugated streptavidin activation for signal amplification. The blue DAPI stained chromosomes provided the reference point for p-Mek1/2 cellular location. Immunofluorescent images of p-Mek 1/2 assay results after 14 hour culture of Vemurafenib were photographed and evaluated under a Zeiss A1 inverted fluorescent microscope.

All 1C and Fragmented/ Degenerated embryos after 14h culture in Vemurafenib serial dilution solutions showed negative response in the Mek 1/2 phosphorylation by C-Raf. 2C embryos after 14h Vemurafenib culture showed either positive or negative p-Mek 1/2 fluorescence depending on Vemurafenib concentrations (Figure 14). Abnormal 2C appearance often demonstrated negative or diminished p-Mek 1/2 fluorescence. Most of embryos in the 0.1% DMSO control, negative control groups, and 1 μM, 0.1 μM, and 0.01 μM of Vemurafenib formed 2C embryos with positive phosphorylation of Mek 1/2 (Table 18). Morphologically, embryos in 100 μM Vemurafenib showed that 7 ± 3 (49% ± 6%) were unable to progress to 2C and within 2C stage cells; 4 ± 1 of the 2C embryos appeared to have either unequal blastomeres or prominent perivitelline spaces. A highly significant difference in morphological development ($p \leq 0.001$) was observed between the control groups and a concentration of 100 μM Vemurafenib. However, a concentration of 10 μM or lower, which is 10 times the therapeutic concentration or lower, showed no significant statistical and morphological difference from the control groups.

Similar to spindle-formation chromosome-alignment and DNA-integrity results, some morphological normal 2C embryos in concentrations of 10 μM and 1 μM showed a negative result of p-Mek phosphorylation by C-Raf.

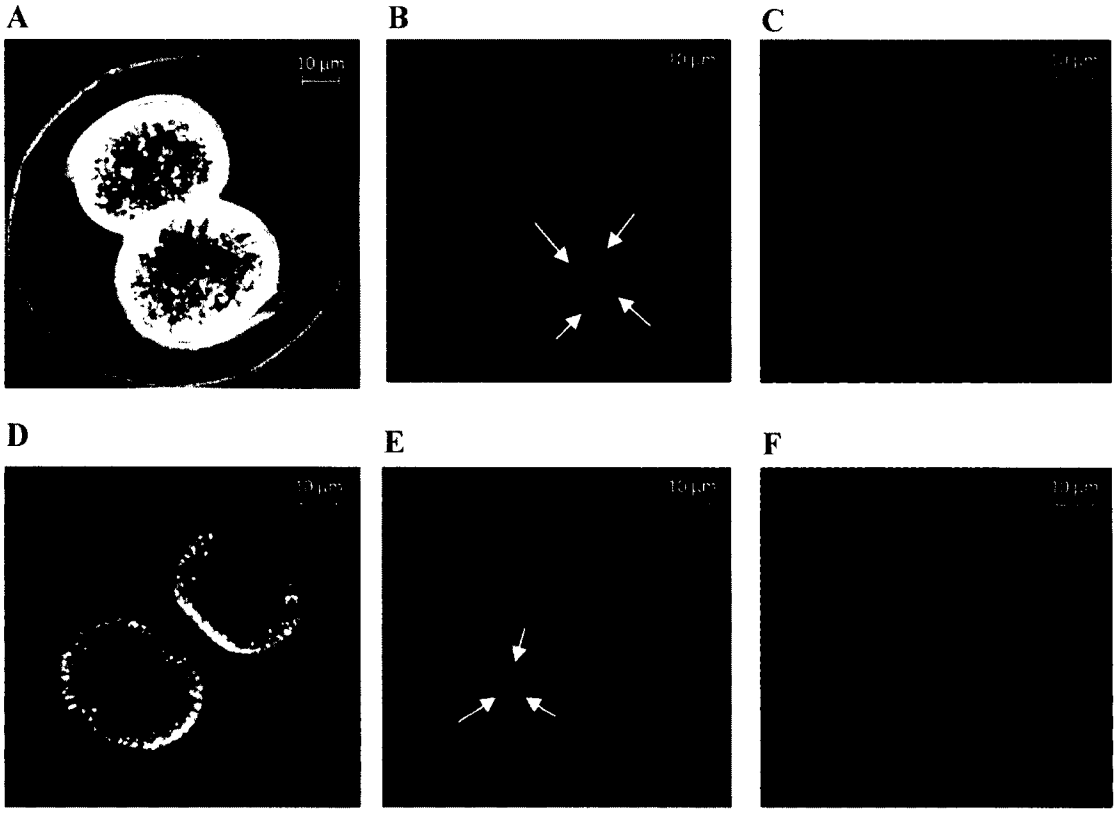

Figure 14. Embryo Responses of C-Raf Activity after 16h Vemurafenib Exposure
(A, B and C) Pictures from one cell show A, normal 2C; B, p-Mek 1/2 IF staining positive (Green stained cytoplasmic substances); C, DAPI stained nucleus location (D, E and F) Pictures from one cell show D, abnormal 2C; E, p-Mek 1/2 IF staining negative(Green stained cytoplasmic substances); F, DAPI stained nucleus location. Concentration related response of embryo C-Raf activity (1C and 2C) by after 16h in presence of Vemurafenib. Figures showed the p-Mek 1/2 IF staining of different responses of embryos under influence of Vemurafenib. Arrow heads show the nucleus outlines which indicate cytoplasmic location of the p-MEK 1/2.

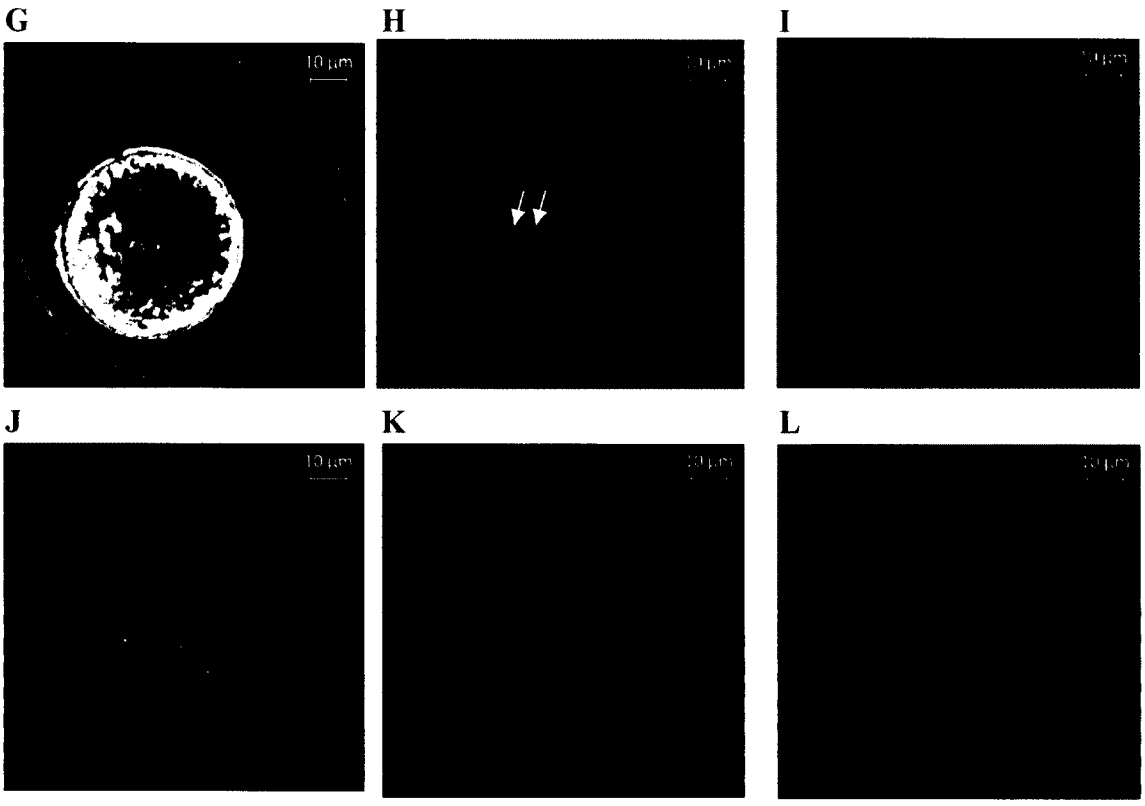

Figure 14 (Continued). Embryo Responses of C-Raf Activity after 16h Vemurafenib Exposure

(G, H and I) Pictures from one cell show G, abnormal 1C; H, p-Mek 1/2 IF staining negative (Green stained cytoplasmic substances); C, DAPI stained nucleus location

(J, K and L) Pictures from one cell show J, degenerated embryo; K, p-Mek 1/2 IF staining negative (no stain); L, DAPI stained nucleus location.

Concentration related response of embryo C-Raf activity (1C and 2C) by after 16h in presence of Vemurafenib. Figures showed the p-Mek 1/2 IF staining of different responses of embryos under influence of Vemurafenib. Arrow heads show the nucleus outlines which indicate cytoplasmic location of the p-MEK 1/2.

Table 18. Triplicate *ex vivo* 1C Embryo Development Evaluation in the Presence Of Vemurafenib after 16h Cultures

Groups	Replicate Number	Mean Number of Embryos±SD (Mean Percentage ±SD)		
		1C	2C	Frag/Deg
Positive Control[a]	3	4 ± 2 (26 ± 3)*	7 ± 4 (48 ± 5) ***	3 ± 1 (24 ± 4)*
Negative Control[b]	3	0 ± 1 (2 ± 3)	15 ± 4 (94 ± 5)	1 ± 1 (4 ± 4)
0.1 % DMSO[c]	3	0 ± 1 (2 ± 4)	15 ± 5 (95 ± 4)	0 ± 1 (2 ± 4)
100 μM[d]	3	5 ± 2 (34 ± 3)*	8 ± 3 (51 ± 5) ***	2 ± 1 (15 ± 3)*
10 μM[d]	3	2 ± 1 (12 ± 9)	13 ± 5 (82 ± 9)	1 ± 0 (7 ± 2)
1 μM[d]	3	1 ± 1 (8 ± 3)	15 ± 4 (90 ± 1)	0 ± 1 (2 ± 3)
0.1 μM[d]	3	1 ± 1 (5 ± 4)	14 ± 3 (94 ± 6)	0 ± 1 (2 ± 3)
0.01 μM[d]	3	0 ± 0 (0 ± 0)	16 ± 4 (100 ± 0)	0 ± 0 (0 ± 0)

*** Highly significantly difference from negative control, $p \leq 0.0001$

* Significantly different from negative control, $p \leq 0.05$

a. Positive Control: composed of 0.0000025% Zephiran Chloride with modified Kreb's Bicarbonate Buffer (mKBB), which has proven gemmate/embryo toxicity.

b. Negative Control: mKBB without DMSO.

c. 0.1% DMSO: DMSO dissolved in mKBB at a final concentration of 0.1% as DMSO control.

d. Serial dilution: Serially diluted from 100X stock solution made by Vemurafenib dissolved in DMSO and subsequently in mKBB to reach the concentration of 100 μM Vemurafenib 0.1% DMSO mKBB. And each concentration was adjusted to maintain the final DMSO concentration to 0.1%.

Two from 1 μM and four from 10 μM morphologically normal embryos showed negative responses to the Mek 1/2 phosphorylation, which represents 2% and 17% respectively of actual incompetency of the morphological normal 2C embryos. Combined results from the 1C embryo development assay in 3.2.2, indicate that while the negative p-Mek 1/2 2C embryos may develop through preimplantation stages, the embryos will not survive during post-implantation stages.

In 100 μM Vemurafenib, on the other hand, all abnormal appearance 2C (6 ± 2 (41% ± 2%)) possessed a negative p-Mek 1/2 and morphologically normal 2C embryos (2 ± 1 (10% ± 3%)) showed a positive p-Mek 1/2. This indicates that 100 μM had a higher embryotoxicity in the early stage of embryo development. This higher toxicity indicates that embryos progressing into 2C were incompetent to develop through the preimplantation stages.

Therefore, in addition to 1C and Frag./Deg. embryos, 100 μM and 10 μM Vemurafenib caused 13 ± 4 (83% ± 2%) and 5 ± 1 (35% ± 13%)respectively of C-Raf inhibition and showed a significant difference (100 μM, $p \leq 0.001$; 10 μM, $p = 0.035$) from the control groups (Table 19). However, a concentration of 1 μM or lower, which is equal to or lower than therapeutic concentrations, showed no significant difference from the control groups after 16h of culture.

Instead of a complete block of C-Raf activity, most of the negative p-Mek 1/2 showed diminished fluorescence. Since no other kinase exists for the phosphorylation of Mek1/2, the diminished fluorescence was completely due to the incomplete inhibition of C-Raf activity. Even with this incomplete blockage, the reduction of C-Raf activity is thought to be unable to support development of embryos through pre- and post-implantation stages (Yamauchi N et al., 1994; Yufen Xie et al., 2005).

Finally, regardless of whether p-Mek 1/2 is inhibited, the presence of phosphorylated Mek 1/2 in the cytoplasm indirectly supports the conclusion that C-Raf located on the cell membrane activates the downstream effector Mek 1/2. Thus, negative p-Mek 1/2 by C-Raf inhibition prevents the further development of the embryos regardless of the

Table 19. Triplicate *ex vivo* Embryo Phospho-Mek 1/2 Staining for C-Raf Activity in Presence of Vemurafenib Solutions after 16h Cultures

Groups	Replicate Number	Mean Number of Oocytes ±SD (Mean Percentage ±SD)	
		Phospho-Mek Positive	Phospho-Mek Negative
Positive Control[a]	3	1 ± 1 (5 ± 5)***	13 ± 6 (95 ± 5)***
Negative Control[b]	3	15 ± 4 (90 ± 2)	2 ± 1 (10 ± 2)
0.1 % DMSO[c]	3	15 ± 5 (93 ± 6)	1 ± 1 (7 ± 6)
100 μM[d]	3	3 ± 1 (19 ± 5)***	13 ± 4 (83 ± 2)***
10 μM[d]	3	10 ± 5 (65 ± 13)*	5 ± 1 (35 ± 13)**
1 μM[d]	3	14 ± 4 (88 ± 3)	2 ± 1 (12 ± 3)
0.1 μM[d]	3	14 ± 3 (91 ± 2)	1 ± 1 (9 ± 2)
0.01 μM[d]	3	16 ± 5 (97 ± 5)	0 ± 1 (3 ± 5)

*** Highly significantly different from negative control, $p \leq 0.001$

** Significantly different from negative control, $p \leq 0.01$

*Significantly different from negative control, $p \leq 0.05$

a. Positive Control: composed of 0.0000025% Zephiran Chloride with modified Kreb's Bicarbonate Buffer (mKBB), which has proven gemmate/embryo toxicity.

b. Negative Control: mKBB without DMSO.

c. 0.1% DMSO: DMSO dissolved in mKBB at a final concentration of 0.1% as DMSO control.

d. Serial dilution: Serially diluted from 100X stock solution made by Vemurafenib dissolved in DMSO and subsequently in mKBB to reach the concentration of 100 μM Vemurafenib 0.1% DMSO mKBB. And each concentration was adjusted to maintain the final DMSO concentration to 0.1%.

morphological appearance. TC_{50} is considered as 10 μM, whereas NC is 1 μM.

3.3 *In Vivo* Mouse Embryo Development Quality Control Assay

3.3.1 The 2C Embryo Development Evaluation Standards and Statistics

Two cell embryos with two equal blastomeres and narrow perivitelline spaces were collected from sexually mature B_6CBAF_1/J female mice. The 3-week-old females were subjected to sequential 5 IU PMSG and 5 IU hCG injections 48h apart, followed by immediately mating with CD1 males. Seven doses i.p. of Vemurafenib (10 mg/kg) were also pre-injected in vivo twice daily. The first injection was administered 12h after PMSG injection and the last dose was administered 36h after hCG injection. Embryos in fallopian tubes from plug positive females 42h post-hCG were isolated and cultured in pre-tested mKBB culture medium. Embryos in each developmental stage were evaluated by scores. Scores of Embryos at different developmental stages ranging from -1 to 5 points after 24, 48, 72 and 96h culture: -1 point for Degenerate or Fragmented embryos; 0 point for 2C embryos; 1 point for 3-4C embryos; 2 points for 5-8C embryos; 3 points for morula embryos; 4 points for blastocyst stage embryos, 5 points for hatching stage embryos and 3.5 points for collapsed embryos.

The treated (Vemurafenib serial dilution) groups and the control (positive, negative, 0.1%DMSO) groups were ranked by calculating and statistically analyzing the mean rank of embryo development staging scores by ANOVA Kruskal-Wallis test. The higher the developmental score, the better the embryo development.

A Post-hoc Mann-Whitney test was performed for testing the statistical ranking differences between paired comparisons groups of each concentration and with control groups. A Bonfeeroni adjustment was used to reduce the type I error, the small degree of freedom, and to increase the accuracy of the test.

The trend of the mean rank scores was plotted to explain the tendency of the 2C embryo developmental behavior after in vivo Vemurafenib i.p. injections compared with control groups in 24, 48, 72 and 96h culture.

All preimplantation embryos in the Vemurafenib dam injection group and control groups were regrouped into four developmental categories to magnify and pinpoint the toxicity effects of the Vemurafenib in 24, 48, 72 and 96h culture. The categories were defined as the same as in Aim 2. One-way ANOVA was applied for testing statistical differences.

3.3.2 The *In Vivo* 2C Embryo Development Evaluation after the Vemurafenib Dam Injection Procedure

Results of Kruskal-Willis test showed a significant difference among groups in 24, 48, 72 and 96h of culture. In a Mann-Whitney paired comparison, the DMSO control group showed a higher score than negative control and Vemurafenib groups in the early culture. Therefore, a stimulating effect on embryos was observed in the DMSO group [mean rank score DMSO control 40.69 ± 18.43 versus negative control 19.36 ± 12.07, pairwise $p \leq 0.001$). The experimental group in which Vemurafenib was dissolved by DMSO demonstrated a similar development rate compared with the negative control group [Mean rank score 10 mg/kg Vemurafenib 24.55 ± 10.43 versus negative control 19.36 ± 12.07, pairwise $p = 0.263$]. Therefore, the Vemurafenib group had either offset the stimulating effect of the DMSO or showed a significant delay in embryo development in early culture. As the time approached 72 and 96h culture (Table 20), embryo development of the control group approached that of the DMSO group [negative control

Table 20. Triplicate *in vivo* Embryo Development Evaluation In the Presence Of Vemurafenib

Dose	Replicate Number	Kruskal-Willis Mean Rank ANOVA Test of Embryo scorings ±SD			
		24 h	48 h	72 h	96 h
Negative Control[a]	3	19.36 ± 12.07	23.85 ± 13.47	24.31 ± 14.51	28.00 ± 13.55
0.1 % DMSO[b]	3	40.69 ± 18.43 ***	33.09 ± 14.68*	29.74 ± 14.80	32.06 ± 14.49
10 mg/kg Vem.	3	24.55 ± 10.43	23.71 ± 12.60	24.67 ± 12.26	19.31 ± 12.23 **

*** Highly significantly different from negative control, $p \leq 0.001$

** Significantly different from negative control, $p \leq 0.01$

* Different from negative control, $p \leq 0.05$

a. Negative Control: mKBB only without DMSO.

b. 0.1% DMSO: DMSO dissolved in mKBB as final concentration of 0.1% as DMSO control.

24.31 ± 14.51 (72h) and 28.00 ± 13.55 (96h) versus DMSO control 29.74 ± 14.80 (72h) and 32.06 ± 14.49 (96h)], whereas the Vemurafenib group showed a gradual decline of development rate and. a significant delay in embryo development [mean rank score= 19.31 ± 12.23 (96h), $p = 0.007$]. Vemurafenib also clearly prevented hatching of the blastocyst in expanded blastocyst embryos.

Similar to the mean rank score comparisons, the plotted trend of mean rank scores (Figure 15) showed that the embryo development of the 10 mg/kg Vemurafenib injection group, compared with the DMSO and negative control groups, had either offset the stimulating effect of the DMSO or showed a significant decline in embryo development at the early time of culture (24, 48 and 72h). However, 10 mg/kg Vemurafenib injections possibly delay the process and significantly compromise the blastocyst hatching process. 9 ± 3 (53% ± 14%) embryos failed to hatch out of the zona pellucida at 96h post-culture.

Categorized data analyzed by the one-way ANOVA test showed a pattern similar to the mean rank Kruskal-Willis ANOVA analysis. Although no significant differences between experimental and control groups were observed at 48 and 72h, at 24h of culture the one-way ANOVA test revealed that the DMSO group approached the more

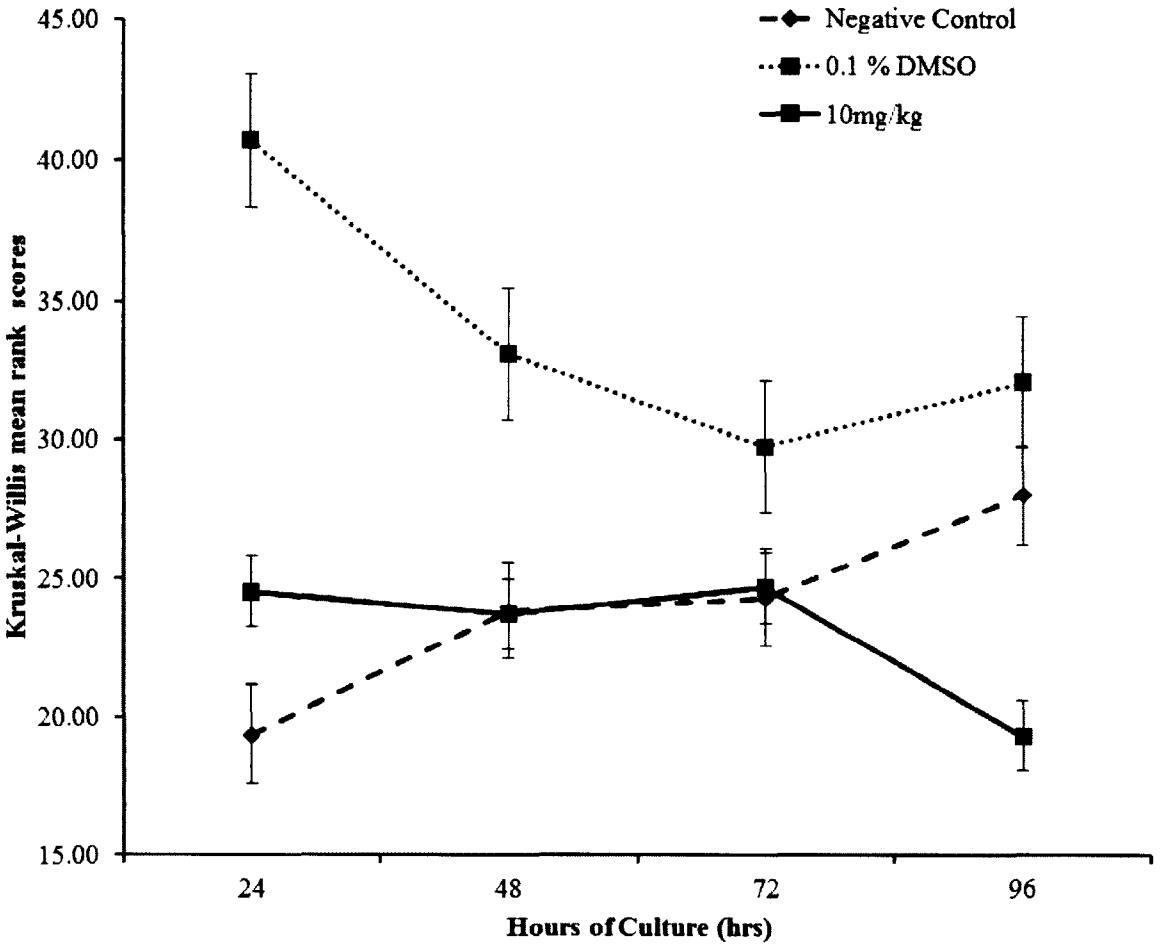

Figure 15. The Plotted Kruskal-Willis Mean Rank Scores Trend

The plotted Kruskal-Willis mean rank scores trend of embryo development after Vemurafenib dam injections at 24, 48, 72 and 96h of culture. The Vemurafenib dam injection group showed a delayed effect on embryo development in the embryo preimplantation stages. Dotted lines and squares represent the mean rank scores and score trend of DMSO control group. The solid line and squares are the mean rank scores and score trend of the Vemurafenib dam injection group. The dashed line and diamonds are the mean rank scores and score trend of the negative control group.

Table 21. Triplicate *in vivo* 24 h Embryo Development Evaluation in the Presence of Vemurafenib Solutions

Groups	Replicate Number	Mean Number of Embryos ±SD (Mean Percentage ±SD)			
		Premorula	Morula-Blastocyst	Hatched	Frag/Deg
Negative Control[a]	3	21 ± 10 (96 ± 3)	1 ± 1 (4 ± 3)	0 ± 0 (0 ± 0)	0 ± 0 (0 ± 0)
0.1 % DMSO[b]	3	5 ± 7 (26 ± 32)***	6 ± 2 (74 ± 32)***	0 ± 0 (0 ± 0)	0 ± 0 (0 ± 0)
10 mg/kg Vem.	3	16 ± 9 (86 ± 10)	2 ± 1 (11 ± 7)	0 ± 0 (0 ± 0)	0 ± 0 (0 ± 0)

*** Highly significantly different from negative control, $p \leq 0.001$

a. Negative Control: mKBB only without DMSO.

b. 0.1% DMSO: DMSO dissolved in mKBB as final concentration of 0.1% as DMSO control.

Table 22. Triplicate *in vivo* 48 h Embryo Development Evaluation in the Presence of Vemurafenib Solutions

Groups	Replicate Number	Mean Number of Embryos ±SD (Mean Percentage ±SD)			
		Premorula	Morula-Blastocyst	Hatched	Frag/Deg
Negative Control[a]	3	0 ± 1 (3 ± 4)	20 ± 12 (87 ± 16)	0 ± 0 (0 ± 0)	0 ± 0 (0 ± 0)
0.1 % DMSO[b]	3	0 ± 0 (0 ± 0)	11 ± 9 (100 ± 0)	0 ± 0 (0 ± 0)	0 ± 0 (0 ± 0)
10 mg/kg Vem.	3	1 ± 1 (2 ± 4)	17 ± 7 (95 ± 4)	0 ± 0 (0 ± 0)	0 ± 0 (0 ± 0)

a. Negative Control: mKBB only without DMSO.

b. 0.1% DMSO: DMSO dissolved in mKBB as final concentration of 0.1% as DMSO control.

Table 23. Triplicate *in vivo* 72h Embryo Development Evaluation in the Presence of Vemurafenib Solutions

Groups	Replicate Number	Mean Number of Embryos ±SD (Mean Percentage ±SD)			
		Premorula	Morula-Blastocyst	Hatched	Frag/Deg
Negative Control[a]	3	0 ± 0 (0 ± 0)	18 ± 7 (83 ± 14)	4 ± 4 (16 ± 14)	0 ± 1 (1 ± 2)
0.1 % DMSO[b]	3	0 ± 0 (0 ± 0)	7 ± 6 (62 ± 22)**	4 ± 4 (38 ± 22)**	0 ± 0 (0 ± 0)
10 mg/kg Vem.	3	0 ± 0 (0 ± 0)	14 ± 8 (80 ± 9)	3 ± 2 (18 ± 12)	0 ± 0 (0 ± 0)

** Highly significantly different from negative control, $p \leq 0.001$

a. Negative Control: mKBB only without DMSO.

b. 0.1% DMSO: DMSO dissolved in mKBB as final concentration of 0.1% as DMSO control.

Table 24. Triplicate *in vivo* 96 h Embryo Development Evaluation in the Presence of Vemurafenib Solutions

Groups	Replicate Number	Mean Number of Embryos ±SD (Mean Percentage ±SD)			
		Premorula	Morula-Blastocyst	Hatched	Frag/Deg
Negative Control[a]	3	0 ± 0 (0 ± 0)	3 ± 2 (16 ± 6)	18 ± 9 (83 ± 6)	0 ± 1 (1 ± 2)
0.1 % DMSO[b]	3	0 ± 0 (0 ± 0)	0 ± 0 (0 ± 0)	10 ± 8 (98 ± 3)	0 ± 1 (2 ± 3)
10 mg/kg Vem.	3	0 ± 0 (0 ± 0)	9 ± 3 (53 ± 14)***	8 ± 6 (44 ± 13)***	2 ± 3 (17 ± 26)

*** Highly significantly different from negative control, $p \leq 0.001$

a. Negative Control: mKBB only without DMSO.

b. 0.1% DMSO: DMSO dissolved in mKBB as final concentration of 0.1% as DMSO control.

advanced stages faster than the Vemurafenib and negative control groups ($p = 0.0006$) stages. At 96h, the group with a 10 mg/kg dose of Vemurafenib injection showed a significant incompetency in blastocyst hatching and delayed progression to an expanded blastocyst. ($p = 0.003$).

Therefore, Vemurafenib injections did not show an acute toxicity. The long half-life of Vemurafenib, cultured only in media after embryo collection, showed a mild and delayed toxic influence throughout embryo development. However, the drug did not show any *in vivo* massive degenerative embryotoxicity in preimplantation embryos.

CHAPTER 4

DISCUSSION

One of the important concerns of the safety of the anticancer drug therapy is whether the drug supports the normal development of the embryo and fetus. Vemurafenib is approved by the FDA as a MM target therapy because of its rapid response and the overall increase of survival rate and free progression period compared with the classical chemotherapeutical agent dacarbazine in malignant melanoma (MM) (Chapman et al., 2011). However, lack of research data and clinical references to Vemurafenib safety has greatly limited the medical treatment options for pregnant, lactating and potentially pregnant MM patients who are urgently seeking effective medications. Therefore, evaluation of the embryo and oocyte toxicity of the anti-melanoma B-Raf^{V600E} inhibitor Vemurafenib is essential to provide an understanding of its benefit to newly pregnant, lactating and potentially pregnant women with MM. We hypothesized that Vemurafenib has detrimental effects on oocyte maturation and/or the embryo development. Results from the tested hypothesis, explanation of the results, and its putative underlying mechanism will be discussed in this chapter.

4.1 Impacts on *Ex Vivo* Oocyte Maturation, Spindle-Chromosome Behavior and DNA Integrity

The tested hypothesis was that Vemurafenib produced detrimental effects on *ex vivo* mouse oocyte maturation from the GV-intact oocyte to the MII arrest, as well as spindle apparatus formation, chromosomal alignment, and DNA integrity.

After 16h of culture, the majority of oocytes from 10 μM to the 0.1% DMSO control successfully progressed to the MII-arrest stage. All oocytes in the negative control group progressed to the MII-arrest stage. Only a few oocytes in these groups were confined to GV-intact, MI and Fragmented/Degenerated stages. Most of the oocytes in the 100 μM group were arrested at the MI stage [5 ± 2 (36% ± 10%) versus 0

± 1 (2% ± 4%) at MI stage]. The difference between the MI and Control groups showed that the majority of oocytes were incompetent to mature into MII-arrest stage and that fragmentation and degeneration could also be seen in this group. The 100 μM group displayed a pattern similar to the positive control group, which produced a clear oocyte toxic effect. A significant oocyte toxic effect had been observed at 100 μM. One hundred μM Vemurafenib caused 8 ± 3 (54% ± 16%) spindle formation abnormalities, and the majority (72% ± 13%) of chromosome misalignments (Table 8). At concentrations of 1 μM or lower, almost all oocytes progressed to the MII-arrest stage with barrel shaped spindle fibers and correctly aligned chromosomes.

Morphologically normal 10 μM Vemurafenib oocytes showed 8 ± 0 (53% ± 0%) chromosome misalignment (P=0.0009) after 16h Vemurafenib exposure. An additional 31% ± 6% increase in incompetency of the MII-arrest oocyte number --added to the pool of GV-intact, MI and Fragmented/ Degenerated oocytes at the 10 μM level--revealed the underlined oocyte toxicity on the spindle formation and chromosome alignment, in which 24% ± 11% of oocytes were incapable for further developmental events. We observe that the higher the concentration, the greater the number of oocytes confined at MI stages.

Similarly, 100 μM Vemurafenib produced 82% ± 4% of DNA fragmentations. In 1 μM Vemurafenib or lower, almost all MII-arrest oocytes demonstrated a negative response to the DNA damage effect of Vemurafenib. However, morphologically-normal MII-arrest oocytes with disintegration of DNA in 10 μM Vemurafenib contributed to an additional 33% weight to the actual incompetency of MII-arrest oocytes, with 10 μM showing clear toxicity to the oocyte DNA.

The Ras/C-Raf MAPK pathway acts as an important self-enhancing and self-promoting system. The pathway is involved in MPF synthesis and activation, which in turn affects GVBD and MII progression. The MAPK pathway also actively participates in spindle apparatus formation and chromosome alignment. Specifically, the MAPK pathway has been shown to be involved in Microtubule Organizing Center (MTOC) formation in mouse oocyte maturation (Verlhac et al., 1994). The spatial co-localization of MAPK with the metaphase spindle during meiosis I to II transition indicates a close relationship between them in the mouse oocyte (Hatch et al., 2001; Lee et al., 2000). Several studies of the mouse oocyte have found that the genetic knockouts along the

MAPK pathway (like Mos, Erk2) showed a failure to achieve the normal spindle assembly (Araki et al., 1996; Bodart et al., 2002; Choi et al., 1996; Zhao et al., 1991). Moreover, recent research shows that 75% MAPK activity causes a disturbed spindle with dispersed chromosomes, whereas 45% MAPK activity leads to a disintegrated spindle with scattered chromosomes. A disturbed spindle apparatus and unaligned chromosomes triggers apoptotic events and results in fragmentation of the DNA molecule. Not only are 10 μM and 100 μM Vemurafenib a B-Raf inhibitor, but also C-Raf, which is the main component of the MAPK pathway, is inhibited. Therefore, 10x and 100x Vemurafenib concentrations were shown to lead to spindle disturbance, chromosome misalignment, and DNA damage.

4.2 Impacts on *Ex Vivo* 1C Embryo Development and Quality

The tested hypothesis was that Vemurafenib produced detrimental effects on *ex vivo* 1C mouse embryo development and Mek 1/2 phosphorylation through C-Raf activity.

The concentrations below 10 μM, which was 10X the therapeutic concentration or lower, did not appear to be significantly different compared with control groups at 38, 62, 86 and 110h (Table 13).

A significant toxic effect on embryo development was observed at the 100 μM level, with no embryos reaching the blastocyst hatching stage. Toxicity was observed at the very beginning of drug exposure (Mean rank score 100 μM (33.73 ± 10.92) versus a negative control rate (63.57 ± 14.07), 38h after culture, pairwise $p \leq 0.0001$). Embryos showed massive fragmentation and degeneration (mean rank score 100 μM (33.73 ± 10.92) compared with the positive control (30.30 ± 11.64)) at 38h after culture. Toxicity remained to the end of 110h observation frame.

The categorized data analyzed he general trend by the one-way ANOVA test, showed a pattern similar to the mean rank Kruskal ANOVA analysis. At 62h of culture, not only did 100 μM Vemurafenib show high toxicity in embryo development, but also 10 μM Vemurafenib demonstrated a delay in embryo development, during which most of the embryos were at 7C or 8C stage (Table 14). However, the 10 μM group recovered the rate of embryo development as the time elapsed.

In the 1C p-Mek 1/2 IF assay, developmental morphology of 1C to 2C was again evaluated. Similarly, embryos in 100 μM Vemurafenib showed 7 ± 3 (49% ± 6%) were unable to progress to 2C, and within 2C stage cells, 4 ± 1 2C embryos appeared to have either unequal blastomeres or a prominent perivitelline space. The 10 μM or lower Vemurafenib showed no obvious morphological toxicity compared with control groups. However, 2 and 4, respectively, from 1 μM and 10 μM morphologically normal embryos showed negative responses to the Mek 1/2 phosphorylation by C-Raf, giving a difference of 2% and 17%, respectively, of abnormal morphology when compared to the normal 2C embryos. In addition to 1C and Frag/ Deg embryos, 100 μM and 10 μM showed a phosphorylation inhibition of p-Mek 1/2, decrease of C-Raf activity, and clear toxicity to the 1C to 2C transition of embryos.

All abnormal 2C showed negative p-Mek 1/2 and were incompetent to develop through the preimplantation stages. More than 80% of named "negative" p-Mek 1/2 showed diminished fluorescence, which was an incomplete block of the C-Raf activity but proved to be unable to support embryo development.

The Ras/C-Raf/Mek MAPK pathway functions as the downstream effectors of the FGF receptor and other Receptor Tyrosine Kinase (RTK) receptors. Ras inhibitions halted the mouse embryo in the early 2C stage and could be completely recovered by constitutive transduction of the C-Raf molecule. C-Raf is the downstream effector of Ras in the embryo development (Yamauchi et al., 1994). Later experiments showed that phosphorylated C-Raf activation was found in the M-phase-specific cell cycle in early cleavage stage of 2C embryos (Haraguchi et al., 1998). Membrane localization in active pC-Raf in embryonic day 2.5 indicates that C-Raf activates the MAPK pathway from the cell membrane instead from the nucleus as usual (Wang et al., 2004). Further, phosphorylation of Mek, the only downstream effector of C-Raf, was shown to be expressed in the preimplantation embryo (Liu et al., 2004). C-Raf was shown to be one of six causes of lethal null post-implantation mutations, resulting in the post-implantation or placental lethality (Yufen Xie et al., 2005). Therefore, 10x and 100x Vemurafenib concentrations inhibit C-Raf activity and led to abnormal 2C formation. However, 1 μM Vemurafenib appears to nontoxic to the *ex vivo* 1C embryo transition to 2C and p-Mek 1/2 by complete C-Raf activity.

The 10 μM Vemurafenib-exposed embryos in *ex vivo* culture progressed with no significant morphological toxicity to the blastocyst hatching stage; however, the p-Mek 1/2 IF assay proved to be significantly different from the control group. This difference indicated that some 2C could still survive. Other pathways may bypass the MAPK pathway blocking effects of the embryo.

4.3 Impacts on *In Vivo* 1C Embryo Development and Quality

The current study tested the hypothesis that Vemurafenib possessed detrimental effects on 2C mouse embryo development after multiple *in vivo* 10 mg/kg Vemurafenib dam's injections.

Results showed that a stimulating effect on embryos had been observed in the DMSO group (Mean rank score DMSO control (40.69 ± 18.43) versus negative control (19.36 ± 12.07), pairwise $p \leq 0.001$) at 24 and 48h of culture. However, the experimental group in which Vemurafenib was dissolved by DMSO lost this stimulating effect and showed a similar rate of development as the negative control group (Mean rank score 10 mg/kg Vemurafenib (24.55 ± 10.43) versus negative control (19.36 ± 12.07), pairwise P=0.263). As the time progressed from 72 to 96h culture, embryo development of the control group recovered the of the DMSO group [negative control 24.31 ± 14.51 (72h) and 28.00 ± 13.55 (96h) versus DMSO control 29.74 ± 14.80 (72h) and 32.06 ± 14.49 (96h)]. The 10 mg/kg therapeutic dose of Vemurafenib showed a delay in embryo development in earlyh of culture, a gradual decline in the development rate, and significant delay in embryo development (mean rank score= 19.31 ± 12.23 (96h), P=0.007). Vemurafenib also caused 9 ± 3 (53% ± 14%) embryos to fail to hatch out of the zona pellucida and eventually to collapse. The categorized data analyzed by one-way ANOVA showed a similar pattern of the mean rank Kruskal-Willis ANOVA analysis.

4.4 Future Work

The question of whether normal looking 2C embryos of the incomplete p-Mek 1/2 blockage are capable of future developmental is yet not answered. Also, a detailed study of the mechanism of a delayed effect (collapsed embryos) of *in vivo* Vemurafenib

injections is required to assure the toxicity-free effect to the preimplantation embryo and oocyte. This current research did not provide all safety information for the post-implantation stage of embryo and fetal development. Because all oocytes have already completely formed in female's fetus stage, any permanent damage to the oocytes will remain in her reproductive age and cause potential incompetency of pregnancy. Research on toxicity of Vemurafenib on oocyte competency by testing post-implantation embryo and fetus in multiple ending pregnancy test will show clear evidence of oocyte permanent damage by Vemurafenib exposure. Therefore, assessments and data for fetal and/or childhood organ and systemic differentiations, development, and function are required to address the safety of the drug. The risk of congenital malformations also needs to be ruled out if embryogenesis occurred after exposure of cytotoxic drugs. Further developmental evaluation, toxicity mechanisms and combinational therapies for the drug must be addressed. Finally, since some aneuploidy such as blastocysts with Down's Syndrome (trisomy 21), Patau Syndrome (13 trisomy), Edward Syndrome (18 trisomy), Klinefelter Syndrome (extra X in males), Turner Syndrome (lack of one X in females)) have perfectly normal morphology, detailed mechanism researches about chromosome karyotype analysis should be performed to rule out the possibilities of chromosome abnormality under the influence of Vemurafenib.

4.5 Dissertation Significance

Although 46 ongoing Vemurafenib clinical trials are being conducted and multiple studies on pharmacological mechanisms, efficiency, toxicities and resistance of Vemurafenib have been completed, none related mouse oocyte maturation toxicity and embryo toxicity to Vemurafenib exposure. This lack of research data on the potential toxicity of Vemurafenib in MM patients has caused doctors to be hesitant to prescribe or even suggest this first-line drug to the pregnant, lactating and potentially-pregnant woman with MM. The current study evaluated Vemurafenib exposure on mouse oocyte maturation and embryo toxicity. Results will enhance our understanding of whether Vemurafenib is suitable for pregnant, lactating and potentially-pregnant patients with MM. Such information is a critical benefit for women facing the legal issues of abortion,

the family expectation on having offspring, time urgency and, most importantly, drug safety on oocyte, embryo and fetal development and maturation. This study suggests many further directions of Vemurafenib exposure upon (1) mouse embryo implantation in the uterus; (2) mouse embryo post-implantation and fetal toxicity and teratogenicity including, organ and systemic differentiations, development and functionalities; (3) cytogenic, histological and molecular biological mechanisms of the above toxicity and teratogenicity; (4) future toxicological studies concerning larger animals; (5) future clinical trials of Vemurafenib effects on human oocyte maturation, embryo and fetal toxicity, and teratogenicity; (6) detailed cytogenic, histological and molecular biological mechanism study for postpartum infant evaluation; and (7) evaluation of potential childhood psychological, intellectual and organ growth development.

CHAPTER 5

CONCLUSIONS

The current research hypothesized that Vemurafenib causes detrimental effects on oocyte maturation and/or embryo development.

Aim 1 sought to determine whether Vemurafenib produced detrimental effects on *ex vivo* mouse oocyte maturation from the GV-intact oocyte to MII arrest, as well as spindle apparatus formation, chromosomal alignment, and DNA integrity. Results showed that 10 μM and higher toxicities to the oocyte disturb spindle apparatus formation and cause chromosomal misalignment and DNA damage. The higher the concentration, the more the oocytes are confined at MI stages whereas 1 μM Vemurafenib, the therapeutic concentration, does not possess significant oocyte morphological toxicity in *ex vivo* oocytes. Concentrations of 10x and 100x Vemurafenib lead to spindle disturbance, chromosome misalignment and DNA damage. But the therapeutic concentration of the Vemurafenib appears to be nontoxic to the *ex vivo* oocyte maturation, spindle formation, chromosome alignment and DNA integrity. TC_{50} is considered as 10 μM, whereas NC is 1 μM. This study did not study whether Vemurafenib at therapeutic concentrations promoted aneuploidy oocytes which will be relevant for future healthy embryo development.

Aim 2 sought to determine whether Vemurafenib possessed detrimental effects on *ex vivo* 1C mouse embryo development and Mek 1/2 phosphorylation through C-Raf activity. Results showed that 100 μM and 10 μM concentrations produced the phosphorylation inhibition of p-Mek 1/2, a decrease of C-Raf activity, and clear toxicity to the 1C to 2C transition of embryos. All abnormal 2C showed negative p-Mek 1/2 and were incompetent to develop through the preimplantation stages. However, Vemurafenib in 1 μM concentration is no significant morphological toxicity on *ex vivo* preimplantation 1C embryo development; especially, on the *ex vivo* 1C to 2C embryo transition and p-Mek 1/2 by complete C-Raf activity was observed. TC_{50} is considered as 10 μM, whereas NC is 1 μM.

Aim 3 sought to determine whether Vemurafenib produced detrimental effects on 2C mouse embryo development after *in vivo* multiple 10 mg/kg Vemurafenib dam injections. The results showed that the 10 mg/kg Vemurafenib dam injections did not produce an acute toxicity. The long half-life of Vemurafenib showed only a mild delayed toxic influence (delay effect) throughout embryo development. However, most of the embryos could progress to at least normal blastocysts and did not show any *in vivo* massive degenerative embryotoxicity in preimplantation embryos.

Finally, this research concludes that Vemurafenib in a therapeutic concentration was free of *ex vivo* oocyte and embryo morphological toxicity, but *in vivo* toxicity on mechanisms and survivability of collapsed unhatched embryos requires further clarification.

REFERENCES

Ackerman, S., Swanson, R., Adams, P. et al. (1983), .Comparison of strains and culture media used for mouse *in vitro* fertilization. Gamete Res. *7*, 103-109.

Ackerman S, Taylor S., Swanson R. (1984). Mouse embryo culture for screening in human IVF. Arch. Androl. *12*, 129-134.

Amelia Lissia and Antonio Cossu. (2013). Targeted Therapies in Melanoma: Successes and Pitfalls In: Melanoma - From Early Detection to Treatment" Chapter 2.

Angell RR, Xian J, Keith J, Ledger W, Baird DT. (1994). First meiotic division abnormalities in human oocytes: mechanism of trisomy formation. Cytogenet Cell Genet. *65*:194-202.

Araki, K., Naito, K., Haraguchi, S., Suzuki, R., Yokoyama, M., Inoue, M., Aizawa, S., Toyoda, Y., Sato, E. (1996). Meiotic abnormalities of c-mos knockout mouse oocytes: activation after first meiosis or entrance into third meiotic metaphase. Biol. Reprod. *55*, 1315–1324.

Artavanis-Tsakonas S, Rand MD & Lake RJ (1999) Notch signaling: cell fate control and signal integration in development. Science *284*, 770–776.

ASRM: American society for reproductive medicine. (1992). Guidelines for human embryology and andrology laboratories. Fertility and Sterility. *58*, (4); 9S.

Barrett, C. B., Schroetke, R. M., Van der Hoorn, F. A., Nordeen, S. K., and Maller, J. L. (1990), Ha-rasVal-12,Thr-59 activates S6 kinase and p34 cdc2 kinase in Xenopus oocytes: evidence for c-mosxe-dependent and -independent pathways. Mol. Cell. Biol. *10*, 310–315.

Bastias, M., C, McGee-Belser, S., T., Bryan, S., H., and Vasquez, J., M. (1993). *In vitro* deleterious effect of hypoxanthine in ham's nutrient medium and early embryonic development. Fertility and Sterility, *60*(5), 876-880.

Bayne RAL, Eddie SL, Collins CS, Childs AJ, Jabbour HN, Anderson RA. (2009). Prostaglandin E2 as a regulator of germ cells during ovaria0n development. J Clin Endocrinol Metab. *94*:4053-60.

Bodart J.-F.L., F.Y. Baert, C. Sellier, N.S. Duesbery, S. Flament, J.-P. Vilain. (2005). Differential roles of p39Mos–Xp42Mpk1 cascade proteins on Raf1 phosphorylation and spindle morphogenesis in Xenopus oocytes. Developmental Biology. *283*, 373-383.

Bodart, J.F., Gutierrez, D.V., Nebreda, A.R., Buckner, B.D., Resau, J.R., Duesbery, N.S. (2002). Characterization of MPF and MAPK activities during meiotic maturation of Xenopus tropicalis oocytes. Dev. Biol. *245*, 348– 361.

Bollag G, Hirth P, Tsai J, Zhang J, Ibrahim PN, Cho H, Spevak W, Zhang C, Zhang Y, Habets G, Burton EA, Wong B, Tsang G, West BL, Powell B, Shellooe R,Marimuthu A, Nguyen H, Zhang KY, Artis DR, Schlessinger J, Su F, Higgins B, Iyer R, D'Andrea K, Koehler A, Stumm M, Lin PS, Lee RJ, Grippo J, Puzanov I, Kim KB, Ribas A, McArthur GA, Sosman JA, Chapman PB, Flaherty KT, Xu X, Nathanson KL, Nolop K. (2010). Clinical efficacy of a RAF inhibitor needs broad target blockade in B-RAF-mutant melanoma. Nature. *467*, 596-599.

Bolton, V. N., P. J. Oades, and M. H. Johnson. (1984). The relationship between cleavage, DNA replication, and gene expression in the mouse 2-cell embryo. J. Embryol. Exp. Morphol. *79*:139-163.

Borysov SI, Guadagno TM. (2008). A novel role for Cdk1/Cyclin B in regulating B-Raf activation at mitosis. Molecular Biology of the Cell. *19*, 2907–2915.

Braude, P., H. Pelham, G. Flach, and R. Lobatto. (1979). Posttranscriptional control in the early mouse embryo. Nature, *282*:102-105.

Brunet S, Maro B. (2007). Geminal vesicle position and meiotic maturation in mouse oocyte. Reproduction. *133*:1069-72.

Chapman PB, Hauschild A, Robert C. (2011). Improved survival with Vemurafenib in melanoma with B-RafV600E mutation. N Engl J Med. *364* 2507-2516.

Chapman, P. (2009). Early efficacy signal demonstrated in advanced melanoma in a phase I trial of the oncogenic B-Raf-selective inhibitor PLX4032. Eur. J. Cancer. *7*, 5.

Choi, T., Rulong, S., Resau, J., Fukasawa, K., Matten, W., Kuriyama, R., Mansour, S., Ahn, N., Vande Woude, G.F. (1996). Mos/mitogen activated protein kinase can induce early meiotic phenotypes in the absence of maturation-promoting factor: a novel system for analyzing spindle formation during meiosis I. Proc. Natl. Acad. Sci. *93*, 4730– 4735.

Conaghan J, Hardy K, Handyside AH, Winston RM, (1993). Leese HJ. Selection criteria for human embryo transfer: a comparison of pyruvate uptake and morphology. J Assist Reprod Genet, *10*:21-30

Condon-Mahony, M., Wortham Jr., J., W., E., Bundren, J., C., Witmyer, J., Shirley, B. (1986). Evaluation of human fetal cord sera, ham's F10 medium, and *in vitro* culture materials with a mouse *in vivo* fertilization system. Fertility and Sterility. *44(4)*. 521-525.

Conti M, Andersen CB, Richard F, Mehats C, Chun SY, Horner K, Jin C, Tsafriri A. (2002). Role of cyclic nucleotide signaling in oocyte maturation. Mol Cell Endocrinol. *187*,153-9.

Crowson, AN; Haskell, H. (2013). The role of sentinel lymph-node biopsy in the management of cutaneous melanoma. Giornale italiano di dermatologia e venereologia : organo ufficiale, Societa italiana di dermatologia e sifilografia. *148*, 493–9.

Dandekar, P., V. and Quigley, M., M. (1984). Laboratory setup for human *in vitro* fertilization. Fertility and Sterility. *42*(1), 1-11.

Davies H, Bignell GR, Cox C. (2002). Mutations of the B-Raf gene in human cancer. Nature. *417*, 949–954.

Dhomen, N. & Marais, R. (2007). New insight into B-Raf mutations in cancer. Curr. Opin. Genet. Dev. *17*, 31–39.

Dhomen, N. (2009). Oncogenic B-Raf induces melanocyte senescence and melanoma in mice. Cancer Cell. *15*, 294–303.

Downs SM & Eppig JJ (1984). Cyclic adenosine monophosphate and ovarian follicular fluid act synergistically to inhibit mouse oocyte maturation. Endocrinology. *114*, 418–427.

Downs SM, Coleman DL, Ward-Bailey PF & Eppig JJ (1985). Hypoxanthine is the principal inhibitor of murine oocyte maturation in a low molecular weight fraction of porcine follicular fluid. PNAS. *82*, 454–458.

Durlinger AL, Gruijters MJ, Kramer P, Karels B, Ingraham HA, Nachtigal MW, et al. (2002). Anti-Mullerian hormone inhibits initiation of primordial follicle growth in the mouse ovary. Endocrinology. *143*:1076-84.

Eichenlaub-Ritter U; Chandley AC; Gosden RG. (1986). Alterations to the microtubular cytoskeleton and increased disorder of chromosome alignment in spontaneously ovulated mouse oocytes aged *in vivo*: an immunofluorescence study. Chromosoma. *94*, 337-45.

Eichenlaub-Ritter, U. and Betzendahl, I. (1995). Chloral hydrate induced spindle aberrations, metaphase I arrest, and aneuploidy in mouse oocytes. Mutagenesis. *10*, 477-486.

Eichenlaub-Ritter, U. and Boll, I. (1989). Nocodazole sensitivity, age-related aneuploidy, and alternation in cell cycle during maturation of mouse oocytes. Cytogenet. Cell Genet. *52*, 170-176.

Eppig JJ, Vivieros MM, Marin-Bivens C, De La Fuente R. (2004). Regulation of mammalian oocyte maturation. In: The Ovary. Ed PCK Lueng and EY Adashi. Elsevier Academic Press. 113-29

Ernstoff MS, Christopher PG, Tretter MD, Titus-Ernstoff L. (2003). Update: Medical therapy for cutaneous melanoma. Am Soc Clin Oncol. 198–207.
Fan, H.Y., Tong, C., Lian, L., Li, S.W., Gao, W.X., Cheng, Y., Chen, D.Y., Schatten, H., Sun, Q.Y. (2003). Characterization of ribosomal S6 protein kinase p90rsk during meiotic maturation and fertilization in pig oocytes: mitogen-activated protein kinase-associated activation and localization. Biol. Reprod. *68*, 968–977.

FDA Center for Drug Evaluation and Research, clinical pharmacology and biopharmaceutics review(s). http://www.accessdata.fda.gov/drugsatfda_docs/nda/2011/202429Orig1s000ClinPharmR.pdf. Accessed March 1,2012.

Fisher, D. L., Brassac, T., Galas, S., and Doree, M. (1999). Dissociation of MAP kinase activation and MPF activation in hormone-stimulated maturation of Xenopus oocytes. Development. *126*, 4537–4546.

Flach, G., M. H. Johnson, P. R. Braude, R. A. S. Taylor, and V. N. Bolton. (1982). The transition from maternal to embryonic control in the 2-cell mouse embryo. EMBO J. *1*, 681-686.

Flaherty, K. (2009). Phase I study of PLX4032: Proof of concept for V600E B-Raf mutation as a therapeutic target in human cancer. J. Clin. Oncol. *27*, 9000.

Fleming, T., P., Pratt, H., P., M., and Braude, P., R. (1987). The use of mouse preimplantation embryos for quality control of culture reagents in human *in vitro* fertilization programs: a cautionary note. Fertility and Sterility, *47(5)*, 858-860.

Fre´de´ ric Baert, Jean-Franc¸ois Bodart‡, Be´atrice Bocquet-Muchembled§, Arlette Lescuyer-Rousseau, and Jean-Pierre Vilain. (2003). p42Mpk1 Activation Is Not Required for Germinal Vescicle Breakdown but for Raf Complete Phosphorylation in Insulin-stimulated Xenopus Oocytes. biol chem J. *278*, 49714–49720.

G. Bradley Alsop and Dahong Zhang. (2003). Microtubules are the only structural constituent

Gardner DK, Lane M, Stevens J, Schoolcraft WB. (2001). Noninvasive assessment of human embryo nutrient consumption as a measure of developmental potential. Fertil Steril, *76*:1175-80

Gautier J, Solomon MJ, Booher RN, Bazan JF, Kirschner MW. (1991). Cdc25 is a specific tyrosine phosphatase that directly activates p34cdc2. Cell. *67*:197-211.

Gershon E, Plaks V, Dekel N. (2008). Gap junctions in the ovary: expression, localization and function. Mol Cell Endocrinol. *282*:18-25.

Gross VS, Hess M & Cooper GM. (2005). Mouse embryonic stem cells and preimplantation embryos require signaling through the phosphatidylinositol 3-kinase pathway to suppress apoptosis. Mol Reprod Dev *70*, 324–332.
Hallare A, Nagel K, Köhler HR, Triebskorn R. (2006). Comparative embryotoxicity and proteotoxicity of three carrier solvents to zebrafish (Danio rerio) embryos. Ecotoxicol Environ Saf. Mar. *63*, 378-88.

Hansson EM, Lendahl U & Chapman G. (2004). Notch signaling in development and disease. Semin Cancer Biol. *14*, 320–328.

Hassold T and Hunt P. (2001). To err (meiotically) is human: the genesis of human aneuploidy. Nature Rev. *2*:280-91.

Haraguchi S, Naito K, Sato E. (1998) MAP kinase cascade, but not Erks, activated during early cleavage of mouse embryos. Mol Reprod Dev. *51*, 148–155.

Hartshorne GM, Lyrakou S, Hamoda H, Oloto E, Ghafari F. (2009). Oogenesis and cell death In human prenatal ovaries: what are the criteria for oocyte selection? Mol Hum Reprod. *15*:805-19.

Hatch, K.R., Capco, D.G. (2001). Co-localization of CaM KII and MAP kinase on architectural elements of the mouse egg: potentiation of MAP kinase activity by CaM KII. Mol. Reprod. Dev. *58*, 69– 77.

Hatzivassiliou, G. (2010). Raf inhibitors prime wild-type Raf to activate the MAPK pathway and enhance growth. Nature. *464*, 431–435.

Hedge G, Colby HD, Goodman BL. (1987). Clinical Endocrinology. W.B. Saunders, Phila London pp. 400.

Heidorn, S. J. (2010). Kinase-dead B-Raf and oncogenic Ras cooperate to drive tumor progression through C-Raf. Cell. *140*, 209–221.

Hingorani, S. R., Jacobetz, M. A., Robertson, G. P., Herlyn, M. & Tuveson, D. A. (2003). Suppression of B-RafV599E in human melanoma abrogates transformation. Cancer Res. *63*, 5198–5202.

Hogan B, Beddington R, Constantini F, Lacy B. (2002). Manipulating the mouse embryo, a laboratory manual. Cold Spring Harbor, NY: Cold Spring Harbor Laboratory Press.

Iwashita, J., Shima, H., Nagao, M., Sagata, N. (1997). cDNA cloning of a novel B subunit of Xenopus protein phosphatase 2A and its biological activity in oocytes.. Biochem. Biophys. Res. Commun.

Jashoman Banerjee1, Dhiman Maitra1, Michael P. Diamond1 and Husam M. Abu-Soud1,2. (2012). Melatonin prevents hypochlorous acid-induced alterations in microtubule and chromosomal structure in metaphase-II mouse oocytes. J. Pineal Res. *53*:122–128.

Kalma Y, Granot I, Galiani D, Barash A, Dekel N. (2004). Luteinizing hormone induced connexin 43 down regulation: inhibition of transation. Endocrinology. *145*:1617-24.

Keller G. (2005). Embryonic stem cell differentiation: emergence of a new era in biology and medicine. Genes Dev. *19(10)*:1129-55.

Knofler M, Vasicek R, Schreiber MKey. (2001). regulatory transcription factors involved in placental trophoblast development--a review. Placenta, Suppl A. S83-92

Langagergaard V. (2011). Birth outcome in women with breast cancer, cutaneous MM, or Hodgkin's disease: a review. Clinical epidemiology. *3*, 7-19.

Latham, K. E., J. I. Garrels, C. Chang, and D. Solter. (1991). Quantitative analysis of protein synthesis in mouse embryos. I. Extensive reprogramming at the one- and two-cell stages. Development. *112*:921-932.

Lee, J., Miyano, T., Moor, R.M. (2000). Localisation of phosphorylated MAP kinase during the transition from meiosis I to meiosis II in pig oocytes. Zygote. *8*, 119–125.

Lefebvre, C., Terret, M.E., Djiane, A., Rassinier, P., Maro, B., Verlhac, M.H. (2002). Meiotic spindle stability depends on MAPK-interacting and spindle-stabilizing protein (MISS), a new MAPK substrate. J. Cell Biol. *157*, 603– 613.

Lens M, Bataille V. (2008). Melanoma in relation to reproductive and hormonal factors in women: current review on controversial issues. Cancer Causes Control.*19*, 437–442.

Liu J, Puscheck EE, Wang F, Trostinskaia A, Barisic D, Maniere G, Wygle D, Zhong W, Rings EHHM, Rappolee DA. (2004). Serine-threonine kinases and transcription factors active in signal transduction are detected at high levels of phosphorylation during mitosis in preimplantation embryos and trophoblast stem cells. Reproduction. *128*, 643–654.

Liu, L. and Keefe, D. (2002). Ageing-associated aberration in meiosis of oocytes from senescence-accelerated mice. Hum. Reprod. *17*, 2678-2685.

Lloyd S, Fleming TP & Collins JE. (2003). Expression of Wnt genes during mouse preimplantation development. Gene Expr Patterns. *3*, 309–312.

Machtinger R, Racowsky C. (2013). Morphological systems of human embryo assessment and clinical evidence. Reprod BioMed Online. *99*, 667-672.

Maekawa M, Yamamoto T, Tanoue T, Yuasa Y, Chisaka O & Nishida E. (2005). requirement of the MAP kinase signaling pathways for mouse preimplantation development. Development. *132*, 1773–1783.

Maekawa M, Yamamoto T, Kohno M, Takeichi M, Nishida E. (2007). Requirement for Erk MAP kinase in mouse preimplantation development. Development. *134*, 2751–2759. Mahmoud, Nervana Talaat-Elsebaei. (2003) Embryo and Gamete Development upon Exposure to CCA components: CrO_3, CuO and As_2O_5. ProQuest Dissertation and Theses.

Makabe S, Naguro T, Stallone T. (2006). Oocyte-follicle cell interactions during ovarian follicle development, as seen by high resolution scanning and transmission electron microscopy in humans. Microsc Res Tech. *69*:436-49.

Margulis S, Abir R, Felz C, Nitke S Krissi H, Fisch B. (2009). Bone morphogenetic protein 15 expression in human ovaries from fetuses, girls and women. Fertil Steril. *92*:1666-73.

Maro B, Kubiak JZ, Verlhac MH, Winston NJ. (1994). Interplay between the cell cycle control machinery and the microtubule network in mouse oocytes. Seminars Dev Biol. *5*:191-8.

Masatoshi Hara, Yusuke Abe, Toshiaki Tanaka, Takayoshi Yamamoto, Eiichi Okumura & Takeo Kishimoto. (2013). Greatwall kinase and cyclin B-Cdk1 are both critical constituents of M-phase-promoting factor. Nature Communications. *3*, 1059.

Masui Y, Markert CL (1971). Cytoplasmic control of nuclear behavior during meiotic maturation of frog oocytes. J Exp Zool. *177*, 129-145.

Maton, G., Lorca, T., Girault, J.A., Ozon, R., Jessus, C. (2005). Differential regulation of Cdc2 and Aurora-A in Xenopus oocytes: a crucial role of phosphatase 2A. J. Cell. Sci.

McDowell, J., S., Swanson, R., J., Maloney, M., Veeck, L. (1988). Mouse embryo quality control for toxicity determination in the Norfolk *in vitro* fertilization program. Journal of In Vitro Fertilization and Embryo Transfer. *5*, 144-148.

Michaloglou, C. (2005). B-RafE600 associated senescence-like cell cycle arrest of human nevi. Nature. *436*, 720–724.

Mikula M, Schreiber M, Husak Z, Kucerova L, Ruth J, Wieser R, Zatloukal K, Beug H, Wagner EF, Baccarini M. (2001). Embryonic lethality and fetal liver apoptosis in mice lacking the c-raf-1 gene. EMBO J. *20*,1952–1962.

Munne S, Magli C, Cohen J, Morton P, Sadowy S, Gianaroli L, et al. (1999). Positive outcome after preimplantation diagnosis of aneuploidy in human embryos. Hum Reprod. *14*, 2191-2199.

Muslin AJ; MacNicol AM; Williams LT. (1993). Raf-1 protein kinase is important for progesterone-induced Xenopus oocyte maturation and acts downstream of mos. Mol Cell BiolVol. *13*, 4197-202.

Naz, R., K., Janousek, J., T., Moody, T., and Stillman, R., J. (1986). Factors influencing murine embryo bioassay: effect of proteins aging of medium, and surgical glove coatings. Fertility and Sterility. *46(5)*, 914-919.

Nebreda, A.R., Hunt, T. (1993). The c-mos proto-oncogene protein kinase turns on and maintains the activity of MAP kinase, but not MPF, in cellfree extracts of Xenopus oocytes and eggs. EMBO J. *12*, 1979–1986.

Negoescu A, Guillermet C, Lorimier P, Brambilla E, Labat-Moleur F. (1998). Importance of DNA fragmentation in apoptosis with regard to TUNEL specificity. Biomed Pharmacother. *52* (6): 252–8

Nurse P; Masui Y; Hartwell L, Nature Medicine. (1998). Understanding the cell cycle. Nat. Med. *4*, 1103–1106.

Oh JS1, Han SJ, Conti M. (2010). Wee1B, Myt1, and Cdc25 function in distinct compartments of the mouse oocyte to control meiotic resumption. J Cell Biol. *188*, 199-207.

Paliga AJ, Natale DR & Watson AJ. (2005). p38 mitogen-activated protein kinase (MAPK) first regulates filamentous actin at the 8–16-cell stage during preimplantation development. Biol Cell. *97*, 629–640.

Palmer, A., Gavin, A. C., and Nebreda, A. R. (1998). A link between MAP kinase and p34(cdc2)/cyclin B during oocyte maturation: p90(rsk) phosphorylates and inactivates the p34(cdc2) inhibitory kinase Myt1. EMBO J. *17*, 5037–5047.

Pangas SA. (2012). Regulation of the ovarian reserve by members of the Transforming Growth Factor Beta family. Mol Reprod Dev. *79*, 666-79.

Pavlidis NA. (2002). Coexistence of pregnancy and malignancy. Oncologist. 7, 279-87.

Peters H, McNatty KP. (1980). Chapter 6. Ovulation. In: The Ovary. Univ. of California press. Berkly and Los Angeles.

Poueymirou, W. T., and R. M. Schultz. (1989). Regulation of mouse preimplantation development: inhibition of synthesis of proteins in the two-cell embryo that require transcription by inhibitors of cAMP-dependent protein kinase. Dev. Biol. *133*:588-599.

Poulikakos, P. I., Zhang, C., Bollag, G., Shokat, K. M. & Rosen, N. (2011). Raf inhibitors transactivate Raf dimers and Erk signaling in cells with wild-type B-Raf. Nature *464*, 427–430.

Pratt, H. P. M., V. N. Bolton, and K. A. Gudgeon. (1983). The legacy from the oocyte and its role in controlling early development of the mouse embryo. Ciba Found. Symp. *98*:197-227.

Qing-Yuan Sun, Yi-Liang Miao and Heide Schatten. (2009). Towards new understanding on the regulation of mammalian oocyte meiosis resumption. Cell Cycle. *8*:17, 2741-2747

Richardson SJ, Senikas V, Nelson JF. (1987). Follicular depletion during the menopausal transition- evidence for accelerated loss and ultimate exhaustion. J Clin Endo Metab. *65*:1231-7.

Riley JK, Carayannopoulos MOH, Wyman A, Chi M, Ratajczak CK & Moley KH. (2005). The PI3K/Akt pathway is present and functional in the preimplantation mouse embryo. Dev Biol. *284*, 377–386.

Rime, H., Jessus, C., Ozon, R. (1995). Tyrosine phosphorylation of p34cdc2 is regulated by protein phosphatase 2A in growing immature Xenopus oocytes. Exp. Cell Res.

Russell DL, Robker RL. (2007). Molecular mechanisms of ovulation: co-ordination through the cumulus complex. Hum Reprod Update. *13*:289-312.

Sagata, N., Oskarsson, M., Copeland, T., Brumbaugh, J., Vande Woude, G.F. (1988). Function of c-mos proto-oncogene product in meiotic maturation in Xenopus oocytes. Nature *335*, 519– 525.

Santanu De and Douglas Kline. (2013). Evidence for the requirement of 14-3-3eta (YWHAH) in meiotic spindle assembly during mouse oocyte maturation. Developmental Biology. *13*:10

Sharma A, Shah SR, Illum H, Dowell J. (2012). Vemurafenib: targeted inhibition of mutated B-RAF for treatment of advanced melanoma and its potential in other malignancies. Drugs. *72*, 2207-22.

Scott, L. F., Sudaram S. G., and Smith S. (1993). The relevance and use of mouse embryo bioassays for quality control in an assisted reproductive technology program. Fertility and Sterility. *60(3);* 559-568.

Shibuya EK; Morris J; Rapp UR; Ruderman JV, Cell Growth & Differentiation. (1996). Activation of the Xenopus oocyte mitogen-activated protein kinase pathway by Mos is independent of Raf. Molecular Biology Journal Vol. 7, 235-41.

Smith, G.D., Sadhu, A., Wolf, D.P. (1998). Transient exposure of rhesus macaque oocytes to calyculin-A and okadaic acid stimulates germinal vesicle breakdown permitting subsequent development and fertilization. Biol. Reprod.

Soewarto, D., Schmiady, H. and Eichenlaub-Ritter, U. (1995). Consequences of non-extrusion of first polar body and control of the sequential segregation of homologous and chromatids in mammalian oocytes. Hum. Reprod. *10*, 2350-2360

Steuerwald N, Cohen J, Herrara R, Brenner C. (1999). Analysis of gene expression in single oocytes and embryos by real time rapid cycle fluorescence monitored RT-PCR. Mol Hum Reprod. *5*, 1034-1039.

Sudipta Paul, Kousik Pramanick, Sourav Kundu, Arun Bandyopadhyay, Dilip Mukherjee. (2009). Involvement of PI3 kinase and MAP kinase in IGF-I- and insulin-induced oocyte maturation in *Cyprinus carpio.* Molecular and Cellular Endocrinology. *309*, 93–100.

Swanson, R. and Leavitt, M. (1992). Fertilization and mouse embryo development in the presence of midazolam. Anesth. Analg. *75*, 549-554.

Terret, M.E., Lefebvre, C., Djiane, A., Rassinier, P., Moreau, J., Maro, B., Verlhac, M.H. (2003). DOC1R: a MAP kinase substrate that control microtubule organization of metaphase II mouse oocytes. Development. *130*, 5169– 5177.

Tingen CM, Bristol-Gould SK, Kiesewetter SE, Wellington JT, Shea L, Woodruff TK. (2009). Prepubertal primordial follicle loss in mice is not due to classical apoptotic pathways. Biol Reprod. *81*:16-25.

Tucker KE, Jansen CAM. (2004). The mouse embryo bioassay: Is it the "Gold Standard" for quality control testing in the IVF laboratory? In: Proceedings 2nd International workshop for Embryologists: Troubleshooting Activities in the ART lab. Ed. R. Basuray and D Mortimer.

Van Blerkom J. (1991). Extrinsic and Intrinsic influences on human oocyte and early embryonic developmental potential. In: Elements of Mammalian Fertilization. Wassarman PM, ed. Boca Raton, FL. CRC Press. 81-109.

Verlhac, M.H., Kubiak, J.Z., Clarke, H.J., Maro, B. (1994). Microtubule and chromatin behavior follow MAP kinase activity but not MPF activity during meiosis in mouse oocytes. Development. *120*, 1017–1025.

Wang Y, Wang F, Sun T, Trostinskaia A, Wygle D, Puscheck E, Rappolee DA. (2004). Entire mitogen activated protein kinase (MAPK) pathway is present in preimplantation mouse embryos. Dev Dyn. *231*, 72–87.

Wei Cui, Jie Zhang, Hua-Yu Lian, Hui-Li Wang, De-Qiang Miao, Chuan-Xin Zhang, Ming-Jiu Luo, Jing-He Tan. (2012). Roles of MAPK and Spindle Assembly Checkpoint in Spontaneous Activation and MIII Arrest of Rat Oocytes. PLoS ONE *7*, 2.

White RM. (2011). The natural history of malignancies under conditions of B-Raf inhibitor stimulation. Expert Opin Investig Drugs. *20*, 135–136.
Winston N. (1997). Stability of cyclin B protein during meiotic maturation and the first mitotic cell division in mouse oocyte. Biol Cell. *89*:211-9.

Wojnowski L, Zimmer AM, Beck TW, Hahn H, Bernal R, Rapp UR, Zimmer A. (1997). Endothelial apoptosis in B-Raf-deficient mice. Nat Genet. *16*, 293–297.

Wolfgang Staiber. (2012). Germ line-limited and somatic chromosomes of Acricotopus lucidus differ in distribution and timing of alterations of histone modifications in male gonial mitosis and meiosis. Chromosome Res. *20*, 717–734.

Wyrobek AJ, Eskanazi B, Young S, Arnheim N, Tiemann-Boege I, Jabs EW, et al. (2006). Advancing age has differential effects on DNA damage, chromatin integrity, gene mutations, and aneuploidies in sperm. Proc Natl Acad Sci. *103*, 9601-6.

Xiang-Hong Ou, Sen Li, Zhen-Bo Wang, Mo Li, Song Quan. (2012). Maternal insulin resistance causes oxidative stress and mitochondrial dysfunction in mouse oocytes. Human Reproduction. *27*, 2130–2145.

Yamauchi N, Kiessling AA, Cooper GM. (1994). The Ras/Raf signaling pathway is required for progression of mouse embryos through the two-cell stage. Mol Cell Biol. *14*, 6655–6662.

Yang H; Higgins B; Kolinsky K; Packman K; Go Z; Iyer R; Kolis S; Zhao S; Lee R; Grippo JF; Schostack K; Simcox ME; Heimbrook D; Bollag G; Su F. (2010). RG7204 (PLX4032), a selective B-RafV600E inhibitor, displays potent antitumor activity in preclinical melanoma models. Cancer Research. *13*, 5518-27.

Yufen Xie, Yingchun Wang, Tong Sun. (2005). Six Post-Implantation Lethal Knockouts of Genes for Lipophilic MAPK Pathway Proteins Are Expressed in Preimplantation Mouse Embryos and Trophoblast Stem Cells. Molecular reproduction and development. *71*, 1–11.

Zernicka-Goetz M. (2002). Patterning of the embryo. The first spatial decisions in the life of a mouse. Development. *129*, 815–829.

Zhang Y, Xiong Y, Yarbrough WG. (1998). ARF promotes MDM2 degradation and stabilizes p53: ARF-INK4a locus deletion impairs both the Rb and p53 tumor suppression pathways. Cell. *92*, 725–734.

Zhao, X., Singh, B., Batten, B.E. (1991). The role of c-mos proto-oncoprotein in mammalian meiotic maturation. Oncogene. *6*, 43– 49.

APPENDIX A

METHOD MECHANISMS

1. Mouse Oocyte Maturation Assay and Mouse 1C and 2C Embryo Development Quality Control Assay

Until the present time, mouse oocyte maturation and embryo development assays have been considered the most reliable bioassays for quality assurance/quality control (QA/QC) determination and validation of gamete and embryo research (Tucker & Jansen, 2004).

The mouse embryo assay, either zygote stage or 2C stage, is a recommended bioassay for evaluating culture medium prior to use in human clinical treatment (ASRM, 1992; Dandekar et al., 1984). In addition the oocyte cell progression from GV to GVBD to M-II also showed the value of oocyte maturation evaluation over a long period (Bodart JFL el al., 2005). Mouse oocyte and embryo models are used to evaluate aspects of new protocols, physical materials, and culture media which cannot be assessed using physical equipment (Scott, et al., 1993; Naz et al., 1986).

Mouse oocyte and embryo models have significant financial, management and ethical advantages over human embryos in toxicity studies. Mouse oocyte maturation and embryo development assays have been used to screen compounds added to cultures for potential toxicities (Condon-Mahony et al., 1986; Fleming et al., 1987; McDowell et al., 1988; Bastias et al., 1993). Both assays have also been used for testing potential developmental toxic effects of clinical drugs (anesthetic formulations), environmental pollutants (methyl tertiary butyl ether) as well as pressure-treated lumber additives (CrO_3, CuO and As_2O_5). Mouse gametes and embryo development assays remain valuable models for evaluating operational procedures, drugs, and potentially toxic agents before using these drugs in clinical situations.

Scoring systems in *in vitro* fertilization (IVF) have been used for many years for oocyte, zygote and embryo parameters evaluation. The most frequently applied method for evaluating gamete and embryo competencies is the morphology analysis. An analysis must possess the quality of being easy to assess, causing minimal impact on gametes and

embryos, and maintaining result objectivity (Machtinger R et al., 2013). Further analysis such as chromosome integrity, metabolic activity, and genomic activation detection, while potentially beneficial, is not necessary for gamete and embryo evaluation (Munne S et al., 1999, Steuerwald N et al., 1999; Van Blerkom J el al., 1991; Conaghan J et al., 1993; Gardner DK, 2001). Because the accuracy or precision of oocyte competency prediction could not be achieved by any indirect assays, evaluation of the morphology of the oocytes is believed to be the most efficient marker of oocyte maturation competency. Also, oocyte spindle formation and chromosome alignment in MI and MII nuclear maturation is the best indicator of cytoplasmic maturation.

2. Spindle Apparatus and Chromosome IF Staining

The correct separation of homologous chromosomes during the telophase of meiosis I and segregation of the sister chromatids during meiosis II play a critical role in avoiding aneuploidy (Hassold T, et al., 2001). Abnormal segregation of the chromosomes or chromatins is often due to the meiotic non-disjunction and is normally incompatible with normal oocyte and embryo development. Many non-lethal chromosomal diseases are associated with incorrect non-disjunction segregation [e.g., Down Syndrome (21 trisomy), Patau Syndrome (13 trisomy), Edward Syndrome (18 trisomy), Klinefelter Syndrome (extra X in males), Turner Syndrome (lack of one X in females)] (Angell RR et al., 1994). Approximately one third of all miscarriages and twenty percent of human embryos are aneuploidies and are the leading cause of the genetic disorders, development disabilities and mental retardations (Wyrobek AJ et al., 2006).

Direct immunofluorescence staining has demonstrated its accuracy in capturing the spindle apparatus formation and chromosome alignment in much research over a long period of time (Santanu De et al., 2013; Nervana TEM, 2003; Jashoman Banerjee et al., 2012; Wei Cui et al., 2012; Wolfgang Staiber, 2012; G. Bradley Alsop 2003). In the present study, the microtubules and chromosomes of Vemurafenib-exposed oocytes in all developing stages were directly stained by fluorescence-dye-conjugated antibody after being fixed and permeated with Microtubule-stabling buffer (MTSB) and blocked by blocking solution. In this way, variously shaped spindle apparatus and chromosomal

alignments were examined and evaluated under the Zeiss A1 inverted fluorescent microscope.

3. DNA Integrity TUNEL Assay

Even with a perfect appearance at the microscopic level of the formation of the barrel shaped spindle apparatus and chromosome alignment after IF staining, we could not rule out the possibility of tiny damages to the DNA molecules by Vemurafenib exposure. This technique is suitable for fixed samples from all stages of the oocyte culture. Apoptosis in any stage of the oocyte is landmark of programmed self-destruction. Oocyte apoptosis is carefully executed by the activation of the nucleases, which break down the nuclear DNA into approximately 200bp DNA in length. Large numbers of 3'-hydorxyl ends are exposed when DNA breaks after initiation of the apoptosis. These 3' hydroxyl endings are the major target for deoxynucleotidyl transferase (TdT), which adds deoxyribonucleotide in a template-independent manner. The 5-bromo-2′-deoxyuridine 5′-triphosphate (Br-dUTP) can be added to the mixture of reaction-led TdT to act as the labelling units of deoxyribonucleotide extensions. The Br-dU can be detected by the anti-Br-dU antibody conjugated by fluorescent dye. This immunohistochemical technique, named Terminal Deoxynucleotide Transferase dUTP Nick End Labeling, or TUNEL, accurately and unambiguously detects DNA fragments and is considered one reliable method for apoptotic cells identification. In our case, the Br-dU was detected by Alexa Fluor® 488 dye–labeled anti-Br-dU antibody, which has an excitation and emission spectrum similar to FITC. The fluorescence was observed by a Zeiss A1 inverted fluorescence microscope. The chromosomes were detected concomitantly by DAPI staining to prove the *in situ* DNA damage.

4. *Ex vivo* 1C embryo p-Mek 1/2 *In Situ* IF Staining for Embryo C-Raf Activity

Activity of the C-Raf in the developing embryo plays a key role in the MAPK pathway for 1C to 2C transition and post- implantation embryo development. The inhibitory nature of Vemurafenib on the C-Raf protein hinders development of the embryo. C-Raf by nature is a kinase (phosphotransferase) which phosphorylates its only

substrate Mek by adding a phosphate group on it at Serine 217 and 221 in the mouse. Mek 1/2 is the direct and only substrate of C-Raf in the MAPK pathway. The phosphorylation of Mek 1/2 directly reflects the kinase function and activity of C-Raf, the potential target of Vemurafenib. Therefore, C-Raf activity in Vemurafenib-exposed 2C embryos was collectively tested by the embryo p-Mek 1/2 *in situ* IF Staining. Phosphorylated Mek 1/2 was subjected to indirect IF staining with signal amplification by biotin-streptavidin system. Results were examined under a Zeiss A1 inverted fluorescent microscope.

5. Laboratory Quality Control and Quality Assurance

To ensure optimal quality and repeatability of experiment results, all equipment involved in each assay was closely monitored. In order to maintain in a constant pH of the medium at the physiological pH 7.4, CO_2 levels of 5% in the water jacketed incubator (Model, NU4750) were checked on daily basis. A Fyrite CO_2 indicator was used to guarantee exact CO_2 levels in the event that the sensor of the incubator became either disabled or disturbed by other factors (e.g. humidity). The optimal growth temperature for mouse embryos is 37°C. Incubator temperatures did not deviate from this optimal temperature by more than 0.5°C. A thermometer was inserted in the middle of the incubator chamber to guarantee temperature accuracy in the event that the sensor of the incubator was not working properly. Internal humidity was maintained by use of a humidity pan at the bottom of the incubator chamber which held a maximum of 5L of distilled water. To insure that temperature remained constant, water was not added during a culture cycle. The incubator was dismantled and cleaned once every three months or at any time that evidence of bacterial growth was noted.

Deionized water was used for the surgical instrument sterilizer and was changed monthly. Surgical stainless steel instruments were placed in the sterilizer for a minimum of three minutes prior to use under sterile conditions. Test-tube block heaters were disinfected weekly with STX-100 solution. The tolerance limit for block heaters was 37°C ± 0.5°C and a thermometer was used for temperature guarantee.

Temperatures of the Revco deep freeze and refrigerator were checked daily. Tolerance limits for the freezer were -15°C ± 5°C for IF staining preservation. Temperature ranges between 5°C and 0°Cwere maintained in the refrigerator for formulated media and other hormones. All chemicals for formulation of culture media were replaced annually or whenever a suspicion contamination arises.

APPENDIX B

SUPPLEMENTAL IMAGES

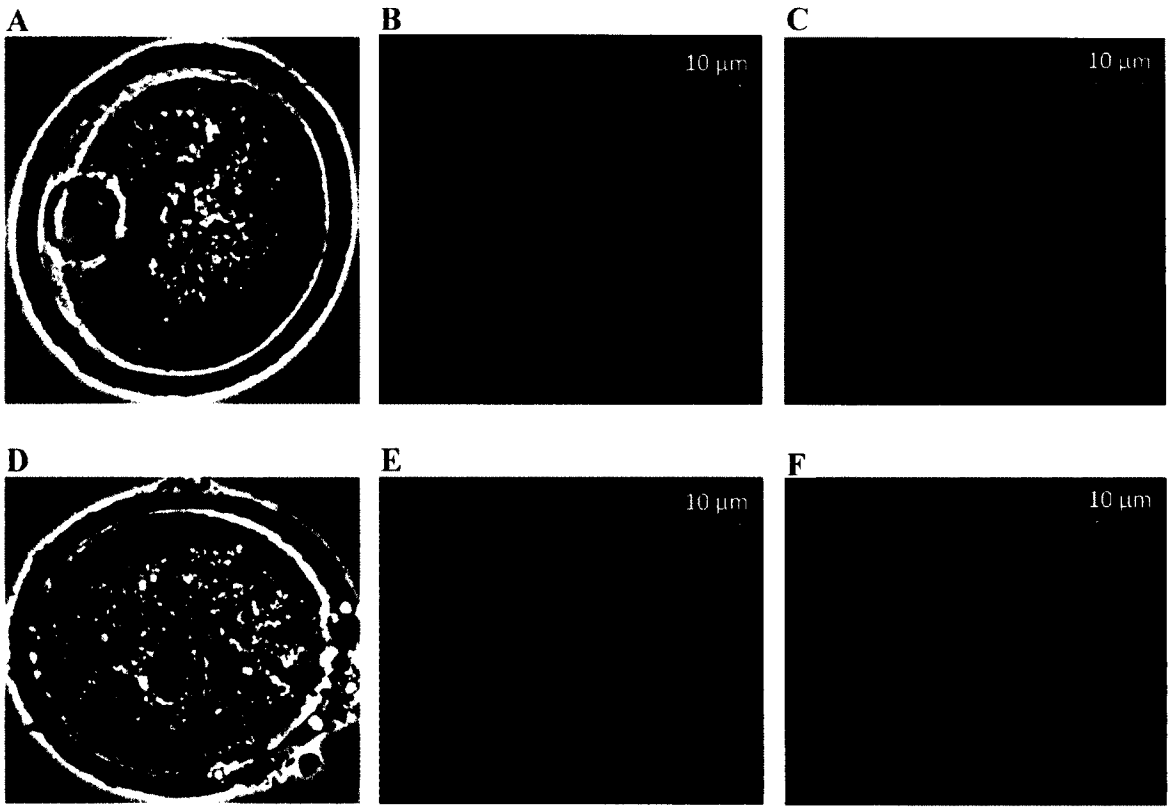

(A, B and C)Pictures from one cell show A, MII stage; B, Misaligned shaped spindle; C, Unaligned aligned chromosome.

(D, E and F) Pictures from one cell show D, MI; E, Barrel spindle fiber; F, Unaligned chromosome.

Concentration related response of spindle apparatus formation and chromosome alignment (GV, GVBD, and MII) after 16h in the presence of Vemurafenib. Figures showed the immunofluorescence staining of different responses of oocytes under the influence of Vemurafenib. MI = Metaphase I; MII = Metaphase II. Cell was taken by DAC phase. Spindle fiber was stained as green and chromosomes were stained as blue.

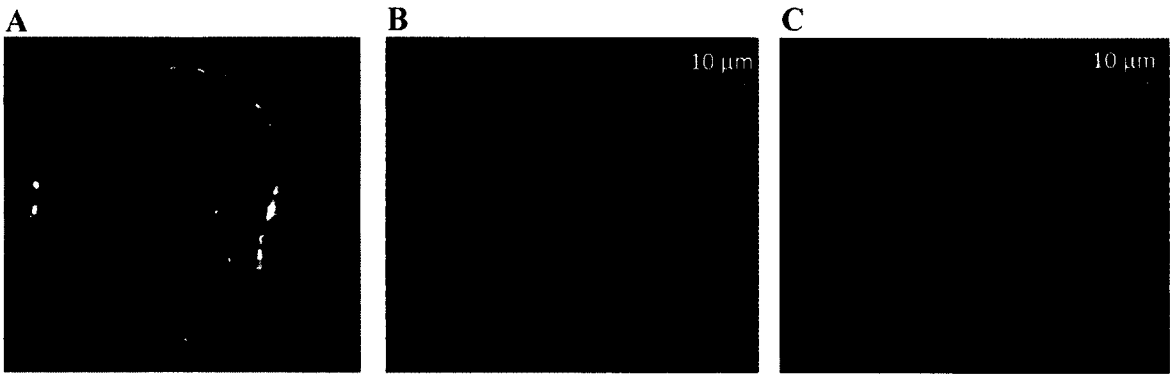

(A, B, and C) Pictures from one cell show A, MII stage; B, TUNEL negative; C, aligned chromosome.

Concentration related response of DNA integrity (GV, MI, and MII) after 16h in presence of Vemurafenib. Figures showed the TUNEL IF staining of different responses of oocytes under influence of the Vemurafenib. MI: Metaphase I; MII: Metaphase II. Cell was taken by phase. Positive TUNEL was stained as green and chromosomes were stained as blue. Polar body showed a positive TUNEL (green, internal control).

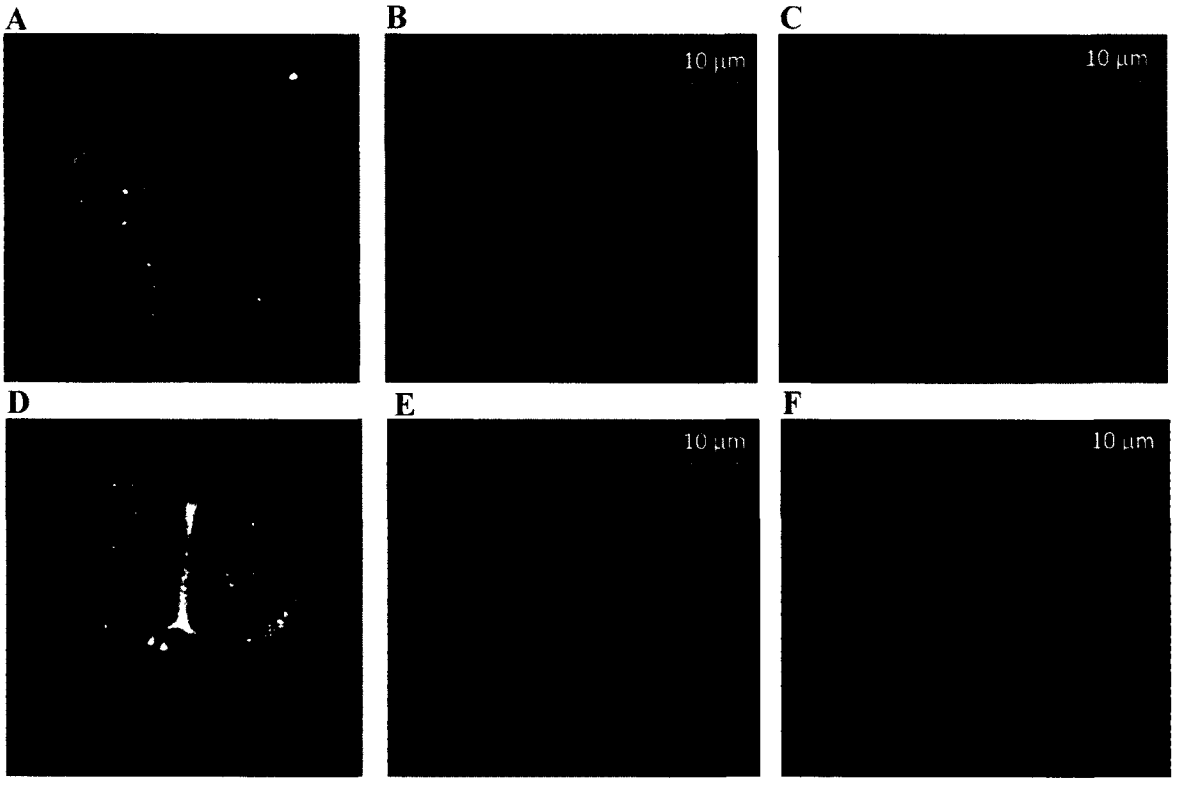

(A, B and C) Pictures from one cell show A, abnormal 1C B, p-Mek 1/2 IF staining negative (Green stained cytoplasmic substances); C, DAPI stained nucleus location (D, E and F) Pictures from one cell show D, normal 2C; E, p-Mek 1/2 IF staining positive (Green stained cytoplasmic substances); F, DAPI stained nucleus location. Concentration related response of embryo C-Raf activity by after 16h in presence of Vemurafenib. Figures showed the p-Mek 1/2 IF staining of different responses of embryos under influence of Vemurafenib.

VITA

Bo Liu

Department of Biological Sciences

Old Dominion University

Norfolk, VA 23529

Education:

- Doctor of Philosophy in Biological Science (Sep. 2010~Dec. 2014)
  Biomedical Science (BIMD), Old Dominion University, Norfolk, VA, USA, 23529.
- Bachelor of Medicine (BM) (Sep. 2004~Jun. 2009)
  Department of Medicine, Guangzhou Medical University, Guangzhou, China.

Internship:

- Research Fellow, Liberty University College of Osteopathic Med. (Jan.~ Aug 2014);
- Guangzhou 1st Municipal People's Hospital. (Jan. ~Dec 2008).

Awards

In Old Dominion University

- *Awardee,* Dominion Scholar Scholarship. (Sep. 2010~Present);
- *Awardee,* Embryonic Laboratory Research Award. (2012~2014).

In Guangzhou 1st Municipal People's Hospital

- Awardee, Outstanding Intern. (2007-2008).

In Guangzhou Medical University

- Recipient, First Grade Scholarship (5%). (Sep. 2004);
- Recipient, Principal Scholarship (2%). (Jun. 2005);
- Winner, Second Prize, 3rd Guangzhou Medical Colleges Professional Knowledge Competition-Systematic Anatomy Contest (Apr. 2006).

Teaching Experience:

- Graduate Teaching Assistant (GTA) Biol 789/889 Gross Anatomy, Cadaver dissection instructor& Lab manager (Summer. 2012, 2013);
- GTA Biol 461/561 Human Cadaver Dissection. Cadaver Dissection Instructor & Lab Manager (Fall, 2012, 2013);
- GTA Biol 250 Anatomy and Physiology I. Lab Instructor. (Summer, Fall, 2013).